TECHNO-ECONOMIC ASSESSMENT OF AN INTEGRATED PLANT TO PRODUCE AMMONIA AND UREA FROM BIOGAS

Matheus Calheiros Fernandes Cadorini

Dissertação de Mestrado apresentada ao Programa de Pós-graduação em Engenharia Química, COPPE, da Universidade Federal do Rio de Janeiro, como parte dos requisitos necessários à obtenção do título de Mestre em Engenharia Química.

Orientadores: Argimiro Resende Secchi
Príamo Albuquerque Melo Junior

Rio de Janeiro
Março de 2024

TECHNO-ECONOMIC ASSESSMENT OF AN INTEGRATED PLANT TO PRODUCE AMMONIA AND UREA FROM BIOGAS

Matheus Calheiros Fernandes Cadorini

DISSERTAÇÃO SUBMETIDA AO CORPO DOCENTE DO INSTITUTO ALBERTO LUIZ COIMBRA DE PÓS-GRADUAÇÃO E PESQUISA DE ENGENHARIA DA UNIVERSIDADE FEDERAL DO RIO DE JANEIRO COMO PARTE DOS REQUISITOS NECESSÁRIOS PARA A OBTENÇÃO DO GRAU DE MESTRE EM CIÊNCIAS EM ENGENHARIA QUÍMICA.

Orientadores: Argimiro Resende Secchi
Príamo Albuquerque Melo Junior

Aprovada por: André Luiz Hemerly Costa
Fábio de Almeida Oroski
Argimiro Resende Secchi
Príamo Albuquerque Melo Junior

RIO DE JANEIRO, RJ – BRASIL

MARÇO DE 2024

Cadorini, Matheus Calheiros Fernandes

Techno-economic assessment of an integrated plant plant to produce ammonia and urea from biogas. / Matheus Calheiros Fernandes Cadorini – Rio de Janeiro: UFRJ/COPPE, 2024.

XVII, 136 p.: il.; 29,7 cm.

Orientadores: Argimiro Resende Secchi

Príamo Albuquerque Melo Junior

Dissertação (mestrado) – UFRJ/ COPPE/ Programa de Engenharia Química, 2024.

Referências Bibliográficas: p. 107-113.

1. Biogas. 2. Ammonia. 3. Urea. 4. Simulation. 5. Process Integration. I. Secchi, Argimiro Resende *et al.* II. Universidade Federal do Riode Janeiro, COPPE, Programa de Engenharia Química. III.Título.

Acknowlegments

I would like to thank my mother Delfina for all the love and partnership throughout my entire life. You will always be my model. To my uncle Carlos, for all the dedication he put into my development as a human being. To my grandparents, Maria and Manoel, for their unconditional love at all times. To my cousin Lucas and aunt Lúcia, for reminding me every day that there is still purity in the world.

To my wife, Letícia, for the companionship and support given at all times. Along with me, you also renounced several moments for this to arrive. We're about to complete this dream together. I love you!

To my advisors, Argimiro and Príamo, for their dedication and commitment to this project despite all the obstacles encountered along the way. You've always been able to show a path despite the adversities with words of encouragement and guidance so that this work could continue. You are fundamental to completing this stage of my career and to my personal and professional growth. Thank you very much for your all the lessons learned during our journey together.

To the Human Resources Program (PRH) 3.1 and ANP for the financial support during my period as a full-time master student. This support was essential for me to be able to develop this topic with the best resources available.

To professionals and beloved friends Luciana Siqueira and John Jeffries, for the dedication they put into my qualification.

Finally, I thank PEQ, COPPE and UFRJ for the opportunity to study at a public institution which provides quality education for all its students based on pioneering lines of research.

Resumo da Dissertação apresentada à COPPE/UFRJ como parte dos requisitos necessários para a obtenção do grau de Mestre em Ciências (M.Sc.)

AVALIAÇÃO TECNO-ECONÔMICA DE UMA PLANTA INTEGRADA PARA PRODUÇÃO DE AMÔNIA E UREIA A PARTIR DO BIOGÁS

Matheus Calheiros Fernandes Cadorini

Março/2024

Orientadores: Argimiro Resende Secchi

Príamo Albuquerque Melo Junior

Programa: Engenharia Química

Dentro do contexto econômico brasileiro, o biogás possui grande potencial para construção de uma plataforma química sustentável a partir da verticalização de cadeia de produtos químicos. A partir de estudos feitos pela CIBiogás (2023), constatou-se que o país possuía um número total de 885 plantas, sendo 771 em funcionamento e 114 em fase de construção. Esses dados indicam o aumento da participação do biogás dentro da matriz energética brasileira. Em contrapartida, o gás natural ainda é o principal insumo utilizado para a síntese de amônia, sendo produzida a partir do famoso processo Haber-Bosch. Além disso, estima-se que 80% da sua produção é encaminhada para fabricação de fertilizantes nitrogenados, especialmente, a ureia. As matérias-primas utilizadas são a amônia e CO_2, sendo o primeiro composto o produto principal do processo Haber Bosch e o segundo o principal subproduto do processo de síntese de amônia. Diante deste cenário, o presente trabalho contempla a simulação, validação e avaliação econômica de uma planta integrada de amônia e ureia a partir da alimentação de 1000 kmol/h de biogás utilizando o software comercial *Aspen Plus*, atingindo uma produção diária de 840 ton de ureia e conversão próxima a 60%. Além disso, devido ao alto percentual de CO_2 na corrente de biogás, obtém-se uma vazão residual de 385 kmol/h que não podem ser absorvidos pela síntese de ureia. A avaliação econômica evidenciou que a planta integrada contendo a alimentação completa de biogás possui NPV negativo (-98 MM $) para as condições assumidas no cenário base. Contudo, a análise de sensibilidade a partir de fatores como preço do biogás, comercialização do CO_2 residual e diminuição da taxa de juros podem afetar positivamente o fluxo de caixa, elevando os resultados referentes aos principais indicadores econômicos.

Abstract of Dissertation presented to COPPE/UFRJ as a partial fulfillment of the requirements for the degree of Master of Science (M.Sc.)

TECHNO-ECONOMIC ASSESSMENT OF AN INTEGRATED PLANT TO PRODUCE AMMONIA AND UREA FROM BIOGAS

Matheus Calheiros Fernandes Cadorini

March/2024

Advisors: Argimiro Resende Secchi

Príamo Albuquerque Melo Junior

Program: Chemical Engineering

Within the Brazilian economic context, biogas has enormous potential for building a chemical platform through the verticalization of a sustainable chemical product chain. Based on studies carried out by CIBiogás (2023), it was found that the country had a total number of 885 plants, 771 of which were in operation and 114 under construction. This data indicates the increased participation of biogas within the Brazilian energy matrix; On the other hand, natural gas is still the main input used for the synthesis of ammonia, being produced using the well-known Haber-Bosch process. Furthermore, 80% of its production is sent to the manufacture of nitrogen fertilizer, especially urea. The raw materials used in its process are ammonia and CO_2, the first one being the product of Haber-Bosch process and the second the main by-product of the ammonia synthesis process. Given this scenario, the present work contemplates the simulation, validation and economic evaluation of an integrated ammonia and urea plant from the supply of 1000 kmol/h of biogas using the commercial software *Aspen Plus*, reaching a daily production of 840 ton of urea and conversion close to 60%. Furthermore, due to the high percentage of CO_2 in the biogas stream, a residual flow of 385 kmol/h is obtained and cannot be absorbed by urea synthesis. The economic evaluation showed that the integrated plant containing the complete biogas feed has a negative NPV (- 98 MM $) in the base scenario. The sensitivity analysis based on factors such as biogas price, commercialization of residual CO_2 and decrease in interest rates can positively affect cash flow, increasing results regarding the main economic indicators.

Summary

List of Figures

List of Tables

List of Symbols

α_i	chemical activity of component i	[-]
$\alpha(T_r)$	dimensionless function of the Peng-Robinson equation	[-]
β_1	parameter for calculation of C_{EP}	[-]
β_2	parameter for calculation of C_{EP}	[-]
C_A	administrative cost	[$]
C_{BT}	benefits and training cost	[$]
C_C	contingency cost	[$]
C_{WG}	working capital	[$]
C_{EP}	equipment purchase cost	[$]
C_{SC}	salary charge cost	[$]
C_{CFP}	fixed production cost	[$]
C_I	installed cost	[$]
C_{PDI}	direct permanent investment cost	[$]
C_{IPS}	property and tax insurance cost	[$]
C_{PTI}	total permanent investment cost	[$]
C_M	maintenance cost	[$]
C_L	total labor cost	[$]
C_{RD}	research and development cost	[$]
C_{TP}	production total cost	[$]
C_{SM}	sales and marketing cost	[$]
C_{CVP}	total variable cost	[$]
C_{SA}	operator salary cost	[$]
C_{SM}	month salary cost	[$]
C_{SP}	supervision and management cost	[$]
C_{SU}	startup cost	[$]
C_{CIT}	total capital investment	[$]
C_O	offsite cost	[$]
C_E	engineering cost	[$]
C_{NH_3}	ammonia concentration	[mol L^{-3}]
C_{CO_2}	carbon dioxide concentration	[mol L^{-3}]
C_{CARB}	ammonium carbamate concentration	[mol L^{-3}]
D	depreciation	[$]
DCF	discounted cash flow	[$]
E_A	activation energy	[M L^2 T^2 mol^{-1}]

f_{BM}	parameter for the calculus of C_{CE}	[-]
f_C	civil factor	[-]
f_E	electric factor	[-]
f_{EL}	elevation factor	[-]
f_{EP}	structure factor	[-]
f_{IC}	instrumentation and control factor	[-]
f_l	location factor	[-]
f_P	piping factor	[-]
f_M	material factor	[-]
f_P	pressure factor	[-]
f_i	fugacity of component i	[M L^{-1} T^{-2}]
f_i^0	fugacity of pure component i	[M L^{-1} T^{-2}]
FF	fraction of financed capital	[-]
IR	interest rate	[-]
IRR	internal return rate	[-]
i	capital cost	[-]
i_f	interest rate of financed capital	[-]
i_{cp}	rate of return for equity investment	[-]
I	Inflation index	[-]
k_{dir}	kinetic constant of the direct reaction	[-]
k_{rev}	kinetic constant of the reverse reaction	[-]
K_a	equilibrium constant	[-]
NQE	number of total of pieces of equipment	[-]
P_i	partial pressure of component i	[M L^{-1} T^{-2}]
P_c	critical pressure	[M L^{-1} T^{-2}]
T	temperature	[K]
r_1	ammonium carbamate reaction rate	[mol L^{-3} T^{-1}]
r_2	urea reaction rate	[mol L^{-3} T^{-1}]
r_{dir}	kinetic rate of the direct reaction	[mol L^{-3} T^{-1}]
r_{rev}	reverse rate of the direct reaction	[mol L^{-3} T^{-1}]
r_{NH_3}	kinetic rate of ammonia synthesis reaction	[mol L^{-3} T^{-1}]
U_{PF}	fluid processing unit	[-]
U_{PS}	solid processing unit	[-]
y_i	molar fraction of component i	[-]

x_i, x_j	molar composition of components i, j	[-]
ϕ_i	fugacity coefficient of component i	[-]
V_m	molar volume	[L^3]
NPV	net present value	[$]
t_{IR}	income tax rate	[-]
t_p	project horizon	[-]
t_{dep}	plant operating horizon	[-]
T_c	critical temperature	[K]
T_r	reduced temperature	[K]
S	equipment size factor	[-]
S_V	sales revenue	[$]
ω	acentric factor	[-]
Π	product	[-]
Ξ_i	parameter for the calculus of C_{PE}	[-]
Ω	parameter for the calculus of f_p	[-]

List of Abbreviations

ABiogás	Brazilian Biogas Association
AD	Anaerobic digestion
ANDA	National Fertilizer Association
ANP	National Oil, Gas and Biofuels Agency
ANN	Artificial Neural Network
ARTE	Retro-techno-economic analysis
BNDES	National Bank for Economic and Social Development
CEPCI	Chemical Engineering Plant Cost Index
CI	Internal Combustion
CIBiogás	International Renewable Energy Center
CS	Cryogenic Separation
CCS	Carbon Capture and Storage
CCU	Carbon Capture and Use
CSP	Chemical Scrubbing Process
CTSR	Continuously Stirred Tank Reactor
DA	Anaerobic Degradation
DAP	Diammonium Phosphate
DEA	Diethanolamine
ENRCCI	Engineering News-Record Construction Cost Index
ELEC	Electricity
EPE	Energy Research Company
FAFEN	Nitrogen Fertilizer Factory
FIRJAN	Federation of Industries of the State of Rio de Janeiro
FH	Fired Heat
HDS	Hydrodesulfurization
HPS	High Pressure Steam
HTS	High Temperature Shift
HPWS	High Pressure Water Scrubbing
GDP	Gross Domestic Product
IE	Income Statement
ISBL	Inside Battery Limits
IPCA	National Consumer Price Index
K	Potassium
KAAP	Kellog´s Advanced Ammonia Process

LCA	Leading Concept Ammonia
LTS	Low Temperature Shift
LPS	Low Pressure Steam
OSBL	Outside Battery Limits
OPS	Organic Physical Scrubbing
MAP	Monoammonium Phosphate
MAPA	Ministry of Agriculture, Livestock and Food Supply
MDEA	Methyldiethanolamine
MEA	Monoethanolamine
MPS	Medium Pressure Steam
MS	Membrane Separation
N	Nitrogen
P	Phosphorous
PR	Peng-Robinson
PFR	Plug Flow Reactor
PSA	Pressure Swing Adsorption
RSK	Redlich-Kwong-Suave
RSU	Urban Solid Waste
SSP	Simple Superphosphate
TSP	Triple Superphosphate
STAC	Stamicarbon
SNAM	Snamprogetti
USA	United States of America
VLE	Vapor Liquid Equilibrium
WT	Wastewater treatment

1. Introduction

A sustainable chemical industry has gained increasing relevance within the global economic scenario due to growing concern about climate change and the finiteness of fossil resources. There is a movement towards the use of renewable energy and the adoption of chemical processes that promote the gradual replacement of petrochemical sources. At this juncture, Brazil has a privileged position and the potential to become a global reference in terms of energy transition within the chemical industry, being an important pillar of the national economic development (MORONE *et al*., 2015; SERRANO-RUIZ *et al*., 2012).

The recent volatility in global commodity markets and geopolitical uncertainties have further highlighted the fragility and dependence of Brazil's economy. In this context, the pressing need to explore and invest in alternative sources within chemical industry becomes evident. The security and stability of national supply chain depends on the search for local alternatives which can significantly contribute to reduce the environmental impact and help the sustainable development of the industrial sector. It is important to highlight that the urgency of this search is even more accentuated given the deficit in the trade balance and the loss of competitiveness caused by the prices of imported raw materials and intermediates. Therefore, raw material diversification is presented not only as a strategic measure, but as an urgent need for the strengthening and resilience of the national chemical industry. (EPE, 2019; SAE, 2020).

Envisioning a favorable scenario for sustainability within the Brazilian economy, biogas presents itself as a strong candidate for building a chemical platform either for use as a source of renewable energy and/or as a raw material for the synthesis of products (ABiogás, 2020). According to the definition of the National Petroleum, Gas and Biofuels Agency (ANP), biogas is described as a direct product of the biological decomposition of organic waste. It has interesting characteristics due to the similarity of chemical composition with natural gas, therefore being a viable option for replacing the petrochemical equivalent for a variety of processes (OLIVEIRA, 2013, POBLETE, 2019).

According to reports promoted by the International Center for Renewable Energy (CIBiogás), Brazil shows an increasing trajectory in relation to the number of biogas production plants in the national territory. The numbers released in 2020 revealed the existence of 675 biogas plants and the emergence of 148 new installations, corresponding to an increase of 22% compared to 2019. The updated data for 2021 found a total number of 653 operational plants (16% more than in 2020) and others 102 in the construction stage (CIBiogás, 2022). The expectation for the decade is the

establishment of biogas as a relevant product based on the presence of companies (*e.g.,* Raízen) investing in the expansion of industrial plants and the trading of this raw material.

During the beginning of the 20th century, there was an exponential growth in the world population made possible by technological advances and their productivity gains. Within this context, the Haber-Bosch process is one of the main innovations in the field of chemical engineering. This process is responsible for the synthesis of ammonia under conditions of high pressure and temperature from the reaction between nitrogen and hydrogen gases, being the basis for industrial projects implemented to this day. Within the ammonia production flowsheet, natural gas is the main raw material used, therefore, the replacement focuses on the implementation of a sustainable system. It is worth highlighting that most of the ammonia produced on a global scale is destined for the manufacture of nitrogen fertilizers and, mainly, the production of urea (CARVALHO, 2016; PAIXÃO, 2018).

Fertilizer production and supply is a relevant topic for the global economy in terms of ensuring world food security. These chemical products are important to guarantee agricultural productivity by the renewal of nutrients present in the soil. In this sense, agricultural fertilization has been able to increase the sustainability and stability of production systems, in addition to expanding the food supply in a world with population growth (BNDES, 2012; PAIXÃO, 2018).

Economic data relating to the Brazilian economy demonstrate agribusiness's constantly increasing share within the Gross Domestic Product (GDP), being considered the main sector within a stagnant economy during last decade. Given the importance for Brazilian GDP, fertilizer availability is a decisive factor in sustaining the sector's productive capacity. However, the data released by the National Fertilizer Diffusion Association (ANDA) reveals a conflicting scenario regarding the quantity of fertilizer imported and the national production of fertilizers, as shown in Figure 1

There has been a decrease in the national production capacity of fertilizer at the same time as the growth in the quantity being imported to supply the sector. Therefore, there is an evident trend of decoupling between Brazilian industry and the total amount coming from imports. This scenario could be aggravated in the coming years given the growth trend in the agricultural sector. The maintenance or worsening of this situation provides a vulnerable condition for Brazil in relation to the constant supply of chemical intermediate products and high external dependence to import them. Besides, it's important to realize that the prices of imported raw materials have a direct impact on the entire supply chain, increasing the cost on the intermediates/products. Naturally, the rising food prices affects the end consumer, contributing to inflation levels.

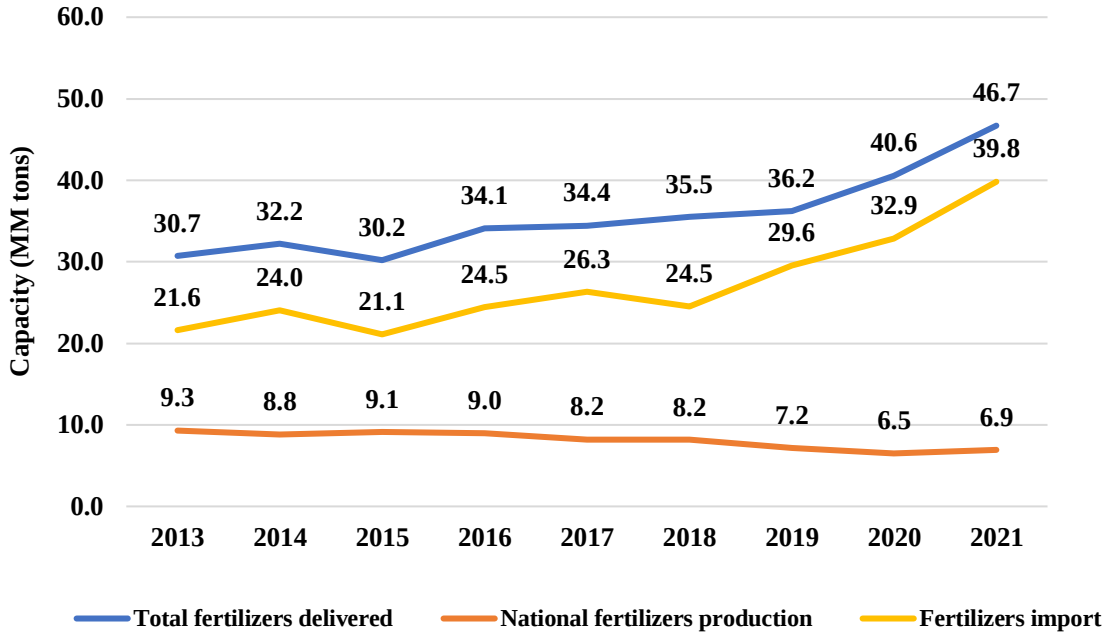

Figure 1 - Macro indicators of fertilizer industry in Brazil. Source: ANDA (2022).

Ammonia and urea are essential products to guarantee the supply of this industry. However, conventional fertilizer manufacturing is carried out through energy-intensive processes that depend on the extraction of finite resources from the natural gas used for the Haber-Bosch process (AZARHOOSH *et al*., 2014, SARTORE, 2014). Considering the availability of raw materials for biogas production, the use of renewable sources in agribusiness can play a fundamental role in reducing environmental impacts associated with production and maintaining the sector's competitiveness in the long term.

In addition to the environmental benefits, the use of alternative energy sources can bring positive impacts from an economic perspective. Brazil has tax incentives and government programs for renewable energy projects, which can boost biogas production as one of the main raw materials within an important value chain for the Brazilian economy. Given the importance of the agricultural sector for Brazilian GDP, fertilizer availability is a decisive factor in sustaining and intensifying the organic growth of the sector.

Therefore, considering that natural gas presents itself as a finite and non-renewable source of energy, this work's main goal is to introduce biogas as an alternative raw material aiming at the construction of a verticalized and sustainable supply chain for the production of ammonia and urea. The contrast between the growth rate of the domestic biogas market and the fertilizer import reveals a favorable scenario for discussing investments to strengthen the national economy. Based on this, the present work seeks to discuss aspects related to the validation and operational performance of an integrated plant for the synthesis of ammonia and fertilizers, identifying the main challenges

related this project. Moreover, based on the results obtained by the simulation, an economic evaluation is carried out to identify the key points for decision-making in relation to the plant's investment, highlighting the key variables for the cost of the plant and the total investment required.

1.1 - Goals

The general goal of this work is to analyze the techno-economic viability of an integrated plant to produce ammonia and fertilizer using biogas as the main raw material. In order to fulfill the purpose of the work, specific objectives were defined to guide the execution of the work:

1. Study and understand the potential of biogas national market.
2. Individual validation of ammonia and urea processes.
3. Process integration considering biogas as raw material.
4. Techno-economic evaluation considering a base scenario.
5. Identification of key variables for plant cost and operation.

1.2 - Work structure

Chapter 1 is the first of six and provides a general introduction to the work.

Chapter 2 contains the literature review structured into three main topics: relevant aspects related to biogas product, descriptions of the ammonia and urea processes, as well as an analysis of the national fertilizer market.

Chapter 3 details the methodology used for all stages of the work. Here, the equipment modeling strategy and the adaptations/considerations made are detailed for the plant simulation and the assumptions adopted for economic analysis.

In Chapters 4 and 5, there is a discussion about the main results obtained from the work and the conclusions arising from this evaluation.

Finally, Chapter 6 aims to propose suggestions for future work to improve or expand the line of research outlined.

2. Theoretical and Bibliographic Review

This chapter has three principal divisions: biogas, ammonia, and urea. The section containing biogas addresses the main aspects related to the composition of biogas, purification processes and the current Brazilian scenario within this sector. The section on ammonia features the characterization of the Haber-Bosch production process. The last subchapter presents the Stamicarbon (STAC) reaction system for urea synthesis, as well as addresses the modeling and simulation the situation of the national fertilizer market. The last two sections highlight works containing the modeling, simulation and optimization of strategies involving ammonia and urea.

2.1 - Biogas

2.1.1 - General context

Biogas can be defined as "raw gas obtained from the biological decomposition of organic products or residues," as set out in Normative Resolution No. 8 of 2015 of the National Agency of Petroleum, Gas and Biofuels (ANP). This biological degradation results from the metabolism of a variety of microbial populations, called anaerobic digestion (AD) and which occurs without the presence of oxygen (CARDOSO, 2017; POBLETE, 2019). This process can also be termed as anaerobic fermentation, biomethanation, biomethanization, and methanization. Among the available biochemical routes, anaerobic digestion is a technically and economically strategy to scale up biogas synthesis. Biodigestion is the main technology used to produce biogas, which can be used for the purposes of treating effluents and/or industrial streams, synthesizing biogas and/or biofertilizer from the digested liquid part, called digestate (CARDOSO, 2017; MARIANI, 2018).

Under different conditions of pressure, temperature, humidity and specific pH ranges, biogas can be produced from various sources, among which domestic sewage, waste from the food industry and agriculture (*e.g.*, straw and vinasse) can be highlighted. The main constituents of biogas are methane and carbon dioxide, accounting for the entire gas mixture. However, other chemical species may be present in lesser amounts such as hydrogen sulfide (H_2S), ammonia (NH_3), hydrogen (H_2), and nitrogen (N_2), and traces of other contaminants resulting from the biological decomposition of organic matter. The composition of biogas is quite variable and directly depends on the constitution of the raw material used during the production process (CARDOSO, 2017; KHAN *et al*., 2017; POBLETE, 2019). Table 1 presents a summary of the main characteristics of biogas.

Table 1 - Main characteristics of biogas. Source: Poblete (2019)

Component	**Range**	**Property**
Methane	50-75 (% v/v)	Energy potential
Carbon dioxide	25-50 (% v/v)	Corrosive Energy potential reduction
Nitrogen	0-5 (% v/v)	Energy potential reduction
Moisture	1-5 (% v/v)	Corrosion tendency
Hydrogen sulfide	0-5000 ppm	Corrosive Combustion gases emission (SO_2)
Ammonia	0-500 ppm	Combustion gases emission (NO_x)
Siloxanes	0-500 ppm	SiO_2 formation Corrosive and equipment incrustation tendency
Parameters	**Range**	**Unit**
Calorific power	4000-5000	kcal/m³
Density	1.19 – 1.21	kg/m³
Ignition temperature	650-750	ºC
Explosive Limit	4.4-16.5	% v/v

Anaerobic digestion consists of a complex metabolic process of decomposition of organic matter resulting from the association of microorganisms in the absence of oxygen. Anaerobic digestion can be divided into four main stages: hydrolysis, acidogenesis, acetogenesis and methanogenesis (KUNZ *et al*., 2019; POBLETE, 2019). Each stage of the process is conducted by distinct groups of microorganisms and different environmental conditions may be required for the process to develop. Figure 2 illustrates the transformations carried out in each stage, depicting the stages of hydrolysis, acidogenesis, acetogenesis and methanogenesis.

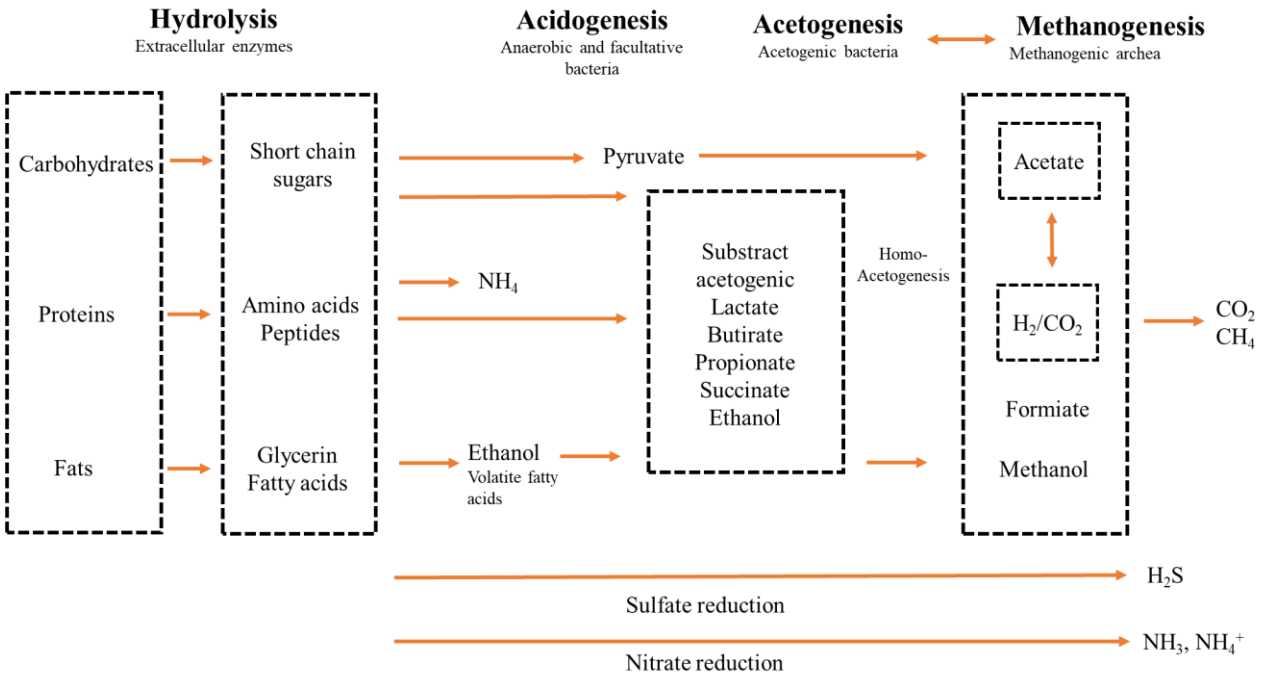

Figure 2 - Block diagram for the anaerobic digestion process. Source: Kunz *et al.* (2019).

Methane is the component of greatest economic interest, since it is an important renewable energy and can be used as a source of heat, electricity, and raw material for other industrial processes. This compound confers the energy potential of biogas, defined as the property of calorific power. Usually, biogas presents calorific values in the range of 5000 kcal/m³, while natural gas assumes values close to 8600 kcal/m³. Due to the higher composition of carbon dioxide in biogas, its calorific power is lower when compared to the petrochemical equivalent. Figure 3 shows the comparison of biogas with different fossil fuels, with the energy equivalence determined for 1 Nm³ of biogas with a composition of 70% CH_4 and 30% CO_2 (OLIVEIRA, 2013; POBLETE, 2019).

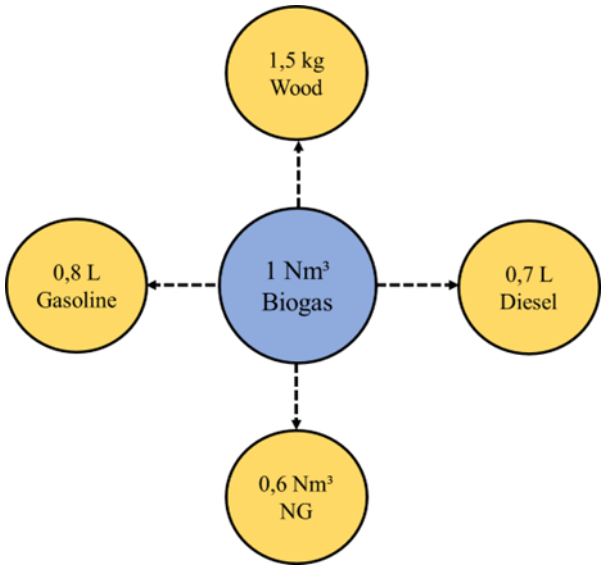

Figure 3 - Energy equivalence of biogas in relation to fossil fuels. Source: Poblete (2019).

The main applications of biogas are for the generation of electricity through turbines or internal combustion engines, heat production and the synthesis of biomethane and carbon dioxide. The focus in many countries shows the application of biogas for electricity production, with biomethane production still a secondary goal to the detriment of the electricity supply (HEIKER *et al*., 2021). It is worth mentioning that due to the similarity of composition with natural gas, biomethane can be considered as a similar gas if its composition meets the specifications determined for commercialization. Thus, biogas needs to be purified and refined, conducting a gas separation process in which the methane composition changes from about 60% (molar basis) to at least 96.5%, the remainder consisting of carbon dioxide and other components in reduced concentrations (ABiogás, 2020; KHAN *et al*., 2017; MARIANI, 2018). Technologies available industrially include absorption (physical and chemical), adsorption, Pressure Swing Adsorption (PSA), cryogenic and membrane separation. Table 2 contemplates a list of the current processes used for the purification of biogas, exploring its advantages and disadvantages.

Table 2 - Advantages and disadvantages of biogas purification technologies. Source: Khan *et al*. (2017)

Process	Advantages	Disadvantages
Pressure Swing Adsorption[a]	95-99% CH_4 concentration Removal of gas humidity Lower energy demand Elimination of O_2 and N_2 Quick installation and operational ease	High capital investment and operating costs (number of PSA columns) H_2S elimination is necessary Water must be removed previously from PSA unit Susceptible to fouling due to impurities
High Pressure Water Scrubbing[b]	> 97% CH_4 concentration Removal of CO_2 and H_2S Easy operation and low loss (< 2% CH_4) Impurities tolerance Water regeneration is possible	High investment and operating costs Lower energy efficiency Low operational flexibility with inlet current concentration (natural gas) Slow process High energy requirement (high pressure) High water requirement even with regeneration Corrosion problems (H_2S)

Table 2 - Advantages and disadvantages of biogas purification technologies. Source: Khan *et al*. (2017) (continue)

Process	Advantages	Disadvantages
Organic Physical Scrubbing[c]	> 97% CH_4 concentration Removal of components such as H_2S, NH_3, HCN e H_2O Low CH_4 loss	High investment and operational costs High energy demand for solvent regeneration Expensive and difficult to handle
Chemical Scrubbing Process[d]	> 99% CH_4 concentration Low operating cost Complete CO_2 removal possible in low pressure operations High selectivity and low loss	High investment High energy required for solvent regeneration Contamination, corrosion, and solvent loss issues
Membrane Separation[e]	> 96% CH_4 concentration Low space required Ease and low cost of maintenance Simple and sustainable process Fast installation and startup operation	Multiple stages for a product with high purity Low yield in single stage Low selectivity of membranes Not recommended for products with a high need for purity
Cryogenic Separation[f]	> 98% CH_4 concentration High CO_2 purity (has use as dry ice) Sustainable process without the use of Chemical agents	High investment, operating and maintenance costs High energy requirement

The biogas production chain can be visualized from Figure 4. The main substrates used for biogas production are organic waste from the agricultural, industrial and sanitation sectors. Each type of substrate has a different pre-treatment procedure due to the heterogeneity of its composition, being sent to the anaerobic digestion section inside the biogas plant. After synthesis, biomethane becomes the main component of interest and can be used in several ways. Currently, the main application is in the production of electricity, which can be exploited within the plant itself or

exported to other users. The presence of CO_2 decreases the biogas heat of combustion, and its removal becomes relevant to increase the heating value of the generated biogas and, consequently, the market value of this asset.

Furthermore, it is known that biogas is synthesized from the degradation of the organic raw material present in the feed substrate, reducing the organic load of this effluent. However, due to the diversity of waste composition, some compounds cannot be removed by the anaerobic digestion process and end up forming the digestate composition. Usually, this digestate has a high inorganic load due to the presence of nutrients such as Nitrogen (N), Phosphorus (P) and Potassium (K). These components can cause environmental problems if they are dumped directly into water bodies. However, this being the case, this composition is extremely beneficial for soil enrichment, containing the macronutrients necessary for fertilization, enabling the reuse of all residues, in addition to promoting increased productivity and reduced costs within agribusiness production chains (KUNZ *et al.*, 2019; MARIANI, 2018).

Finally, biogas stands out as a product with greater added value after a process of purification and upgrading for an increased concentration of biomethane. This product can be used directly as fuel. However, there is also a relevant opportunity for its use as a raw material in the construction of a national chemical platform following a global trend of decreasing dependence on non-renewable sources.

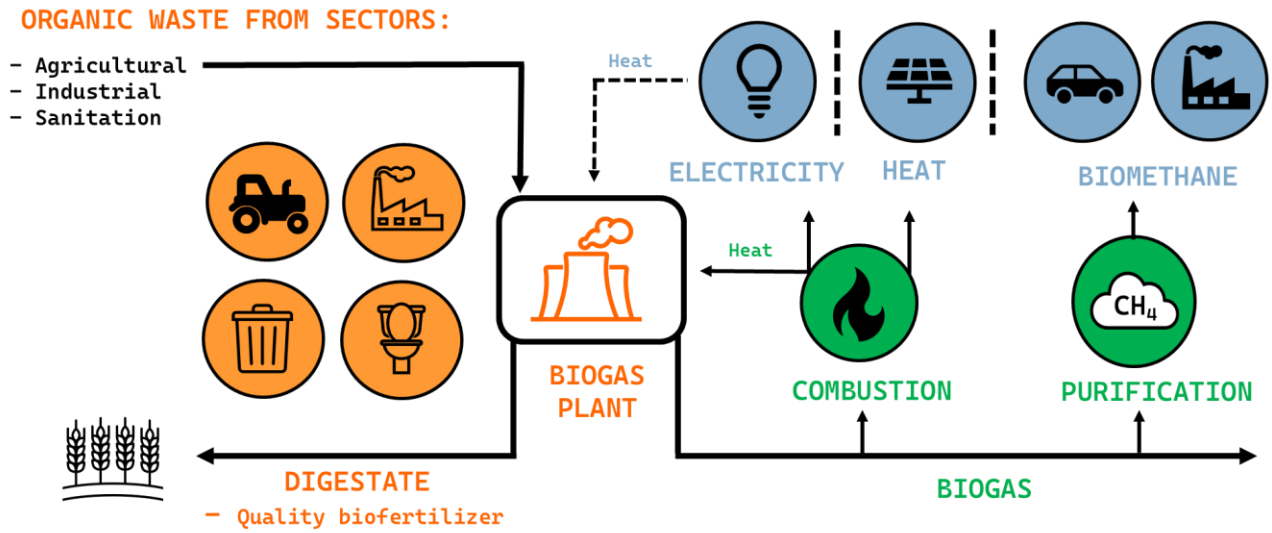

Figure 4 - Productive chain of the biogas sector. Source: ABiogás (2022).

2.1.2 - Brazilian Scenario

Sustainable economic development has driven the chemical industry by seeking solutions which promote the conscious use of resources concomitantly with concern for the environmental impacts involved in all operations. In this context, biogas presents itself as a promising alternative to diversify the composition of the Brazilian sustainable energy matrix, having a theoretical potential of 84.6 billion Nm³/year, with the greatest generation coming from the sugar-energy sector (RABELO, 2019, CIBiogás, 2021; CIBiogás, 2022, CIBiogás, 2023). Figure 5 highlights the data collected in a survey carried out in 2023 by CIBiogás. According to this study, by the year 2022, Brazil had 885 operational biogas plants, 82% of which were applied directly for energy purposes. In addition, 114 new plants were established, representing a growth of 15% compared to 2021. These plants could produce 2.8 billion Nm³ of biogas in the period, adding 530 million Nm³ compared to the total volume registered in 2021. Adding the total capacity, Brazil would be able to produce 2.8 billion Nm³ annually considering all the installed capacity of the biogas plants within the national territory.

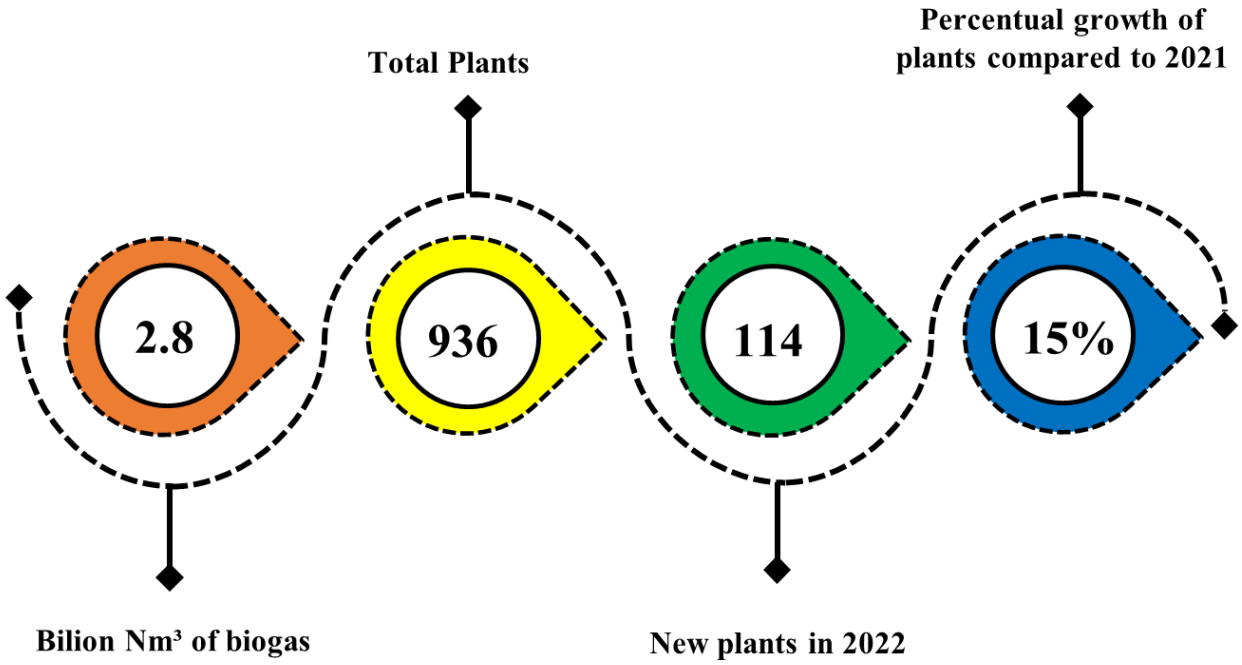

Figure 5 - Key figures for the biogas industry in 2022. Source: CIBiogás (2023).

The methodology of study segmented the capacity of the plants into three categories (small, medium, and large), in which Table 3 highlights the classification adopted by CIBiogás for segmenting the productive capacity of the biogas plants and also Figure 6 details the relationship between the number of plants and the volume of biogas produced according to the production capacity of national plants.

The data from Figure 6 indicates that 77% of the plants in operation in Brazil were classified as small (annual production up to 1 million Nm³ of biogas). However, these plants represent only 7% of the total volume of biogas in the country. Consequently, the largest volume of biogas produced (83%) was concentrated in large plants, this being the category with the smallest number of plants (only 8% of the Brazilian total).

Table 3 - Classification of the production capacity of biogas plant. Source: CIBiogás (2023)

Classification	Biogas Production (10^3 Nm^3/year)
Small capacity	< 500 to 1000
Medium capacity	1001 to 5000
Large capacity	> 5000 to 125000

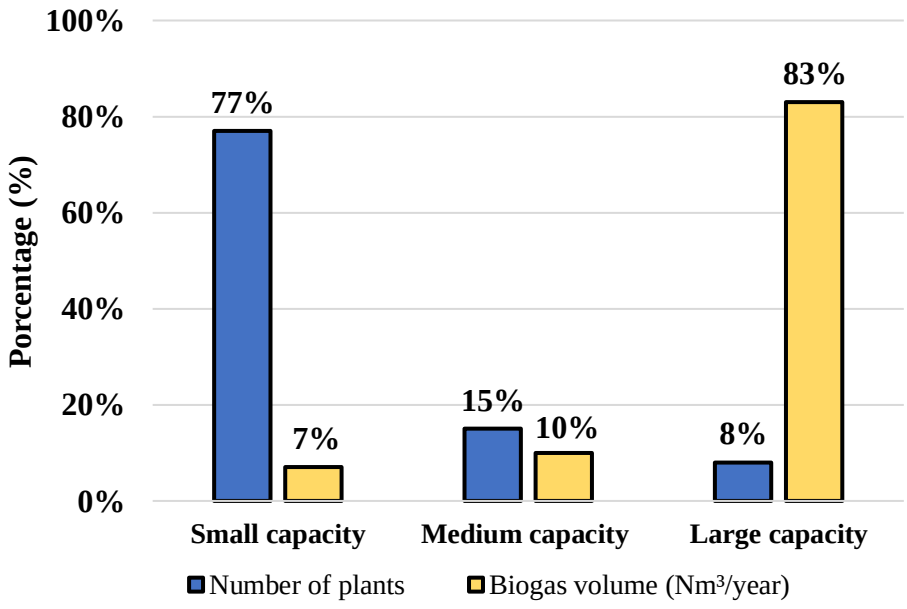

Figure 6 - Relationship between the number of plants and the volume of biogas produced in 2022, distributed by size. Source: CIBiogás (2023).

The origin of the substrate for national biogas synthesis was classified into three major sectors: agriculture, industry, and sanitation, as highlighted in Section 2.1.1. The main source of substrate used in biodigesters came from agricultural activity, corresponding to 78% of the plants in operation within the national territory. However, these plants represented only 10% of the national volume of biogas generated. According to the CIBiogás report, the existence of a high number of small plants performing agricultural activity was observed in previous surveys. Most of these units correspond to rural producers who use waste from their own production regarding animal protein market. Plants

that have urban solid waste (USW) as raw material and wastewater treatment (WT) are equivalent to 10% of the plants in operation, however, they are responsible for 74% of the national synthesis of biogas (2.1 billion Nm³/year) which accounts for the predominant share of total volume produced. In the year of 2022, this sector accounted 91 biogas plants across the country, achieving a remarkable increase of 32% compared to the previous year (2021). This value represents an increment surpassing the average growth rate of the preceding three years, which stood at the range of 23%. Besides, this sector is characterized by the prevalence of large-scale plants, with 56 facilities (62%) falling into the category indicated by Table 3. In that context, the biogas production volume from operational plants experienced a notable growth of 23% in 2022, exceeding the average annual growth rate of 15% observed over the preceding three years. This trend highlights the sector's growing role in leveraging biogas for sustainable energy generation (CIBiogás, 2021; CIBiogás, 2022, CIBiogás, 2023). Figure 7 presents information related to the number of plants and volume of biogas produced in 2022.

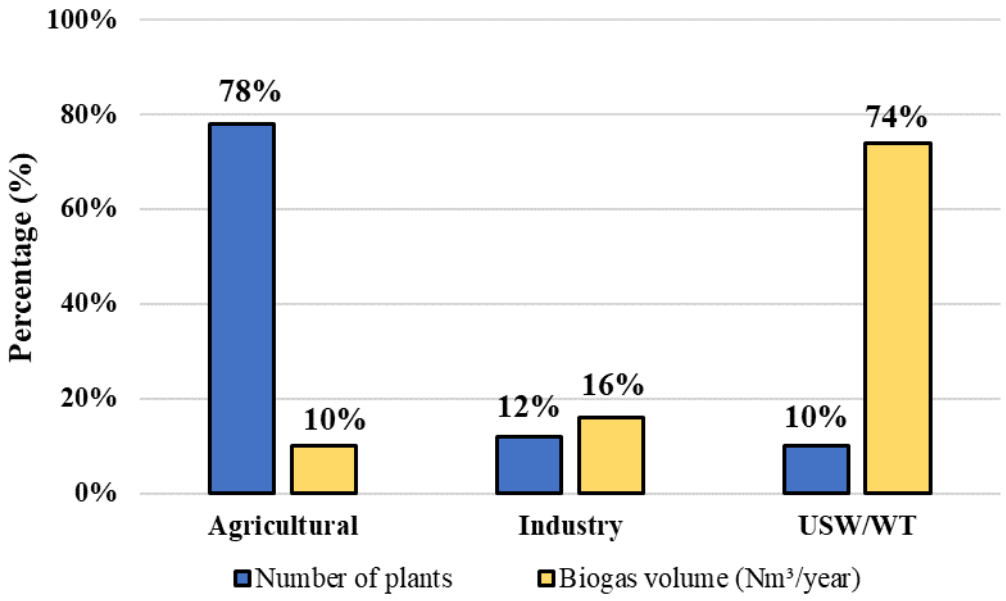

Figure 7 - Relationship between the number of plants and the volume of biogas produced in 2022 distributed by origin of the raw material. Source: CIBiogás (2022).

Table 4 presents the classification of plants divided by application purpose, as well as the percentage distribution for the year 2022. The same report indicates that 97% of total plants have applications for energy purposes (electrical, thermal, and mechanical). Despite the prevalent use of biogas for electricity generation, it can be observed the trend of utilizing biogas for biomethane production has been steadily gaining attention in the national scenario. In 2022, there was a remarkable 82% increase in the number of plants employing biogas purification systems to obtain

biomethane for self-consumption and/or commercial sales, rising from 4 to 20 plants compared to the previous year (2021). The biogas continues to absorb a significant portion of the biogas volume, with 22% of the biogas produced in the country being allocated for this purpose. In this regard, a total of 20 plants were registered as primarily utilizing biogas for biomethane production, with a production capacity of 359.8 million Nm³ per year.

Table 4 - Classification of national plants by energy application. Source: CIBiogás (2020)

Energy Application	**Number of plants**	
Electric energy	763	86.2 %
Thermal energy	96	10.8 %
Mechanical energy	6	0.7 %
Biomethane	20	2.3 %

A similar survey carried out by CIBiogás (2021) indicate the increase of the share of biogas purification for biomethane production in the total volume of biogas increased from 3% to 19% between 2019 and 2020, showing a growth trend for the next decade. In this context, the South, North and Northeast regions of Brazil concentrate the biomethane producing units and, mostly, promote the purification of biogas from the sanitation sector. Plants based in the Southeast region accounted for 313.5 million cubic meters processed in 2020.

The year of 2022 was marked by the ongoing economic recovery post-COVID pandemic and the emergence of the conflict in Ukraine, both of which directly impacted the global energy sector, heightening pressure on the natural gas market even further. The geopolitical conflict had a severe impact on global energy security, resulting in a significant increase in natural gas prices. In Europe, prices surged by up to 50%, while Asian spot prices for liquefied natural gas (LNG) rose by 30%. With the conflict unresolved, expectations are for continued volatility in natural gas prices and the continuous search for energy matrix diversification based on renewable sources. Therefore, the entire supply chain has been affected and resource scarcity has led to increased costs for raw materials and their processing across various sectors, resulting in price impacts and delays in the supply of equipment and inputs. (CIBiogás, 2023).

Despite the scenario described above, there is a clear growing trend in the number of biogas plants within the national territory. In the next coming years, the expectation is to pursuit energy security and mitigate climate changes, strengthening the importance of renewable energy sources for the global and, mainly, national energy matrix. According to the CIBiogás report from 2022, the

biogas operational plants in relation to 2021 was 15%, being slightly lower when compared to the average value recorded over the past 3 years (~ 17 p.y.). In the other hand, the continuous growth in the number of biogas plants in operation, indicates that the biogas market in Brazil continues to expand. Over the last the three years, it has been registered an average of 114 new plants per year. The states of São Paulo and Paraná registered outstanding numbers regarding the rise of operational plants, with a 21% and 18% increase, respectively (CIBiogás, 2022; CIBiogás, 2023).

The temporal evolution of biogas plants in Brazil highlights the emergence of new units and the number accumulated over the years, as illustrated in Figure 8. It is important to highlight that the data demonstrate a very sharp growth trend, especially in the time interval between the years 2017 and 20222. Between 2019 and 2020, the progress was 19% p.y., while between the years 2020 and 2022 it was 16% p.y. The data highlights the points discussed in the previous paragraphs, validating the increased importance of biogas in the national scenario.

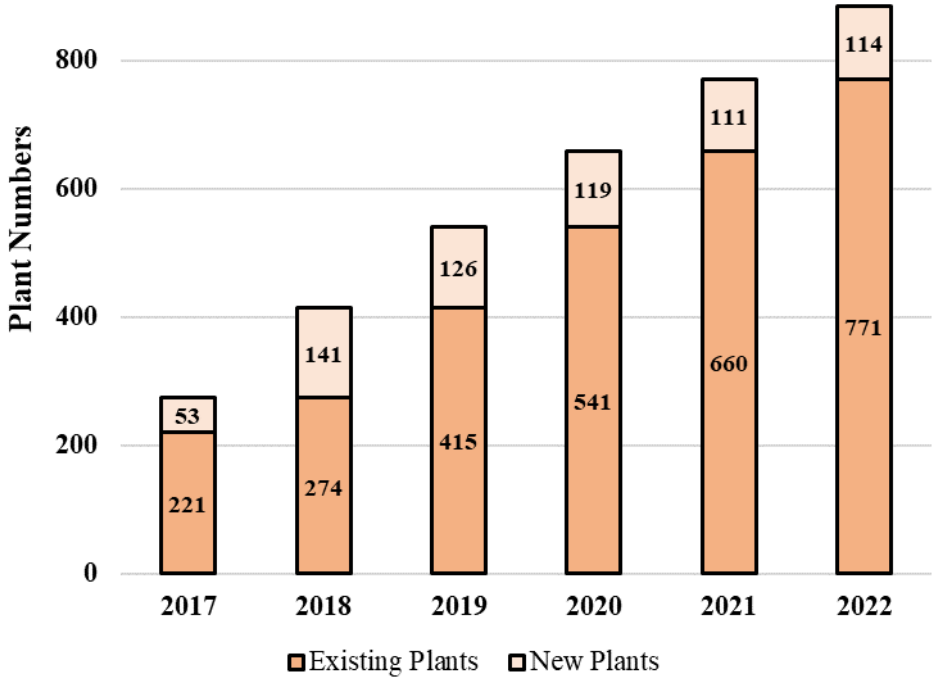

Figure 8 - Growth in the number of biogas plants between 2017 and 2022. Source: CIBiogás (2023).

Considering the geographical location, the Southeast region concentrates the highest number of operational plants (366), as well as the majority of biogas produced, accumulating a total of 1.74 billion Nm^3/year. According to the data from the 2022 report, the 5 states which recorded the highest number of plants are: Minas Gerais (274), Paraná (198), Santa Catarina (82), São Paulo (74), and Goiás (74), accounting for 79% of the total operational plants in the national territory.

In terms of biogas volume for energy purposes, it was found that the state of São Paulo (1.01 billion Nm^3/year) accounts for 35% of biogas production in Brazil. The states of Rio de Janeiro (389.5 MM Nm^3/year) and Minas Gerais (312.7 MM Nm^3/year) rank second and third, respectively. This is due to the presence of large biogas plants in the sanitation sector, mainly in landfills in Rio de Janeiro, and the high number of plants installed in the agricultural sector in Minas Gerais. The states without installed plants remain the same as in 2021, namely the states of Acre, Roraima, Amapá, Piauí, Rio Grande do Norte, and Sergipe. Therefore, there is a window of opportunity to be explored in these states, aiming to bring new business opportunities and renewable energy distribution to the North and Northeast regions.

Considering the scenario outlined, there is a clear trend towards an increase in the number of plants and biogas volume produced within the national territory. The distribution of the plant profile indicates a higher participation of small-scale plants fed by agricultural waste. On the other hand, the largest volume produced is concentrated in large-scale plants at landfills in the Southeast region, probably justified by the higher volume of raw materials generated in the major urban centers.

Additionally, it is observed that a significant portion of the produced biogas is directly employed for energy purposes. However, there has been a continuous towards the utilization of biogas for biomethane purposes between the years 2021 and 2022, indicating the increasing value placed on biogas for the construction of value chains within the chemical industry. Despite a challenging geopolitical and economic context globally, the domestic market remained productive with a high growth rate, indicating the potential to reduce the nation's dependence on petrochemical resources and strengthen the national supply chain. In this way, it is noticeable that biogas can significantly contribute to the Brazilian energy transition, as well as leverage its exploitation as a raw material for the synthesis of chemical intermediates.

.

2.2 - Ammonia

2.2.1 - Ammonia synthesis process

Ammonia represents one of the main compounds produced within the chemical industry, and its process was developed in the early 20th century by the pioneering work of scientists Fritz Haber and Carl Bosch (ANDERSSON *et al*., 2014; CHEEMA *et al*., 2018). This discovery is considered one of the main technological advances of the last century as it allowed the increase in the production of fertilizers and food, enabling and sustaining the growth of the global population (CARVALHO, 2016; PAIXÃO, 2018). The main application of ammonia is as a raw material to produce nitrogen fertilizers, with emphasis on the synthesis of urea. However, its use extends to other fields of industry, in which it is possible to mention the production of nitric acid, a variety of polymers and direct use as a coolant for heat exchange equipment. In addition, the implementation of an ammonia-based economy for the energy sector has been studied, strengthening the idea of a renewable economy (CHEEMA *et al*., 2018).

The synthesis of ammonia occurs by an equilibrium reaction Eq. (1) between nitrogen and hydrogen gases, which is highly exothermic, and generally uses iron catalysts. Recently, the use of ruthenium-based materials has also been explored due to greater catalytic activity and lower operating pressure in the main reactor (ROSSETI *et al*., 2006; TRIPODI *et al*., 2018, YOSHIDA *et al*., 2021). By Le Chatelier's principle, increasing pressure shifts the equilibrium towards the product, while decreasing temperature favors the production of ammonia. However, temperature reduction considerably affects the reaction rate, with the minimum viable temperature being close to 350 ºC (CARVALHO, 2016; ESTURILIO, 2011; MALMALI *et al*., 2016; PAIXÃO, 2018).

$$N_2(g) + 3H_2(g) \leftrightharpoons 2NH_3(g) \qquad \Delta H = -92.4\ kJ\ mol^{-1} \tag{1}$$

In this system, nitrogen gas (from atmospheric air) reacts with hydrogen gas (commonly produced from natural gas) together with the iron catalyst, requiring high ranges of pressure (10 to 25 MPa) and temperature (350 to 550 ºC) to establish favorable conditions for the reaction. Currently, significant amounts of greenhouse gases are emitted by NH_3 production since hydrogen gas is synthesized from fossil sources. Both reactants are fed into the catalytic reactor under stoichiometric conditions (3:1) for optimal operation. Considering the exothermic characteristic, the strategy of reactors with multiple catalytic beds coupled to heat exchangers is used to reduce the inlet temperature of the subsequent bed. The intention is that the release of energy and the rise in temperature during the progress of the reaction does not cause the reactor to operate at thermodynamic equilibrium. Only 20-30% of the synthesized gas is converted to ammonia per pass

within the reaction loop. In this way, the ammonia produced is separated by condensation and cooled down in the output stream, and the gases that do not react are recirculated for reuse (CARVALHO, 2016; PAIXÃO, 2018; TAVARES *et al*., 2013; TRIPODI *et al*., 2018; YOSHIDA *et al.*, 2021). Figure 9 illustrates the flowsheet of the ammonia synthesis process.

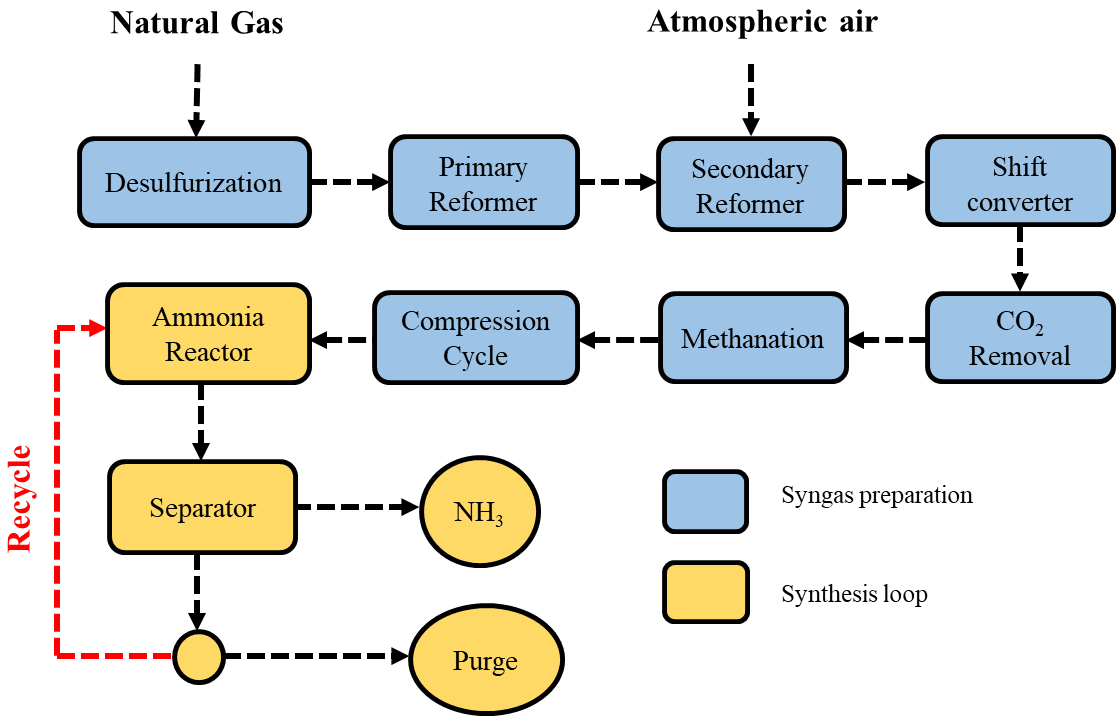

Figure 9 - Simplified flowsheet for ammonia synthesis. Source: Carvalho (2016).

The consolidated ammonia production process consists of the steps of desulfurization, steam reform, shift converter (water-gas shift reaction), CO_2 removal, methanation and synthesis loop/catalytic reactor (CARVALHO, 2016). Natural gas, the main raw material used to produce H_2, must be first purified through the desulfurization process because of the presence of sulfur components (H_2S and mercaptans) which are harmful to the catalysts in the later stages. First, the hydrodesulfurization process (HDS) is carried out using a $CoMo/Al_2O_3$ catalyst, where the output stream is sent for H_2S removal in a ZnO bed (PAIXÃO, 2018; TAVARES *et al*., 2013). Equations (2) and (3) illustrate the characteristic reactions of this process:

$$R - S - H + H_2 \rightarrow R - H + H_2S \quad (2)$$

$$H_2S + ZnO \rightarrow R - ZnS + H_2O \quad (3)$$

At the end of the sulfur elimination step, the purified natural gas is mixed with water vapor (molar ratio between 2.5 and 4 moles of H_2O per mole of C) and heated to a temperature range between 500-600 ºC. This stream is introduced into the primary reformer, where reactions in

Equations (4) and (5) occur (PAIXÃO, 2018). The H_2O/CH_4 ratio must be controlled to avoid deposits of coke on the active surface of the catalyst, causing the active sites to be covered and, consequently, the pores to be blocked.

$$CH_4 + H_2O \leftrightharpoons CO + 3H_2 \qquad \Delta H = +206.0\ kJ\ mol^{-1} \tag{4}$$

$$CO + H_2O \leftrightharpoons CO_2 + H_2 \qquad \Delta H = -41.0\ kJ\ mol^{-1} \tag{5}$$

Considering the endothermic characteristic of the main reaction, Eq. (4), it is necessary to burn fuel to provide constant energy to the primary reformer. At this stage, a nickel catalyst is used, with most of the methane converted and the remainder sent to secondary reform. The outlet temperature of the primary reformer remains in the range between 750 and 820 ºC and this stream is directed to the secondary reform. In this stage, the combustion of the residual methane from the primary reform takes place and atmospheric air is introduced to supply the nitrogen demand of the ammonia synthesis and to supply the necessary oxygen for methane burning. Therefore, in addition to the methane combustion reaction, the secondary reform also promotes the reactions present in the primary reform. The output stream of the secondary reformer presents temperature and pressure ranging between 1000-1100 ºC and 25-35 bar, respectively. In addition, the molar fraction of CO is between 10 and 13%, which is harmful for the catalysts in the later stages, especially for the catalyst used in the synthesis loop (CARVALHO, 2016; TAVARES *et al.*, 2013).

After the reforming stages, the gaseous mixture is sent to the shift stage, conducted in two stages, one at high temperature (HTS) and the other at low temperature (LTS), where reaction in Eq. (5) takes place, since CO_2 is easily removed compared to CO. The favored reaction kinetics are conditions of high pressure and elevated temperatures; however, the equilibrium is unfavored by the exothermic characteristic of the reaction. Thus, the HTS reactor operates at temperatures between 350 and 500 ºC, using a Fe_3O_4 catalyst. This output stream must then be cooled to a temperature range close to 200 ºC and proceed to the LTS, in which the molar concentration of CO is reduced to percentages below 0.2%, having been catalyzed by $CuO/ZnO/Al_2O_3$. After the completion of the two stages of the shift converter, the output stream usually contains a percentage superior to 13% of CO_2 on a molar basis, and its removal is also necessary as it can cause a decrease in the catalyst's performance in the synthesis of ammonia (CARVALHO, 2016; PAIXÃO, 2018 TAVARES *et al*., 2013).

The removal of CO_2 can be done by chemical or physical adsorption, and several types of configurations and adsorbents can be used. The physical absorption processes used are Sulfinol, Rectisol and Selexol. As for chemical absorption systems, it is common to use amine extraction with Monoethanolamine (MEA), Diethanolamine (DEA) and Methyldiethanolamine (MDEA)

solvents. After the CO_2 removal step, the outgoing gaseous stream still has low volumetric concentrations of CO and CO_2 that need to be removed. In fact, the Pressure Swing Adsorption process is currently gaining prominence. This system consists of transferring the adsorbate from the gaseous phase to the surface of an adsorbent material through pressurization and depressurization cycles, and the CO_2 removal step, methanation and the LTS reactor may become unnecessary due to this new configuration. Gas purification and recovery rates depend directly on the plant's production capacity, with fractionation of the components based on the affinity of the gases with the solid contained in the bed (CARVALHO, 2016, KHAN *et al*., 2017).

Finally, the synthesis gas reaches the synthesis section/loop, where reaction in Eq. (1) takes place under conditions of high pressure (100-250 bar) and temperature in the range of 350-500 ºC. Due to the exothermic nature of this reaction, energy integration is essential to optimize plant operation in terms of conversion per pass, flow rate and product purity. Reactor conversion only reaches 20-30%, requiring constant recirculation of unconverted and inert gases (CH_4 and Ar). Ammonia is separated by successive cooling and condensation processes. Due to the recycling of reagents, there must be a purge stream to avoid the concentration of inert gases inside the converter and the drop in the global conversion of the process (CARVALHO, 2016; PAIXÃO, 2018). Figure 10 represents a simplified schematic of the Haber-Bosch cycle.

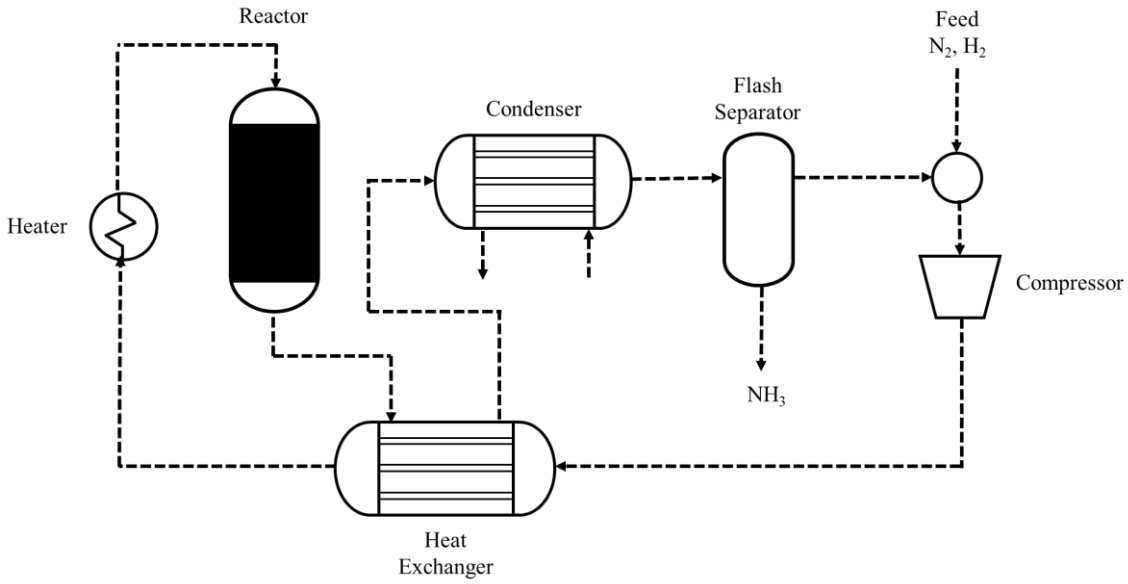

Figure 10 - Simplified schematic of the Haber-Bosch circuit. Source: Reese *et al.* (2016).

2.2.2 - Kinetic models

The first kinetic models studied for the synthesis of ammonia come from the 1930s, with hypotheses being developed from hydrogen and nitrogen under conditions of high temperature and pressure for ferrous catalysts. Under industrial conditions, low temperatures are not able to provide

the necessary energy for high reaction rates. Therefore, high temperatures provide this condition, where the gaseous reaction takes place on the surface of a catalyst (JORQUEIRA, 2018).

For iron catalysts, ammonia synthesis occurs from the individual steps enunciated by the mechanism steps in Equations (6) to (11):

$$N_2 + \Xi \rightleftharpoons 2N\Xi \tag{6}$$

$$H_2 + \Xi \rightleftharpoons 2H\Xi \tag{7}$$

$$N\Xi + H\Xi \rightleftharpoons NH\Xi + \Xi \tag{8}$$

$$NH\Xi + H\Xi \rightleftharpoons NH_2\Xi + \Xi \tag{9}$$

$$NH_2\Xi + H\Xi \rightleftharpoons NH_3\Xi + \Xi \tag{10}$$

$$NH_3\Xi \rightleftharpoons NH_3 + \Xi \tag{11}$$

As can be seen, the reactants are dissociated and adsorbed on the catalyst surface, with the formation of the product and its subsequent desorption. It is worth mentioning that most projects involving the study of kinetic models for ammonia synthesis come from the above mechanism (CARVALHO, 2016). The first efficient kinetic model was proposed by Temkin and Pyzhev (1939), in which the reaction rate described by Eq. (12) depended directly on the partial pressure of hydrogen, nitrogen and ammonia. The expression is defined as the sum of the forward rate r_{dir} and reverse rate r_{rev}:

$$r_{NH_3} = r_{dir} - r_{rev} = k_{dir}\, P_{N_2} \left(\frac{P_{H_2}^3}{P_{NH_3}^2}\right)^{\alpha} - \; k_{rev}\, P_{N_2} \left(\frac{P_{NH_3}^2}{P_{H_2}^3}\right)^{\alpha} \tag{12}$$

$$k_{dir} = 1.78954 \times 10^4 \, e^{\frac{-20800}{(R\,T)}} \tag{13}$$

$$k_{rev} = 2.5714 \times 10^4 \, e^{\frac{-47400}{(R\,T)}} \tag{14}$$

where r_{NH_3} represents the kinetic rate of reaction given in kmolNH_3 m^{-3} h^{-1}, k_{dir} and k_{rev} are, respectively, the forward and reverse rate constants given in kmol m^{-3} h^{-1}, α is a parameter equal to 0.5 for the iron catalyst, P_i the partial pressure of component i in the gaseous mixture (bar), T is the temperature (K) and R is the universal gas constant (1.987 cal mol^{-1} K^{-1}). Eq. (12) has limitations when the partial pressure of ammonia reaches values close to zero, causing numerical singularity for the rate r_{NH_3}. Thus, the kinetic reaction rate equation developed by Temkin and Pyzhev (1939) has restrictions for representing systems with diluted ammonia concentrations (JORQUEIRA, 2018). However, it presents itself as a particularly important work for the evolution of kinetic models for ammonia synthesis and was used by authors such as Araújo and Skogestad (2008),

Angira (2011), Carvalho (2014), Zhang *et al*. (2020) and Zhang *et al*. (2021) to calculate the reaction rate.

After that, Nielsen (1968) proposed a kinetic model based on the chemical activity of the components due to high pressure and temperature conditions. The definition of expressions based on chemical activity contributes to the modeling of gaseous mixtures, being able to quantify the deviation from ideality in operating conditions (TAVARES *et al*, 2020). The reaction rate r_{NH_3}, given in kmolNH_3 m^{-3} h^{-1}, is described by Eq. (15):

$$r_{NH_3} = k_{rev}\left[\frac{\alpha_{N_2} K_a^2 - \frac{\alpha_{NH_3}^2}{\alpha_{H_2}^3}}{\left(1 + K_3 \frac{\alpha_{NH_3}}{\alpha_{H_2}^{1.5}}\right)^2}\right] \tag{15}$$

$$k_{rev} = 7.35 \times 10^{12}\, e^{\frac{-14111}{(R\,T)}} \tag{16}$$

$$K_3 = 3.07 \times 10^{-2}\, e^{\frac{-19361}{(R\,T)}} \tag{17}$$

where k_{rev} is the reverse rate constant (kmol m^{-3} h^{-1}) expressed by Eq. (16), K_a the equilibrium constant, K_3 the adsorption constant represented by Eq. (17), α_i corresponds to the chemical activity of each component of the gas mixture (dimensionless), T is the temperature (K) and R is the universal gas constant (1.987 cal K^{-1} mol^{-1}). Nielsen's model (1968) was used in the work by Moura *et al*. (2021), as well as the Aspen Plus model plant for simulating the ammonia plant (ASPEN TECH, 2008a).

Furthermore, in the same year of 1968, Dyson and Simon (1968) also proposed a pseudo-homogeneous kinetic model based on the chemical activity of the components represented by Eq. (18), suggesting the modification and extension of the expression initially developed by Temkin and Pyzhev (1939):

$$r_{NH_3} = 2\, k_{rev}\left[K_a^2\, \alpha_{N_2}\left(\frac{\alpha_{H_2}^3}{\alpha_{NH_3}^2}\right)^{\alpha} - \left(\frac{\alpha_{NH_3}^2}{\alpha_{H_2}^3}\right)^{1-\alpha}\right] \tag{18}$$

$$k_{rev} = 8.849 \times 10^{14}\, e^{\frac{-40765}{(R\,T)}} \tag{19}$$

where r_{NH_3} represents the kinetic rate of reaction given in kmolNH_3 m^{-3} h^{-1}, k_{rev} is the reverse rate constant (kmol m^{-3} h^{-1}) expressed by Eq. (19), K_a the equilibrium constant, α_i corresponds to the chemical activity of each component of the gaseous mixture (dimensionless), T is the temperature (K) and R is the universal gas constant (1.987 cal K^{-1} mol^{-1}) and α corresponds to a model parameter with value of 0.5 or 0.75. It is worth pointing out that the kinetic model developed by Dyson and

Simon (1968) is widely used in the literature of recent works to calculate the reaction rate of ammonia synthesis using iron catalysts (AZARHOOSH *et al*., 2014; CARVALHO, 2016; CHEEMA *et al*. al., 2018; ESTURILIO, 2011; TRIPODI *et al*., 2018; YOSHIDA *et al*., 2021).

New ruthenium-based catalysts have been studied due to the productivity gain compared to traditional iron catalysts. The reasons are the inhibition of iron catalysts by the presence of ammonia, which directly affects the conversion of the process to values below the conversion in the thermodynamic equilibrium condition (ROSSETI *et al*., 2006; TRIPODI *et al*., 2018; YOSHIDA *et al*., 2021).

Within this context, Rosseti *et al.* (2006) developed a kinetic model for ruthenium catalysts supported on activated carbon (Ru/C), using the ammonia synthesis reaction under industrial operating conditions (T = 370-460 ºC, P = 50-100 bar). The proposal for the reaction rate was developed through the Langmuir-Hinshelwood-Hougen-Watson (LHHW) approach for heterogeneous reactions, obtaining a good representation of the experimental data. Initially, the authors used a modification of the expression by Temkin and Pyzhev (1939), performing the addition of adsorption terms for hydrogen and ammonia. Tripodi *et al*. (2018) and Yoshida *et al.* (2021) used Eq. (20) to carry out studies related to the simulation of ammonia reactors combining the presence of fixed beds containing iron and ruthenium-based catalysts:

$$r_{NH_3} = k_{dir}\left[\frac{\left(\alpha_{N_2}\right)^{0.5}\left[\frac{\left(\alpha_{H_2}\right)^{0.375}}{\left(\alpha_{NH_3}\right)^{0.25}}\right] - \frac{1}{K_a}\left[\frac{\left(\alpha_{NH_3}\right)^{0.75}}{\left(\alpha_{H_2}\right)^{1.125}}\right]}{1 + K_{H_2}\left(\alpha_{H_2}\right)^{0.3} + K_{NH_3}\left(\alpha_{NH_2}\right)^{0.2}}\right] \tag{20}$$

$$k_{dir} = 9.02 \times 10^8 \, e^{\frac{-23000}{(R\,T)}} \tag{21}$$

$$\log_e K_{H_2} = -\frac{56.9024}{R} + \frac{37656}{R\,T} \tag{22}$$

$$\log_e K_{NH_3} = -\frac{34.7272}{R} + \frac{29228}{R\,T} \tag{23}$$

where r_{NH_3} is the kinetic rate of reaction given in kmolNH_3 m^{-3} h^{-1}, k_{dir} the direct rate constant (kmol m^{-3} h^{-1}) expressed by Eq. (21), K_{H_2} e K_{NH_3} represent, respectively, the adsorption constant of hydrogen and ammonia by Eq. (22) and (23), α_i corresponds to the chemical activity of each component of the gaseous mixture (dimensionless), T is the temperature (K) and R is the universal gas constant (8.314 J mol^{-1} K^{-1}). For all mentioned models, the equilibrium constant K_a is calculated from the work of Gillespie and Beatie (1930) by Eq. (24) where T represents the temperature of the

system (K). In addition, the activity of the components can be obtained from the relationship with fugacity according to Equations (25) and (26):

$$log_{10}K_a = -2.691122\ log_{10}(T) - 5.519265 \times 10^{-5}\,T + 1.848863 \times 10^{-7}T^2 + \frac{2001.6}{T} + 2.6899 \quad (24)$$

$$\alpha_i = f_i/f_i^0 \quad (25)$$

$$\alpha_i = y_i\,\phi_i\,P \quad (26)$$

where α_i represents the chemical activity of each component, f_i the fugacity of each compound in the gaseous mixture, f_i^0corresponds to the fugacity of each pure compound in the defined standard condition (pressure of 1 atm and temperature of the system), y_i symbolizes the mole fraction of each component in the gaseous phase, ϕ_i the fugacity coefficient of each component and P the system pressure. The fugacity coefficient (ϕ_i) for hydrogen is determined according to the works by Cooper (1967) and Shaw *et al*. (1964), while the fugacity coefficients of nitrogen and ammonia are calculated according to the equations developed by Cooper (1967) and Newton (1935):

$$\phi_i = A + B\,T + C\,P - D\,T^2 + E\,P^2 \quad (27)$$

$$\phi_j = exp\{exp[(-A\,T^{0.125} + B)]\,P - P^2\,exp[-(C\,T^{0.5} + D)] + 300\,exp\left(\frac{-P}{300}\right)exp[-(E\,T + F)]\} \quad (28)$$

where i is related to the components N_2 and NH_3, while j is related to the compound H_2; T is the system temperature (K) and P corresponds to the pressure (atm). Table 5 summarizes the values obtained for the fugacity coefficient parameters.

Table 5 -Values for fugacity coefficients for ammonia synthesis. Source: Jorqueira, 2018

Coefficient	N_2	H_2	NH_3
A	9.3431737×10^{-1}	- 3.8402	1.438996×10^{1}
B	2.0285380×10^{-4}	5.41×10^{-1}	2.285380×10^{-3}
C	2.9589600×10^{-4}	-1.263×10^{-1}	-4.4876720×10^{-4}
D	-2.7072700×10^{-7}	-1.598×10^{1}	-1.1429450×10^{-6}
E	4.7752070×10^{-7}	-1.1901×10^{-3}	2.7612160×10^{-7}
F[a]	-	-5.941	-

2.2.3 - Modeling and simulation of ammonia synthesis processes

The ammonia production process is based on the classic Haber-Bosch method, using natural gas as the main material to generate hydrogen gas. Furthermore, ammonia synthesis can also occur through partial oxidation of heavy oils and coal gasification (CHEEMA *et al*., 2018; TAVARES *et al*., 2013). Usually, ammonia plants have a large production capacity, exceeding 500 tons/day to supply demand (ARORA *et al*., 2016). Therefore, given the need to generate hydrogen from fossil fuels, the ammonia industry contributes to the emission of high amounts of greenhouse gases. Within this context, challenges have been proposed to stimulate the establishment of new processes based on renewable technologies (REESE *et al*., 2016).

Arora *et al.* (2016) developed a techno-economic study to evaluate small-scale plants for ammonia production based on the Leading Concept Ammonia (LCA) methodology, using biomass as a supply. Initially, the biomass gasification process was implemented to generate synthesis gas using air as an oxidizing agent. The main stages of this project are primary reformer under mild conditions, gas heated reformer, isothermal shift reactor (RSI), PSA units for gas purification and synthesis loop under pressure conditions lower than the conventional large-scale process. Implementing the PSA and RSI system makes the process less susceptible to catalyst performance and plant disturbances. Therefore, it is expected that the changes with the use of the LCA methodology will allow small-scale plants to compete with higher capacity plants (ARORA *et al*., 2016; CARVALHO, 2016). The published work considers a production capacity of 65 tons/day of ammonia, calculating a selling price of \$1153/ton NH_3. For the conditions established for this study, The values obtained for the ammonia's sale price based on LCA methodology are much higher than market conditions, which highlights the loss of competitiveness for the conventional process.

Andersson and Lundgren (2014) proposed the synthesis of ammonia from the biomass supply resulting from the pulp and paper industry. The main goal of the study was to carry out a techno-economic evaluation of the ammonia production integrated into the biomass gasification system from the pulp and paper industry. The authors observed that the performance of the integrated process in terms of energy and economics is superior when compared to individual processes. However, they also concluded that the ammonia produced from biomass gasification needs to be sold at a price higher than market conditions for the system to be economically viable.

Following a similar line of research, Paixão (2018) also developed work exploring municipal solid waste (MSW) gasification for energy generation and ammonia synthesis, performing retro-techno-economic analysis (RTEA) for a small-scale plant project dimensioned for a city with a population size of 100,000 inhabitants with the capacity to produce 21.25 NH_3 ton/day. As well as for Aurora *et al*. (2016), the LCA methodology was used to define and dimension the equipment.

For the initially projected plant, the selling price of ammonia for a zero Net Present Value (NPV) was US$ 2,262.30/ton, well above the market price practiced. However, it was found that for a population range between 550,000 and 1.5 million inhabitants, the selling price of ammonia becomes competitive under market conditions.

The synthesis loop is the main step in the ammonia production process, as it operates under severe pressure and temperature conditions, in addition to low conversion per pass, which is characteristic of the ammonia synthesis reaction. Therefore, in practice, any improvement in the degree of conversion directly affects the economic and operational performance of the plant, highlighting the need for accurate modeling of the reactor (AZARHOOSH *et al.*, 2014). Azarhoosh *et al*. (2014) proposed the mathematical modeling of a one-dimensional heterogeneous reactor, in steady state, to simulate the horizontal flow for the ammonia synthesis. The authors considered two cases: the first had the presence of intermediate heat exchangers between the beds, while the second scenario evaluated the quench of the fed load to favor the reactor temperature control. The authors determined the ideal conditions for the mass flow of ammonia based on the implementation of the genetic algorithm for optimization, using the inlet temperature, total feed flow and operating pressure as adjustment parameters.

Carvalho (2016) simulated the synthesis loop based on rigorous modeling of the reactor, considering thermal exchanges and integration between streams present inside the equipment. The model calibration was carried out based on the availability of industrial data, evaluating the influence of the main process variables, and analyzing the best operating conditions. The reactor model was developed in steady state, pseudo-homogeneous and one-dimensional in the radial direction, considering the effects of radial dispersion of mass and heat. For the reaction rate, the expressions from Nielsen (1968) and Dyson and Simon (1968) were tested, with the second being chosen for the sequence of the work.

The integration of large-scale processes can result in a series of technological and economic benefits for the chemical industry, stimulating the search for new solutions which can promote sustainable development, intelligent use of available resources and the concern associated with environmental issues (ANDERSSON, 2014; SERRANO *et al.*, 2012; MORONE *et al*., 2015). In the conventional process for producing ammonia from natural gas, hydrogen gas is synthesized from the primary and secondary reformers. The idealization of alternative systems has the objective of reducing dependence on fossil fuels and, therefore, fitting into this context is the generation of hydrogen through the gasification of biomass. Furthermore, the production of hydrogen through the electrolysis of water is also a possibility. The University of Minnesota (USA) has a pilot plant to produce ammonia using wind energy as an energy source and the use of electrolysis technology to obtain hydrogen. Economically, the small-scale plant is still not a competitive option compared to

the conventional process due to the seasonality and availability of wind energy and the connection to the local electrical grid is necessary (CARVALHO, 2016; REESE *et al.*, 2016). Despite the environmental advantages, this route still presents high production costs. According to the report "The green hydrogen economy: Predicting the decarbonisation agenda of tomorrow" elaborated by the consultancy Pwc (s.d), green hydrogen production from power electrolysis varies from €3 to €8/kg. The biggest challenges of this production route are the high electricity costs, being a process that demands a lot of energy and water, and the high investment in electrolyzers.

Reese *et al*. (2016) proposed the study of a small ammonia production plant powered by wind energy, boosting the PSA unit for the separation of N_2 from atmospheric air and the generation of hydrogen from the water electrolysis process, characterizing a system power-to-ammonia. They are combined with the small-scale continuous Haber-Bosch cycle to obtain ammonia. Cheema *et al*. (2018) also explored the analysis of the operational flexibility of the Haber-Bosch process in steady state using self-thermal reactors in the design of a power-to-ammonia system. The authors concluded that the self-thermal reactor is viable for process operation, being able to work in different ranges of operating conditions while maintaining stable ammonia synthesis.

In addition to traditional ferrous catalysts, new ruthenium-based materials have been studied to promote an increase in catalytic activity and a decrease in operational conditions related to the synthesis loop. There are already industrial applications using Ru catalysts supported by activated carbon through the process called Kellog's Advanced Ammonia Process (KAAP), present in a total of 7 plants and with a production capacity of 2000 tons NH_3/day (TRIPODI *et al*., 2018; YOSHIDA *et al.*, 2021). Tripodi *et al*. (2018) developed a work for the synthesis of ammonia proposing the combination of iron and ruthenium catalysts based on validated kinetic models and based on experimental conditions. The authors carried out studies to optimize the ammonia synthesis loop and the refrigeration cycle based on different possible configurations for iron and ruthenium catalysts, aiming at increasing productivity, lowering operating and installation costs of the production process. Yoshida *et al*. (2021) also analyzed the synthesis of ammonia considering the possible combination between iron and ruthenium catalysts. The Aspen Plus software was used to simulate the synthesis section and the separation processes based on a production capacity ranging from 0.1 to 500 tons NH_3 per day. The authors detailed the composition of costs and investments for small, medium, and large-scale plants considering the different catalysts (Fe and Ru), highlighting that the price of the catalyst is not dominant in any project scale. The study included sizes of 10, 100 and 500 tonNH_3/day considering different combinations of conditions and catalysts. Naturally, the investment data obtained for larger plants (medium and large) recorded values in the order of 50 and 200 MM$, respectively. Naturally, investment data obtained for larger plants (medium and large) recorded values in the order of 50 and 200 MM$, respectively.

2.3 - Urea

2.3.1 - General aspects

Urea (NH_2CONH_2) is characterized as one of the main compounds produced in the chemical industry. Considering the continuous increase in the world population, the agricultural and fertilizer demand is increasing to guarantee the global supply, with 80% of the urea produced being directly applied as fertilizer. Among all marketed nitrogen fertilizer, urea has the highest nitrogen composition. The existence of consolidated technologies, the ease of application in the soil and the high nitrogen content are relevant factors in establishing urea as the most used compound. In addition, it has an application of a stabilizer in nitrocellulose explosives, additive for dyes in the textile industry, plastics manufacturing, among other purposes, can be highlighted (CHINDA, 2015; EDRISI *et al*., 2016; ZAHID *et al*., 2014; ZHANG *et al,* 2021).

Urea is produced on an industrial scale by the reaction between ammonia and carbon dioxide at high pressures (100-150 bar) and temperatures (170-200 ºC). There are different types of processes for urea synthesis in industrial plants, with total recycling systems being the most used due to operational flexibility and energy efficiency. The Stamicarbon (STAC) and Snamprogetti (SNAM) processes are among the main licensors of the technology in commercial units (HAMIDIPOUR *et al*., 2005; ZAHID *et al*., 2014).

The urea synthesis reaction can be divided into two main steps. The first stage consists of the reaction in Eq. (29) between ammonia and carbon dioxide to form ammonium carbamate (NH_2COONH_4), with a rapid, exothermic, and heterogeneous transformation. The second corresponds to reaction in Eq. (30) of ammonium carbamate dehydration in urea and water, being a slow, endothermic step that occurs only in the liquid phase. In addition, its performance is limited by thermodynamic equilibrium. The overall conversion reaction is exothermic, with the first reaction providing heat to the second through the release of energy (KOOHESTANIAN *et al.*, 2018; RASHEED, 2011; ZAHID *et al*., 2014).

$$2NH_{3\,(g)} + CO_{2\,(g)} \leftrightharpoons NH_2COONH_{4\,(l)} \qquad \Delta H = -38\ kcal\ mol^{-1} \tag{29}$$

$$NH_2COONH_{4\,(l)} \leftrightharpoons CO(NH_2)_{2\,(l)} + H_2O_{\,(l)} \qquad \Delta H = +7.7\ kcal\ mol^{-1} \tag{30}$$

Furthermore, urea can be decomposed to biuret and ammonia at atmospheric pressure and at its melting point. This reaction is slow and endothermic and, therefore, biuret formation occurs at high urea concentrations, low ammonia concentrations, long residence times and high temperatures. As shown by Eq. (31), urea biuret is synthesized from the combination of two urea molecules, releasing an ammonia molecule. This compound is considered a by-product of urea synthesis, and

minimizing its formation is one of the biggest challenges in the production process (CHINDA, 2015; HAMIDIPOUR *et al*., 2005).

$$2CO(NH_2)_{2\,(l)} \rightleftharpoons NH_2CONHCONH_{2\,(l)} + NH_{3\,(l)} \qquad \Delta H = +20.3\ kcal\ mol^{-1} \tag{31}$$

2.3.2 - Stamicarbon process (STAC)

The Stamicarbon (STAC) process can be divided into 5 main blocks: Synthesis, Evaporation, Desorption and Hydrolysis, Recirculation, and Pearling/Granulation. Among all the stages, the synthesis section stands out as the most important, as it is where the formation of ammonium carbamate and, consequently, urea. The other stages of the production process are responsible for the recirculation of non-converted reagents and the purification of the product.

The synthesis section consists of 4 pieces of equipment: condenser (pool condenser), reactor, scrubber, and high-pressure stripper. The carbamate condenser process is relatively new, with its commercialization and implementation in industrial projects dating back to 1994 by the licensing company Stamicarbon (CHINDA, 2015). Figure 11 illustrates the synthesis section of the Stamicarbon process for urea production.

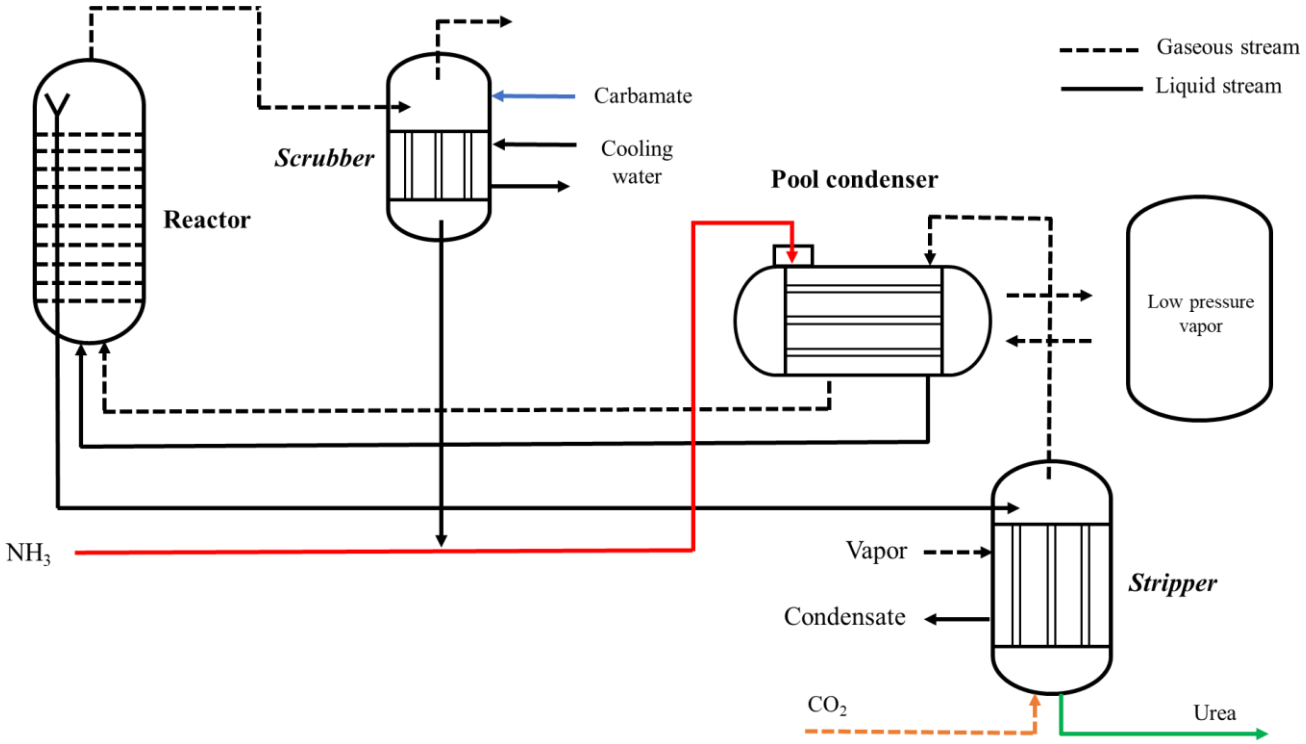

Figure 11 - Stamicarbon process synthesis cycle. Source: Chinda (2015).

During the next paragraphs, the equipment and streams used in the STAC process will be detailed. Therefore, it should be noted that liquid and gaseous streams will be represented by solid and dashed lines, respectively. Furthermore, the color scheme will also be maintained to represent the reactants (NH_3, CO_2 and ammonium carbamate) and products of the system, facilitating the understanding of two-phase operation.

As it can be seen in Figure 12, carbon dioxide is fed to the high-pressure stripper in countercurrent, together with the liquid stream coming from the reactor. This equipment is characterized by a shell-tube heat exchanger, in which the partial pressure of ammonia in the liquid phase is reduced and the carbamate is decomposed. The outlet stream from the top of the stripper contains unconverted NH_3 and CO_2 vapors, while the bottom stream composed of urea, biuret and water is directed to a single recirculation stage at low pressure (4 bar), where occurs urea's concentration and purification. The gas that flows from the top of the equipment is destined for the carbamate condenser (CHINDA, 2015; HAMIDIPOUR *et al.*, 2005).

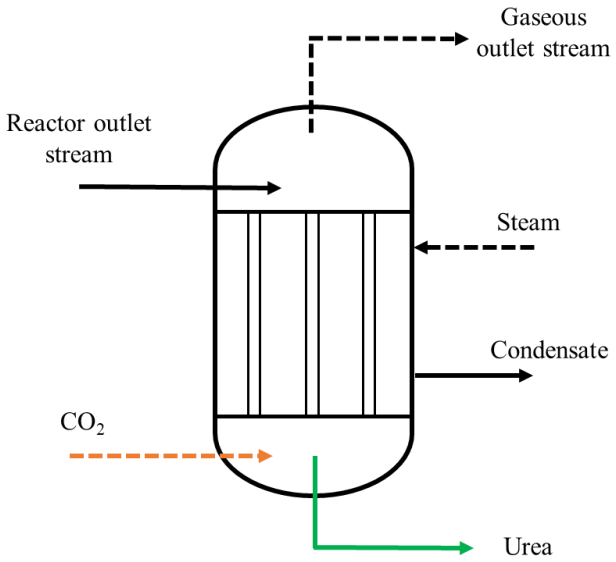

Figure 12 - Schematic illustration of the high-pressure stripper. Source: Chinda (2015).

Like the stripper, the carbamate condenser also consists of a shell-tube heat exchanger (Figure 13). In this step, a portion of the gases coming from the stripper is condensed and the heat from the condensation can be used to generate low pressure steam. The ammonia and carbon dioxide that is fed and condensed is responsible for the formation of the carbamate. More, it participates directly in the synthesis of urea within the STAC unit, helping the reactor in the formation of the product The carbamate condenser generates two streams: liquid and gas. The gaseous stream is made up of the unconverted gases and the liquid stream contains ammonium carbamate, urea, and water. Both streams are directed to the bottom of the reactor (CHINDA, 2015; HAMIDIPOUR *et al.*, 2005).

The reactor operates at high pressure to ensure high conversion per pass, with the effluent sent to the stripper as shown in Figure 14. The equipment has internal trays to optimize contact between the liquid and gaseous phases, with the main goal to ensure that the process fluid has a homogeneous behavior. As the reactants rise inside the reactor, ammonium carbamate is produced. This reaction releases energy so that the same carbamate undergoes a dehydration reaction, forming urea and water. The temperature profile in the reactor gradually increases as the reagents flow upwards, and the internal temperature variation in the reactor usually does not exceed 30°C

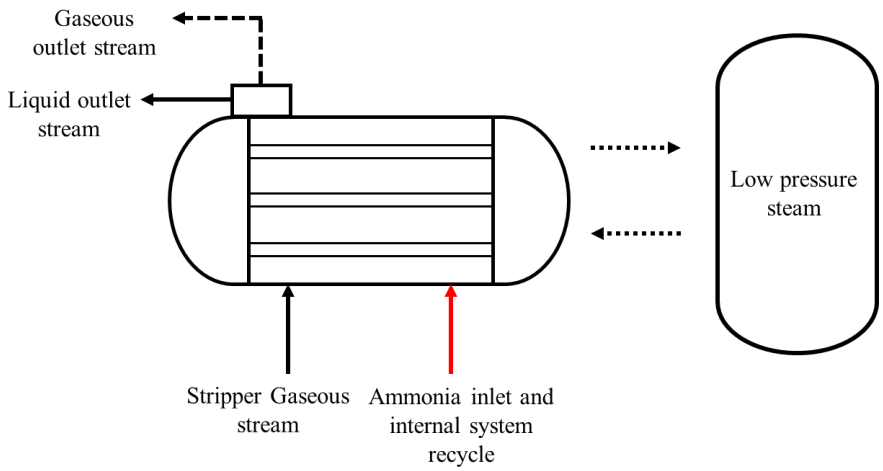

Figure 13 - Schematic illustration of the carbamate condenser. Source: Chinda (2015).

The main justification is given by the constant consumption of energy by dehydration of ammonium carbamate in the generation of urea, as well as preventing the synthesis of biuret from being significant within this system and, consequently, keeping under control the generation of by-products. In this way, the reaction proceeds as the streams meet each stage, and at the top of the reactor there is the exit of a liquid stream containing urea, ammonium carbamate and water and a gaseous stream composed of ammonia and non-carbon dioxide converted. The first is routed to the high-pressure stripper and the second is routed to the scrubber. The residence time usually varies between 20 and 40 minutes due to the slow characteristic of the urea synthesis reaction in the liquid phase (BROUWER, 2009a; CHINDA, 2015; DENTE *et al*., 1992; HAMIDIPOUR *et al*., 2005).

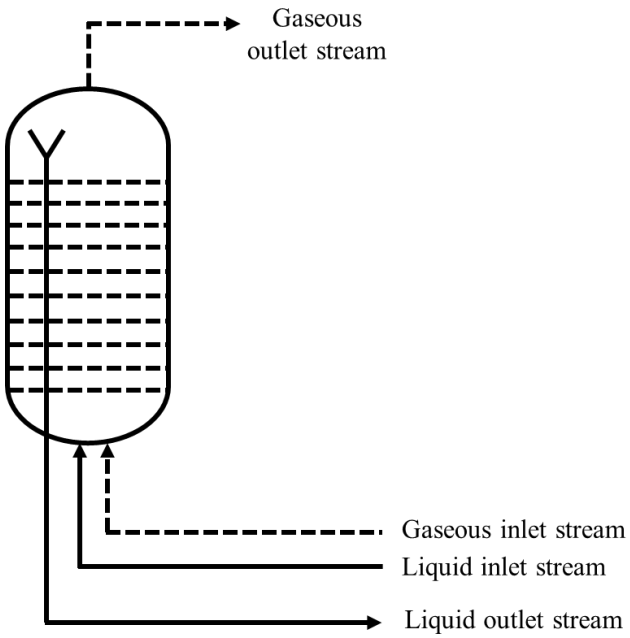

Figure 14 - Schematic illustration of the synthesis reactor. Source: Chinda (2015).

The gaseous stream sent to the scrubber condenses the unconverted vapors and, consequently, there is carbamate synthesis according to Figure 15. Therefore, countercurrent feeding of the carbamate solution from the recirculation section is necessary, and on the shell side there is the presence of water to remove the heat generated by the reaction between NH_3 and CO_2. The carbamate solution is led to the pool condenser together with the ammonia introduced in the process, both being mixed by an ejector before entering the equipment (CHINDA, 2015; HAMIDIPOUR *et al.*, 2005).

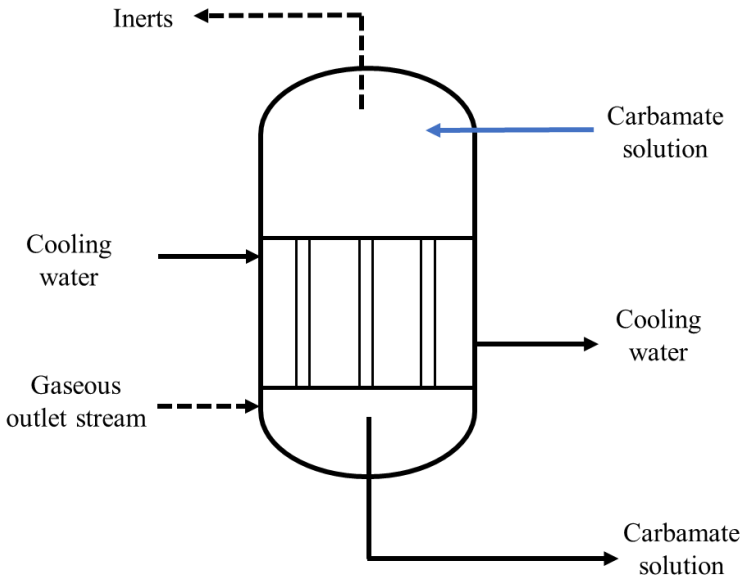

Figure 15 - Schematic illustration of the scrubber Source: Chinda (2015).

2.3.3 - Modeling and simulation of urea synthesis

Despite representing an industrially established technological process, only a few works have been developed to perform the modeling and simulation of the urea synthesis process. Dente *et al*. (1988) aimed to create a simulator for the high-pressure section of urea plants according to the Snamprogetti and Stamicarbon processes. The results indicated robustness and versatility for calculations involving mass and energy balances in the industrial operation range of the process. In addition, the thermodynamic approach considering an electrolytic model for the NH_3-CO_2-H_2O-urea system and the modeling of the equipment showed good convergence with the industrial data available for comparison. Subsequently, the same working group progressed the studies (DENTE *et al*., 1992) detailing the modeling of a gas-liquid reactor for urea synthesis, highlighting the thermodynamic approach for the equilibrium of phases, the fluid dynamic equations and the kinetic model. The authors mentioned average error data for the reactor outlet temperature and conversion being less than 2% for both variables mentioned above.

Isla *et al*. (1993) proposed the simulation of a urea reactor based on the thermodynamic modeling of the NH_3-CO_2-H_2O-urea system. The work was carried out in partnership with the PETROSUR fertilizer factory, located in Argentina, being able to predict the behavior of the system for a wide range of operating conditions. The main objective of the work was the estimation of thermodynamic parameters of the NH_3-CO_2-H_2O and NH_3-CO_2-H_2O-urea systems, in which the results were capable of predicting, satisfactorily, the vapor pressure of the system and the conversion of CO_2 to urea of according to the available experimental data of the plant.

Abensur (1996) was one of the pioneers in the study of the urea synthesis reactor in Brazil. The author used operational data from the Nitrogen Fertilizers Factory (FAFEN) - Bahia, located at the Camaçari unit (Petrobras). The main stages of the work involved the determination of the mathematical model, execution of the simulation, parameter estimation and optimization of the synthesis section using the FORTRAN 77 programming language. During the work, the biuret generation was evaluated. However, it is concluded that the production rate of the by-product was not significant enough to be considered in the continuation of the study. Table 6 presents the average percentage error obtained between the real and simulated data for the mass fractions in the liquid stream leaving the reactor.

The values remained in a range of values lower than 10%, evidencing an efficient prediction from the proposed mathematical model. The author proposed the modeling of the urea reaction kinetics from industrial data, evidenced by Eq. (32) and (33) a parameter adjustment from an elementary power law model:

Table 6 - Mean error calculated for net current out of the reactor. Source: Abensur, 1996

Validation parameter	Mean error (%)
MF[a] CO_2	9.8
MF[a] NH_3	9.7
MF[a] H_2O	3.5
MF[a] Urea	5.0

[a] MF: Mass fraction

Carbamate synthesis $$r_1 = 7.3x10^{-5}\ C_{NH_3}^2 C_{CO_2} \quad (32)$$

Urea synthesis $$r_2 = 0.1\ C_{CARB} \quad (33)$$

where r_1 represents the reaction rate for carbamate formation (mol L^{-1} min^{-1}), C_{NH_3} the ammonia concentration (mol L^{-1}), C_{CO_2} the carbon dioxide concentration (mol L^{-1}), r_2 the reaction rate for the formation of urea (mol L^{-1} min^{-1}) and C_{CARB} the concentration of ammonium carbamate (mol L^{-1}).

Hamidipour *et al.* (2005) proposed the synthesis section modeling of an industrial urea plant, in which the reactor was divided into a series of CSTRs (continuously stirred tank reactors) to represent the equipment's hydrodynamics. The formation of ammonium carbamate was performed by a heterogeneous reaction between ammonia and carbon dioxide, as well as the presence of biuret as a by-product of urea synthesis. The authors compared results obtained from the simulation with real data from the plant for key variables in the process operation, confirming the good representation of the model. Table 7 represents the values obtained for the validation parameters, as well as the average calculated error. However, unlike the Stamicarbon process, in the authors' work the fresh stream of ammonia was fed directly into the main reactor. The conversion obtained for the process was close to 60%, using 10 CSTR reactors to represent the total volume of the reactor.

Table 7 - Comparison between plant and simulated data. Source: Hamidipour *et al*. (2005)

Validation parameter	Plant data	Simulation data	Mean error (%)
Inlet temperature reactor (ºC)	169.3	169.5	-0.1
Outlet temperature reactor (ºC)	183	182.5	0.3
MF urea inside liquid outlet stream (%) [a]	33.9	33.0	2.7
N/C ratio in reactor outlet	2.9	3.1	-6.9

[a] MF: mass fraction

Zhang *et al*. (2005) also carried out the modeling and optimization of the synthesis section of the urea process. The authors proposed the description of the vapor-liquid equilibrium (VLE) of the NH_3-CO_2-H_2O-urea system from the extended electrolytic UNIQUAC equation to characterize the deviation from ideality of the liquid phase. The synthesis section was based on an 8-stage equilibrium model, obtaining satisfactory results compared to industrial data with a conversion close to 60%. This work did not consider the formation of biuret inside the reactor.

Rasheed (2011) investigated the increase in the productive capacity of the company Agritech Limited, headquartered in Pakistan, from the urea synthesis reactor, as well as the change of technology previously used in the plant to the Stamicarbon process. The work was developed using the *Aspen Plus* simulator and the proposed model was validated with data from the existing plant. The author carried out a series of simulations to investigate the effects of the N/C molar ratio, temperature, and pressure on the conversion of CO_2 and urea mass fraction in the liquid phase. The results showed good accuracy for composition of the liquid phase of the reactor (average errors below 5%), however, the gaseous phase presented higher deviation (greater than 15%). Furthermore, the author also did not consider the formation of biuret as a by-product of urea synthesis. The kinetics used by the author was obtained from the adjustment of industrial data through a power law model, as well as Abensur (1996), indicated by Equations (34) and (35):

Carbamate synthesis

$$r_1 = 1628 \exp\left(\frac{-62802}{R\,T}\right) C_{NH_3}^{1.4} C_{CO_2}^{-0.4} \tag{34}$$

Urea synthesis

$$r_2 = 12000 \exp\left(\frac{-62802}{R\,T}\right) C_{CARB}^{0.92} \tag{35}$$

where r_1 represents the reaction rate for carbamate formation (kmol m^{-3} s^{-1}), C_{NH_3} the ammonia concentration (kmol m^{-3}), C_{CO_2} the carbon dioxide concentration (kmol m^{-3}), r_2 the reaction rate for the formation of urea (kmol m^{-3} s^{-1}) and C_{CARB} the concentration of ammonium carbamate (kmol m^{-3}), T symbolizes the temperature (K) and R a universal gas constant (J mol^{-1} K^{-1}).

Zendehboudi *et al*. (2014) worked on the modeling and optimization of a urea reactor based on data from the Shiraz Petrochemical Company, operating using Stamicarbon technology. The authors proposed a comparison between a phenomenological mathematical model and an artificial neural network (ANN) to simulate the plant. As well as Hamidipour *et al*. (2005) and Rasheed (2011), the reactor was modeled considering a series of CSTRs to predict the hydrodynamic non-ideality present in the equipment due to operating conditions. The results of mathematical simulation and neural network prediction compared with industrial data showed good accuracy for the components mass flow rate, urea conversion and temperature variables. Furthermore, the authors concluded that the neural network was more accurate and effective than the proposed mathematical

modeling. The average percentage errors obtained for composition were close to 2.3 and 9.4% for neural network and mathematical modeling, respectively. It is important to highlight that the authors considered the generation of biuret as Hamidipour *et al.* (2005).

Chinda (2015) carried out the modeling and simulation of the synthesis section of a urea plant using Stamicarbon technology and implementation in *Aspen Plus* software for the work of his master's thesis. For the validation stage of the process, industrial data provided by Nitrogen Fertilizers Factory (FAFEN – Paraná/Brazil) were used to evaluate the average percentage error in relation to the data generated by the mathematical model chosen to represent the system. It was verified that the mean deviations for mass compositions and other variables were lower than 6 and 8%, respectively, considering the validation data. The main contribution of Chinda's work (2015) was the analysis and identification of the most influential process parameters for the formation of biuret as the main by-product and contaminant of nitrogen fertilizer in the Synthesis section. Chinda (2015) employed the same strategy used by Abensur (1996) and Rasheed (2011) to adjust the reaction kinetics highlighted from Equations (36) and (37):

Carbamate synthesis $$r_1 = 1628 \exp\left(\frac{-62802}{R\,T}\right) C_{NH_3}^{0.4} C_{CO_2}^{-0.11} \quad (36)$$

Urea synthesis $$r_2 = 12000 \exp\left(\frac{-62802}{R\,T}\right) C_{CARB}^{0.39} \quad (37)$$

where r_1 represents the reaction rate for carbamate formation (kmol m^{-3} s^{-1}), C_{NH_3} the ammonia concentration (kmol m^{-3}), C_{CO_2} the carbon dioxide concentration (kmol m^{-3}), r_2 the reaction rate for the formation of urea (kmol m^{-3} s^{-1}) and C_{CARB} the concentration of ammonium carbamate (kmol m^{-3}), T symbolizes the temperature (K) and R a universal gas constant (J mol^{-1} K^{-1}). As for her doctoral thesis, Chinda (2019) continued her line of research already developed during the master's degree, however the main objective was to carry out the economic, sustainability and life cycle analysis considering the entire urea synthesis plant. The author highlights the lack of availability of industrial data in the open literature, and the non-disclosure of relevant process parameters in some works which do not include industrial data make it difficult to reproduce the results for simulation of other industrial units.

The main industrial route to produce urea is through the reaction between ammonia and carbon dioxide. Virtually all commercialized ammonia for urea synthesis is generated by the Haber-Bosch process, with carbon dioxide being the main by-product of this system and natural gas being used as an essential raw material (EDRISI *et al*., 2016). However, the chemical industry has been looking for new alternatives to reduce dependence on fossil fuels through the diversification of the energy matrix, developing new systems for valuing and converting industrial waste and building chemical

platforms based on the concept of biorefineries (SERRANO-RUIZ *et al.*, 2012; MORONE *et al.*, 2015). Within this context, carbon capture and storage (CCS) technologies can contribute substantially to the reduction of CO_2 emissions, with the capture of flue gases being the most developed technology in thermoelectric power plants and other energy-intensive industries (SHIRMOHAMMADI *et al.*, 2020).

Koohestanian *et al.* (2018) proposed the synthesis of urea from carbon dioxide and nitrogen from the flue gases of thermoelectric power plants. The authors were pioneers in the design of a plant for the formation of ammonia and urea from combustion gases, contributing to the flowsheet of a sustainable system. The STAC process was used as the basis for the urea synthesis section. It was concluded that investments are still needed to establish the system and technology proposed by the authors, requiring the assembly of a pilot-scale unit and more detailed techno-economic assessments to identify vulnerable points, optimize energy integration and mass balances and determining appropriate control parameters.

Shirmohammadi *et al.* (2020) carry out a study for the integration of a carbon dioxide capture process with a urea production plant. The authors used a fertilizer plant based in Iran (Kermanshah Petrochemical Industries Co.) as a case study, responsible for the manufacture and commercialization of fertilizers and chemical inputs for the national market. Carbon capture and utilization (CCU) plant data were provided. From this, a sensitivity analysis was carried out from the main operating parameters and a good representation of the real data was verified from the simulation of the CCU plant.

2.3.4 - National fertilizer market

The fertilizer product can be defined as any organic or mineral compound, obtained industrially or naturally, that supplies the demand for the nutrients which are necessary for plant growth, returning to the soil the elements removed in each harvest, thus increasing productivity. Essential nutrients are divided into two categories (macro and micronutrients), totaling 16 elements that can be found in water, air, and soil. Each compound has a specific function, making them irreplaceable (BNDES, 2012). Macronutrients are those used in large amounts by plant metabolism, the main ones being nitrogen, phosphorus, and potassium (NPK). Nitrogen is mainly associated with plant growth and the synthesis of amino acids and proteins. Phosphorus is directly related to the chemical reactions that occur in plants, contributing to the processes of photosynthesis, respiration, energy storage and transfer, cell division and growth. Potassium is essential for fruit formation, water maintenance, resistance to cold and diseases (BNDES, 2012). As highlighted in Section 2.1.1, the production of biogas itself has digestate as a by-product with commercial value, which can be

applied directly as a biofertilizer due to the load of inorganic macronutrients present in its composition.

Currently, Brazil stands out as an agricultural power, with agribusiness being the majority part of Brazilian exports and representing 21% of the Brazilian GDP in 2019. According to data from the Ministry of Agriculture, Livestock and Food Supply (MAPA), among the ten most exported products in 2019, eight come from the agricultural activity. Thus, it is observed that agribusiness exports have shown a growing trend since 1994 and it is estimated that agricultural production will continue an upward movement until 2028 to meet the demand to produce food and biofuels worldwide (SAE, 2020). Currently, economic data show that all agribusiness production chains already account for 25% of the national GDP, and there are no signs that this growth curve will decrease in the coming years (EXAME JOURNAL, 2023).

Brazil is an important player in the fertilizer consumer market, ranking fourth in the world behind China, India, and the United States (USA). This amount represents about 8% of global consumption and, due to the increase in national demand for agro-industrial production, the trend is for this amount to increase in the coming years. However, it is observed that the accelerated growth of the national demand for fertilizers has significantly extrapolated the increase in supply. Therefore, to sustain Brazilian agribusiness, imports of fertilizers become increasingly necessary, maintaining the current scenario of the national industry of chemical intermediates.

Within this context, the fertilizer's synthesis is closely correlated with agricultural production and the availability of raw materials. Figure 16 illustrates the production chain of NPK fertilizers. The first stage of the chain includes the mineral extractive industry, being responsible for the provision of basic raw materials (phosphate and potassium rock). It is noted that phosphate and potassium fertilizers have the supply of raw material from mineral extraction, that is, the synthesis of both depends a lot on the availability and existence of these minerals within the territory for there to be a significant production. On the other hand, the synthesis of nitrogen fertilizers directly depends on the availability of hydrocarbons, especially natural gas, considering the current productive structure of the industrial sectors (BNDES, 2012; FARIAS, 2015; EPE, 2019). Then, starting from the basic inputs, intermediate raw materials are produced, such as sulfuric acid, phosphoric acid, and anhydrous ammonia. The third link is made up of the manufacture of simple and intermediate fertilizers, of which it is possible to highlight urea, ammonium nitrate, single superphosphate (SSP), triple superphosphate (TSP), ammonium phosphate (MAP and DAP) and potassium chloride. Finally, there is the process of granulation and synthesis of mixed fertilizers, originating the products known as NPK (BNDES, 2012).

Within the national market, the speed of growth of Brazilian demand in the agricultural sector makes the country increasingly dependent on imports. Currently, Brazil imports more than 80% of

the fertilizers used in the domestic market. Consequently, the national production of fertilizers corresponds to less than 20% of the total amount consumed. The country was an exporter until 1992, however it became a major importer from 1992 onwards due to the gap between agribusiness demand and national supply what could be explained by the lack of investment throughout the production process and the absence of a public policy aimed at valuing natural gas and raw materials for the chemical industry. (EPE, 2019; SAE, 2020).

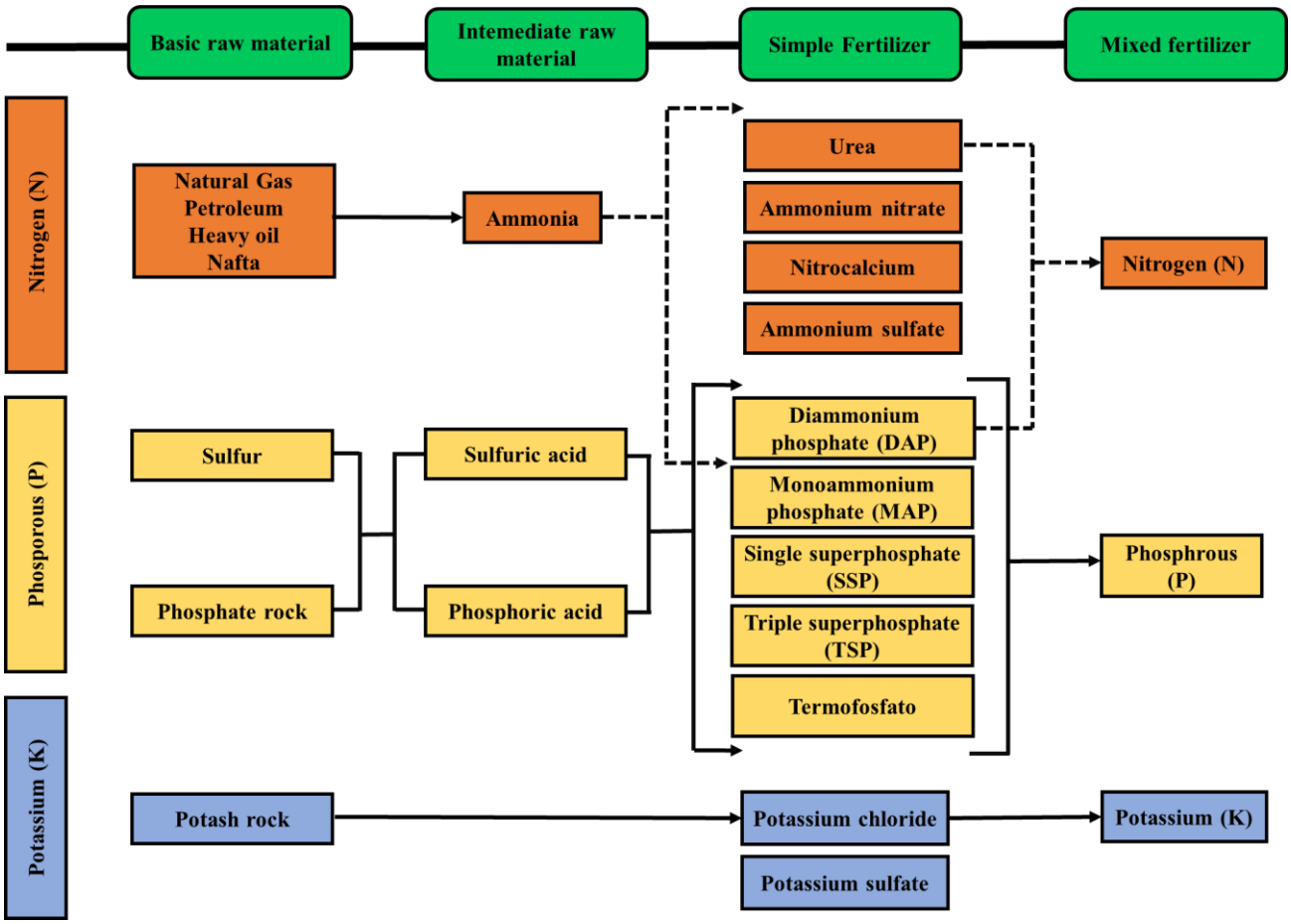

Figure 16 - NPK fertilizer value chain. Source: EPE (2019).

According to the data from MAPA (2018), the volume of fertilizer imports in Brazil was approximately 25 million tons. Nitrogen fertilizers corresponded to 35% of the total volume, totaling 8.77 million tons. Phosphate represented 23%, reaching 5.69 million tons. Finally, potassium chloride constituted 42%, reaching 10.5 million tons. Figure 17 illustrates Brazil's external dependence on fertilizers for the year 2018 (SAE, 2020).

The data suggests a worrying scenario for the national economy, especially for the agricultural sector. As it can be seen, the most delicate situation concerns the import of potassium fertilizers, with this percentage being equivalent to 94% of the total volume consumed. Furthermore, the panorama regarding the import of nitrogen fertilizers also indicates a strong external dependence,

making the country vulnerable in relation to the global macroeconomic scenario, especially in situations such as the current war in Ukraine as both Russia and Belarus (directly involved in the conflict) are important producers and world exporters of nitrogen fertilizers. In relation to phosphate fertilizers, the situation is favorable in relation to other macronutrients, however it also exposes the fragility.

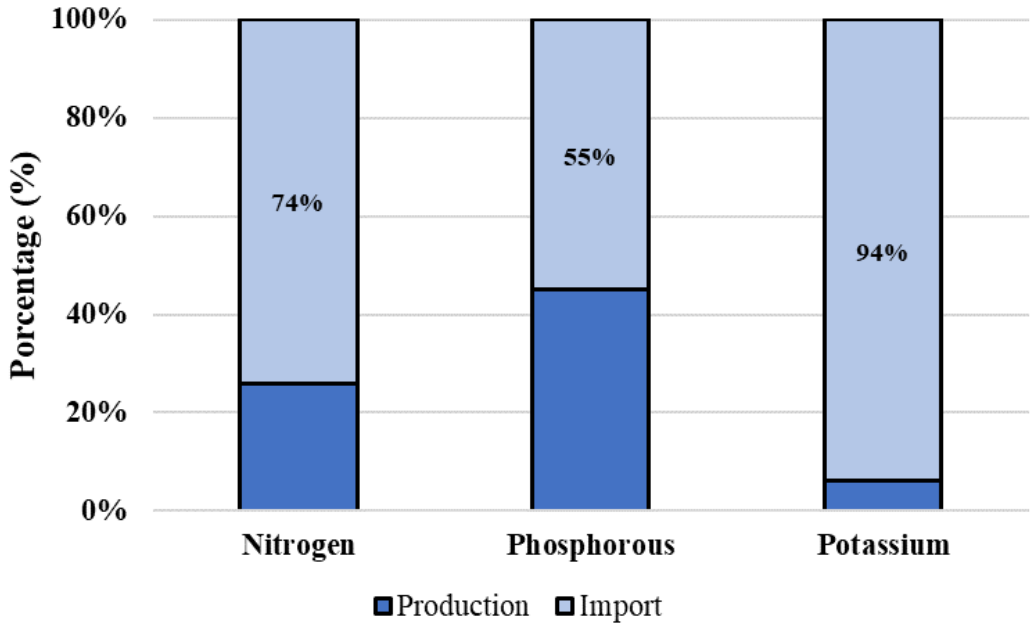

Figure 17 - Brazil's external dependence on fertilizers in 2018. Source: EPE (2018).

It is important to point out that the high demand of the national agricultural sector is not the only reason for Brazil's external dependence. The sector faces port and storage infrastructure problems, in addition to technological, regulatory, and environmental limitations that have been identified as bottlenecks for new investments. This set of factors directly affects the availability of basic raw materials (*e.g.*, natural gas, refinery gas and asphalt waste) and the manufacture of intermediates (*e.g.*, ammonia). In historical terms, the biggest deficit – both in monetary value and in physical quantity of imports – in the trade balance is concentrated in imports of intermediaries for fertilizers. This difference has increased in recent years, while the volume of national production has remained stable over the last decade (BNDES, 2012; EPE, 2019).

Thus, the participation of imports of nitrogenous fertilizers is of great importance. In 2018, Brazil imported approximately 9 million tons of nitrogen fertilizers. This amount is double when compared to the year 2008. Figure 18 illustrates the distribution by product in the import of nitrogen fertilizers between the years 2008 and 2018, according to data from the Ministry of Economy (EPE, 2019). Within this context, the main exporters of nitrogen fertilizers in 2018 were Russia (23%), China (16%), Algeria (12%), Qatar (8%), Nigeria (6%) and the United Arab Emirates (5%).

Notably, the main places of import of urea were Algeria, Russia, Qatar, Nigeria, United Arab Emirates and Egypt (EPE, 2019).

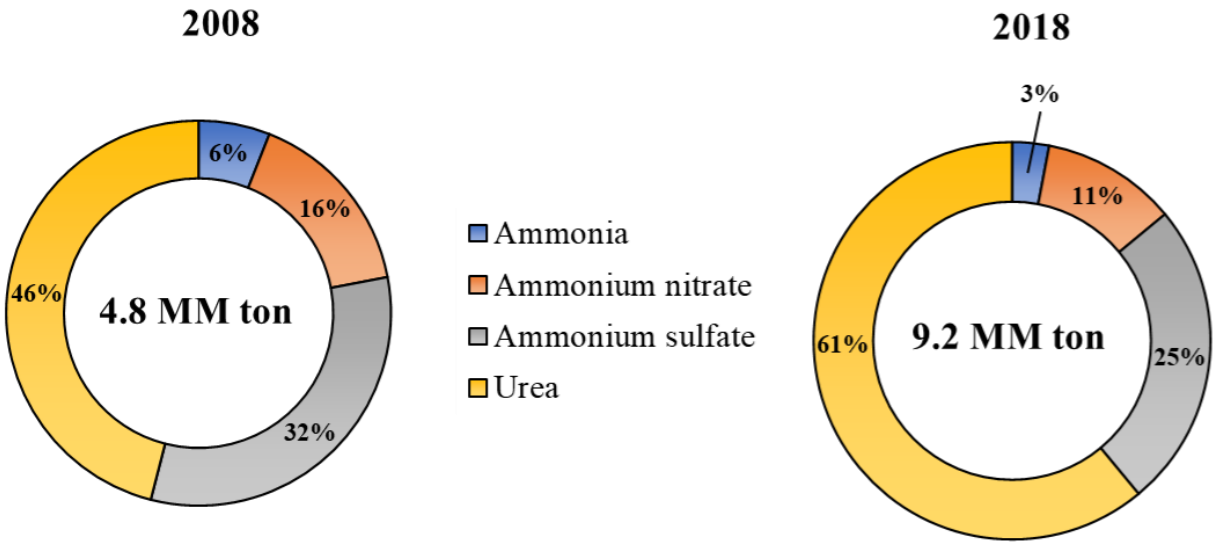

Figure 18 - Distribution by product in imports of nitrogen fertilizers in 2008-2018. Source: EPE (2019).

2.4 - Final considerations

Biogas presents itself as an alternative for diversifying the Brazilian energy matrix, and its potential is associated with both the direct generation of electricity and the synthesis of biomethane for industrial applications. According to data from CIBiogás (2021, 2022) and ABiogás (2020), there is a significant growth in the domestic market both in total number of plants and volume of biogas produced between the period 2015 and 2022. This data reflects the expansion capacity of the national biogas market, being far below the theoretical potential associated with the three main residues: sugar-energy, agroindustry, and sanitation.

In the context mentioned, it is important to discuss the challenges related to investment policies which affect the expansion of the biogas sector in Brazil. A significant topic should be the competition between the use of biogas for electricity generation and its application as a raw material in industrial processes. While electricity generation is most established option, the potential of biogas as a raw material for industrial applications is increasingly being recognized. This scenario may raise questions about resource allocation and incentive policies, as different sectors may have distinct priorities. Additionally, the variety of feedstock sources for biogas production is also a factor to be considered. For example, biogas plants fed by USW/WT have a greater volume produced despite the smaller number of plants. However, other sources such as agricultural also play an important role in providing feedstock for biogas production within Brazilian territory . Therefore, investment policies need to take into account these different sources and their potential applications,

ensuring that resources are allocated efficiently and that the sector as a whole can reach its maximum potential for growth and sustainable development.

Currently, natural gas is the main raw material used in the synthesis of ammonia, being used directly for the preparation of synthesis gas. Alternative technologies have been employed to reduce the emission of greenhouse gases and make the process more sustainable, however they still do not offer competitive conditions in relation to the conventional Haber-Bosch process. Due to the similarity of composition with natural gas, biogas becomes a viable option to replace natural gas and promote a vertical chain for sustainable generation of ammonia and urea, with the main adjustment step associated with the raw biogas pre-treatment due to the higher CO_2 content present in the composition.

Given the importance of the agricultural sector for the Brazilian GDP, the national demand for fertilizers becomes essential to supply the productive capacity and growth of the sector. Within this context, ammonia and urea are essential inputs to ensure the supply of this industry, with ammonia being the main raw material for the synthesis of nitrogen fertilizers, while urea represents the main nitrogen fertilizer sold globally. Thus, establishing a national industry to produce nitrogenous fertilizers configures the possibility of reducing external dependence on imports, national technological development and strengthening of agricultural activity.

Therefore, Brazil has great potential for the production, synthesis, and trading of biogas and biomethane. However, studies and investments in this area are still incipient and, therefore, there is a gap in the literature for the investigation of biogas as a raw material for the construction of a verticalized plant of ammonia and urea through computational tools of modeling and simulation of an integrated plant.

Considering the context outlined above, the work addresses critical aspects surrounding the utilization of biogas in ammonia and fertilizer production within Brazil. The increasing prominence of biogas in diversifying the national energy matrix and its potential for industrial applications underscores the relevance of this research. With significant growth potential in the domestic biogas market, this study focusses on integrating biogas into the production chain for ammonia and urea aligned with economic goals. By leveraging biogas as a substitute raw material, the proposed vertical integration of ammonia and urea production not only promotes sustainability but also offers strategic advantages for Brazil's agricultural sector. With ammonia and urea being indispensable intermediate products, establishing a domestic industry for their production ensures supply security and reduces the negative trade balance effect alongside chemical industry , promoting national technological advancement and reinforcing agricultural activity.

This study focuses on computational modeling and simulation to evaluate the techno-economic feasibility of an integrated ammonia-urea plant, representing a significant contribution to

the existing literature. By filling a gap in research and investment in this area, this work provides insights into the potential benefits and challenges associated with adopting biogas as a raw material for ammonia and urea production. Ultimately, the research contributes to Brazil's efforts towards sustainable energy and agricultural development while addressing the evolving demands of a dynamic global market.

3. Methodology

In this work, the methodology consisted of evaluating individual ammonia and urea synthesis processes to analyze the integration potential of plants considering biogas as raw material. The simulations were performed with the commercial software *Aspen Plus* (version 12.1). This tool has flexibility for specifying (1) input streams, (2) operating conditions of the equipment and (3) introduction of heat and/or work (VIANNA, 2017). Within the next topics, the synthesis processes of ammonia and urea are described, as well as an breakdown made of the methodology to calculate the economic metrics.

3.1 - Ammonia Synthesis

The reference process for this simulation was an ammonia plant based on the generation of synthesis gas from the steam reforming of methane, dimensioned for an industrial capacity in the range of 500 ton/day and capable of supplying the demand of the urea plant: The plant is structured in two main sections:

- Preparation and purification of biogas (biomethane), steam reforming of biomethane (primary and secondary), water-gas shift reaction (CO conversion), CO_2 removal and methanation;
- Ammonia synthesis.

Each section details the choice of specific equipment within the simulator, as well as the specification of important process parameters. The main assumptions adopted are highlighted below:

- The plant model is developed in steady state.
- The biogas stream comes from landfills located in the Southeast region of the country due to the higher volume of biogas produced and the potential for generating raw materials for the production of this asset;
- Biogas feed stream only contains CH_4 and CO_2.and purified from an amine absorption column process. After that, biomethane is mixed with steam and fed to methane reforming;
- Primary/Secondary reformers, shift reactors and the methanator are modeled as equilibrium reactors.
- CO_2 is separated in two different sections: Biogas upgrading and CO_2 removal sections. These two streams can be used as raw materials for urea synthesis.
- Ammonia kinetic model follows Eq. (18).
- Ammonia is main product and can supply urea synthesis section.

3.1.1 - Thermodynamic framework

Considering the non-polar characteristic of the compounds present in the ammonia process, the Peng-Robinson equation of state (PR) was used to simulate the system. Table 8 presents the expressions of this thermodynamic model (SARTORE, 2014; VIANNA, 2017).

Table 8 - Equations used for Peng-Robinson

Relations	Equations
PVT	$P = \frac{R\,T}{V_m - b} - \frac{\alpha_c \alpha(T_r)}{V_m(V_m + b) + b(V_m - b)}$
Parameters	$b = 0.077796\frac{R\,T_c}{P_c}$ $\alpha_c = 0.457235\frac{R^2 T_c^2}{P_c}$
$\alpha(T_r)$	$\alpha = \left[1 + m\left(1 - \sqrt{T_r}\right)\right]^2$ $m = 0.37646 + 1.5422\omega - 0.26992\omega^2$

where $\alpha(T_r)$ represents a dimensionless function of the reduced temperature of the system T_r and the acentric factor ω. The variable V_m corresponds to the molar volume, T_c to the critical temperature and P_c to the critical pressure (TAVARES *et al.*, 2020).

3.1.2 - Biogas purification/upgrading and reactants feed

Figure 20 illustrates the complete flowsheet of the ammonia synthesis process, in which the STM-REF, SHIFT-RF, CO2-SEP and AMMSYNT blocks contains the equipment related to methane steam reforming, shift reactors, CO_2, and ammonia synthesis, respectively. Colors are determined to facilitate the visualization and identification of each step, in addition to delimiting the transition between each one of them. The initial stage consists of the purification of the biogas fed to the ammonia plant, with the goal of promoting the separation of the CH_4 and CO_2 molar composition of 60 and 40%, with a total molar flow of 1000 kmol/h as benchmark. The Component Separator (SEP-01) is used as an simplification and assumes the total removal of CO_2 to produce the biomethane used in the ammonia synthesis, respectively. The processed biomethane stream (CH4-FEED) is sent to the COMP-01 compressor simulated as a 3-stage compressor being pressurized to 25 atm. In addition, a stream of water (FEED-H2O) is fed with a molar flow of 1800 kmol/h to supply steam for the methane reforming section, which is also pressurized to 25 atm in the pump indicated by PUMP-01. The FEED-H2O stream corresponds to the combination of the

make-up streams and the excess condensed water, separated, and recirculated in the CO_2 removal section. The H_2O/CH_4 molar ratio is adjusted to 3.0 to avoid coke deposition on the active surface of the catalysts and increase the useful life within the steam reforming (CARVALHO, 2016; PAIXÃO, 2018). As shown in Figure 20, the red color is attributed to the purification/compression steps of the biogas/water vapor feed streams represented by dashed lines.

3.1.3 - Methane reforming

After the purification/compression section of the feed streams, both water vapor and biomethane are mixed through the MIX-01 mixer and sent to the methane steam reforming section, represented in Figure 20 by the STM-REF hierarchy block. Figure 19 illustrates the steam reforming process represented by the STM-REF block.

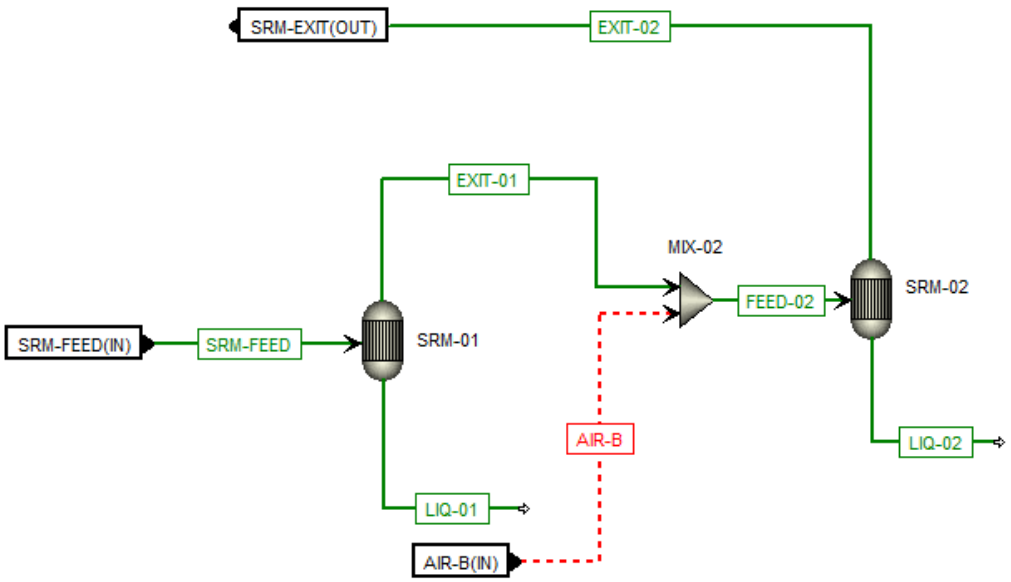

Figure 19 - Methane steam reforming section.

The first (SRM-01) and second (SRM-02) equipment illustrated corresponds to the primary and secondary reform, respectively. An equilibrium reactor was chosen to carry out the simulation because it is possible to determine specific stoichiometric reactions and the products in the equilibrium condition. Therefore, this simulation strategy becomes effective for situations where equilibrium reactions coexist, which is a reasonable approximation for the steam reforming of methane. Reactions (4) e (5) shown in Section 2.2.1 were considered in the reactor model, with the equilibrium constant data available in the software's database. (VIANNA, 2017).

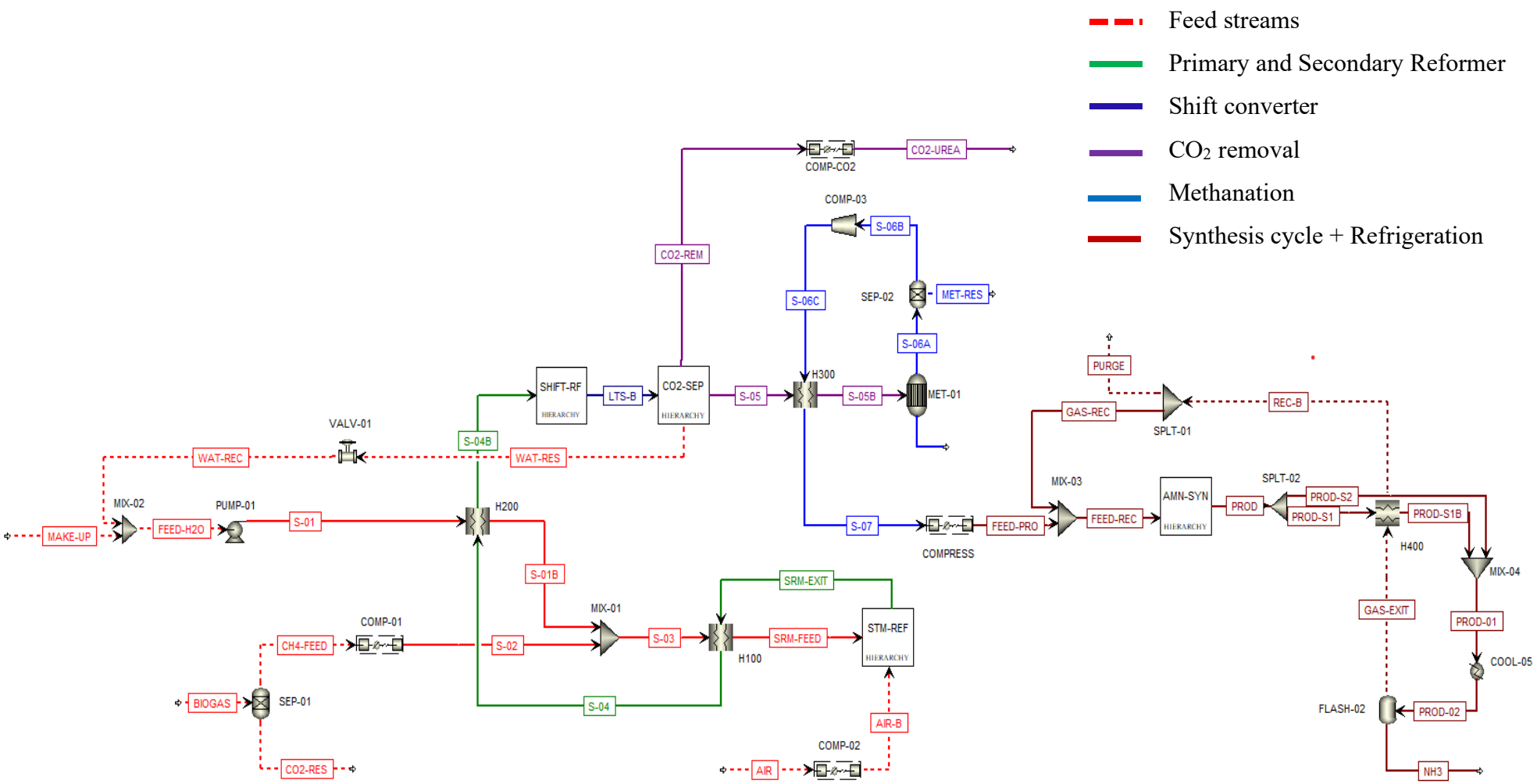

Figure 20 - Flowsheet of the ammonia synthesis process.

The effluent from the primary reformer has an outlet temperature of 820 ºC and 25 atm, responsible for consuming most of the methane fed. The outlet stream of the primary reformer needs to have residual methane to feed the second step. An atmospheric air stream compressed with a 3-stage compressor (25 atm) is mixed with the gas stream leaving the primary reformer and fed to the secondary reformer. Inside the secondary reformer (SRM-02), combustion of methane occurs through its reaction with oxygen present in atmospheric air. Furthermore, N_2 is introduced by the air stream to supply the demand of the synthesis loop. For the secondary reformer, the equilibrium reactor temperature was specified at 1000°C (MOURA, 2021; VIANNA, 2017). With goal to determine the air flow rate, an *Aspen Plus* software tool called *Design Spec* (acronym for design specification) is used to establish the appropriate stoichiometric molar ratio at the reactor inlet (FEED-REC) according to Eq. (1).

The gaseous stream leaving the secondary reformer has a residual methane mole fraction close to 0.001% (wet basis), completing the reaction cycle of the reform section. Table 9 has the main conditions and input data adopted for the reform section.

Table 9 - Assumptions and operating conditions for streams and reactors inside reforming stage

Stream/Equipment	Variable	Value
Primary reformer steam	Temperature (ºC)	550
Primary reformer	Steam/Carbon ratio	3.0
	Inlet temperature (ºC)	550
	Outlet temperature (ºC)	820
Process air	Pressure (atm)	25
	Temperature (ºC)	210
Secondary reformer	Outlet temperature (ºC)	1000

After the methane reform section, the gaseous stream has an outlet temperature of 1000 ºC, being sent to the H100 heat exchanger. This equipment promotes energy integration between the inlet stream (SRM-FEED) and outlet stream (SRM-EXIT) of the methane steam reforming stage. Then, the same stream proceeds to the heat exchanger H200, where energy integration is done with the process water feed stream. Finally, the gaseous stream from the methane steam reforming section is cooled to 210 ºC and sent to the equipment where the water-gas shift reaction takes place.

3.1.4 - Shift conversion (water-gas shift)

This step is conducted in two stages: a high temperature (HTS) and a low temperature (LTS) stage. This stage is justified, mainly, by the continuity of hydrogen production, but also by the ease of removing CO_2 compared to CO from the synthesis gas stream. Shift reactors were also modeled as thermodynamic equilibrium reactors specified by the presence of reaction (5). Figure 21 contains the sub-diagram detailing the shift converters section. From the high temperature shift reactor (HTS-100) most of the conversion of CO into CO_2 occurs, with the residual molar content of 2.0% (wet basis). Then, the gaseous stream is cooled down to a temperature of 200 ºC (COOL-01), being conducted to the low temperature converter (LTS-100), which reduces the CO content to values lower than 0.2% (wet basis). The gaseous effluent from the LTS reactor is at a temperature of 220 ºC, having a CO_2 molar percentage of 13.7%. Table 10 summarizes the main operating conditions used in shift reactors and important process variables for the process.

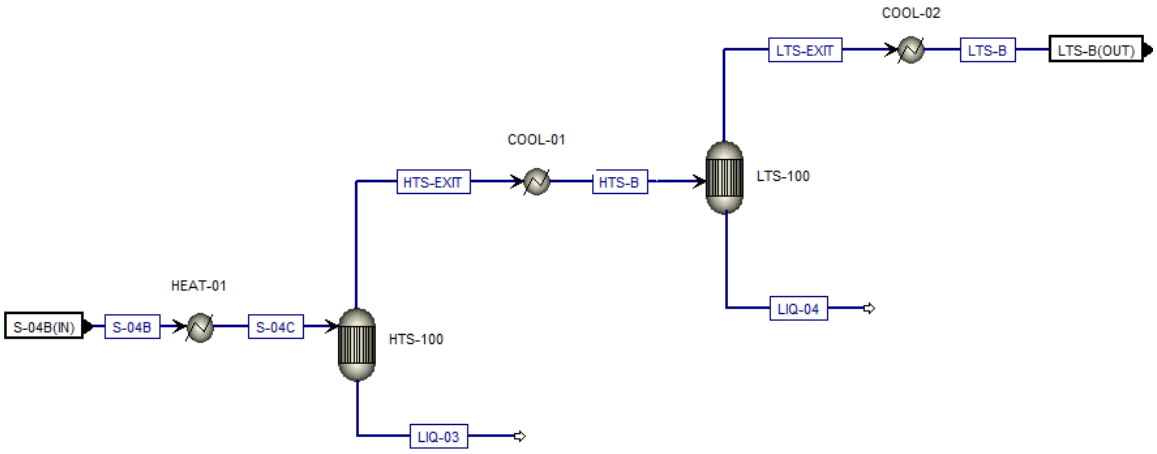

Figure 21 - Shift reaction simulation model.

Table 10 - Assumptions and operations conditions for the shift reactors

Stream/Equipment	Variable	Value
High Temperature Shift	Inlet Temperature (ºC)	330
	Outlet Temperature (ºC)	400
Low Temperature Shift	Inlet Temperature (ºC)	200
	Outlet Temperature (ºC)	220

3.1.5 - CO_2 Removal, Methanation and Compression

The LTS output stream is cooled down to a temperature of 50ºC (COOL-02) and forwarded to separation steps. First, a flash operation (FLASH-01) is performed to condense the excess water vapor present in the gaseous stream. Figure 22 contains the schematic of the CO_2 separation section. The liquid stream from this equipment has a molar composition of water greater than 99.9% purity with the presence of traces of contaminants (CO_2, CO, CH_4). Due to the high flow of condensate generated in the flash operation, it is necessary to recirculate this current (WAT-RES) to feed water into the system. Before being fed back into the system, the WAT-RES stream passes through a decompression valve section (VALV-01), where the pressure is reduced from 25 to 1 atm.

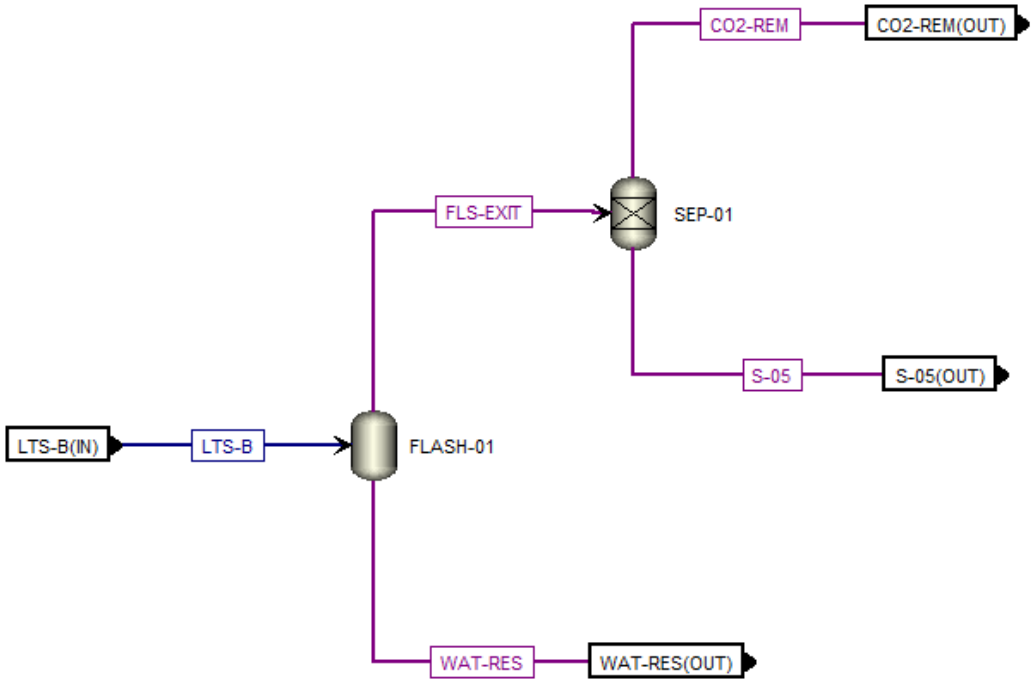

Figure 22 - Simulation model of the CO_2 removal section.

Naturally, the condensate flow rate is high enough for recycling, however there is a need to introduce a fresh stream of water (MAKE-UP) to keep the desired H_2O/CH_4 molar ratio for the reform section. For this demand, *Design Spec* tool was used. This tool allows the mathematical adjustment of an operating condition based on the control of another variable and, in this case, the H_2O/CH_4 molar ratio is adjusted based on the MAKE-UP stream, already considering the stream of condensed recycled water vapor.

After the flash operation, the gaseous effluent is sent to a separator (for example PSA – pressure swing adsorption, separation modules with membranes or chemical/physical absorption with amines), and the CO_2 removal modeling is carried out from a Component Separator (SEP-100), which consists

of a mathematical tool for separating components based on the specification of flowrates or fractions in the stream's composition. In this way, a removal of 99.7% of carbon dioxide was determined (VIANNA, 2017), with the CO_2 stream being channeled to a 3-stage compression, and then conducted to a urea synthesis section with temperature and pressure of 100 ºC and 140 atm, respectively. The synthesis gas is sent to the methanation section for the last stage of stream purification before entering the synthesis loop. Table 11 summarizes the main operating conditions used in the CO_2 removal section.

Table 11 - Assumptions and operating conditions for the CO_2 removal section

Stream/ Equipment	Variable	Value
FLASH-01	Temperature (ºC)	50
	Pressure (atm)	25
WAT-RES	H_2O molar content (%)	99.9
	Temperature (ºC)	50
SEP-01	Pressure (atm)	25
	CO_2 removal specification (%)	99.7

Methanation is responsible for adjusting the supply stream of the synthesis loop. This step of the process takes place to avoid the presence of contaminants and the loss of catalytic activity in the synthesis loop, that is, residual levels of CO and CO_2. Methanation's output stream has in its composition Ar, CH_4 and H_2O, in addition to the necessary reagents for the synthesis of ammonia. The inert Ar and CH_4 will be present within the synthesis loop, while residual water also needs to be removed from this stream to preserve the catalytic activity within the synthesis loop. Thus, before the compression, there is the presence of the separator SEP-02 to promote the split of the residual water formed during the methanation reactor. Figure 23 contains the simulation model for methanation and compression.

After adjustments to the composition of the supply stream, the compression takes place before entering the synthesis loop. Initially, the gaseous effluent is sent to the COMP-03 equipment for an initial stage of compression up to 65 atm. This stream exchanges heat with S-05 in H300 equipment. In this way, energy integration between the input and output streams of the methanator is enabled, as well as facilitating the compression of the feed stream of the synthesis loop. Finally, the S-07 stream is sent directly to the main compression (COMPRESS), which is carried out in 4 stages. The compressors were specified as isentropic equipment, having an equivalent pressure ratio between each stage. The exit conditions of the compression were defined as 390 ºC and 200 atm.

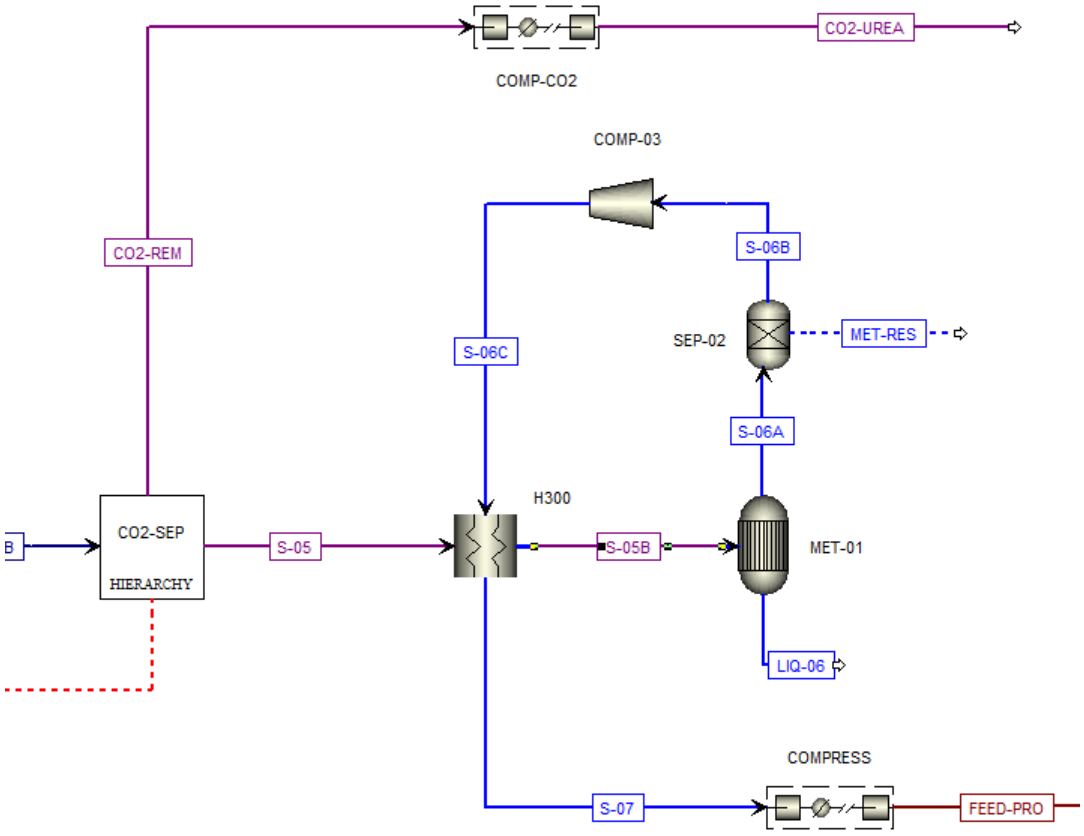

Figure 23 - Simulation model for methanation and compression.

3.1.6 - Synthesis loop

Finally, the ammonia production process occurs by Haber-Bosch synthesis, considering the reaction of N_2 and H_2 to generate NH_3 and the presence of iron catalysts as detailed by Eq. (1) in Section 2.2.1. As previously mentioned, the FEED-PRO fresh stream has a temperature and pressure of 390°C and 200 atm, respectively. In addition, all the previous steps were adjusted so that the H_2/N_2 molar ratio of feed to the first reactor remained close to 3. The operating temperature of the system needs to be high enough to favor the kinetic rate, however the ammonia synthesis reaction is highly exothermic. Therefore, as the reaction progresses through the reactor, the temperature increases close to chemical equilibrium, causing the net rate of reaction to decrease. In this way, the reactor needs to be cooled when the temperature is very high ($T > 500\ ^oC$) and, therefore, industrial plants generally employ a reactor with multiple beds with the presence of intermediate heat exchangers (AZARHOOSH *et al.*, 2014; CARVALHO, 2016; YOSHIDA *et al.*, 2021). For this work, the reactor is simulated as a plug flow reactor (PFR), with the existence of three catalytic beds and two intermediate heat exchangers. Figure 24 contemplates the simulation model established for the synthesis of ammonia.

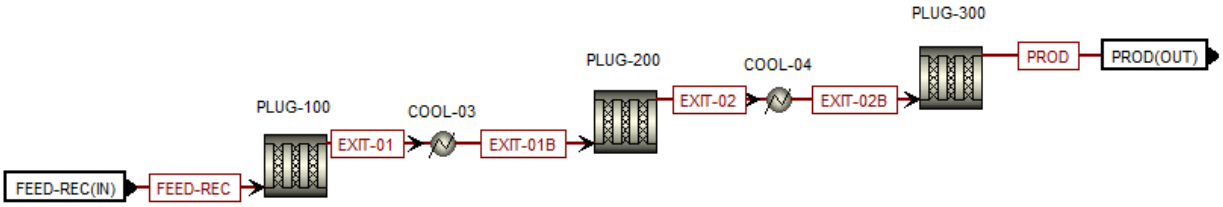

Figure 24 - Ammonia reactor simulation model.

The inlet temperature of the PLUG-100, PLUG-100 and PLUG-300 reactors is 390, 400, 410 ºC, respectively. For operational safety reasons, all reactors have an outlet temperature below 500 ºC, keeping the ΔT ≤ 100 ºC. Furthermore, as the ammonia concentration approaches thermodynamic equilibrium, the reaction rate decreases as the volume of the reactor increases. Therefore, the volume of each reactor is determined considering operational safety rules (ΔT ≤ 100 ºC) or based on the ammonia concentration criteria according to equilibrium conditions under adiabatic conditions (CHEEMA *et al*., 2018; YOSHIDA *et al*.., 2021). Thus, the reaction volume of catalyst PLUG-100 was considerably lower than that of PLUG-200/PLUG-300 in absolute and percentage criteria (CHEEMA et al., 2018; Yoshida *et al*., 2021). Table 12 contains the operating conditions and detailed specifications referring to the main reactor and catalytic beds 1, 2 and 3.

The pseudo-homogeneous kinetic model of Dyson and Simon (1968), through the modification and extension of the expression initially developed by Temkin and Pyzhev (1939), is used in this work. The driving force is the chemical activity of the components involved in the mixture. The equilibrium constant K_a is calculated according to Gillespie and Beatie's expression (1930):

$$r_{NH_3} = 2\, k_{rev} \left[K_a^2\, \alpha_{N_2} \left(\frac{\alpha_{H_2}^3}{\alpha_{NH_3}^2} \right)^{\alpha} - \left(\frac{\alpha_{NH_3}^2}{\alpha_{H_2}^3} \right)^{1-\alpha} \right] \quad (38)$$

$$k_{rev} = 4.916 \times 10^{11}\, e^{\frac{-170298}{(R\,T)}} \quad (39)$$

$$log_{10} K_a = -2.6911\ log_{10}(T) - 5.5193x10^{-5}\,T + 1.8489x10^{-7}T^2 + \frac{2001.6}{T} + 2.6899 \quad (40)$$

where r_{NH_3} represents the reaction's kinetic rate given in kmolNH_3 m^{-3} s^{-1} expressed by Eq. (38), k_{rev} is constant of the reverse rate (kmol m^{-3} s^{-1}) expressed by Eq.(39), K_a the equilibrium constant by Eq.(40), α_i is the chemical activity of each component of the gas mixture (dimensionless), T is the temperature (K) and R is the universal gas constant (8.314 J mol^{-1} K^{-1}) and α corresponds to a model parameter with a value of 0.5.

Table 12 - Assumptions and operations conditions for the reactor and catalytic bed

Stream/Equipment	Variable	Value
PLUG-100	Inlet Temperature (ºC)	390
	Outlet Temperature (ºC)	486
	Diameter (m)	1.5
	Length (m)	0.8
PLUG-200	Inlet Temperature (ºC)	400
	Outlet Temperature (ºC)	493
	Diameter (m)	1.5
	Length (m)	2.4
PLUG-300	Inlet Temperature (ºC)	410
	Outlet Temperature (ºC)	468
	Diameter (m)	1.5
	Length (m)	3.3

Based on the chosen kinetic model, there is a need to adapt this expression to the *Aspen Plus* environment. Within this tool, there are already pre-defined reaction classes such as power law models and LHHW isotherms. Considering the pseudo-homogeneous nature of the Dyson and Simon (1968) model, the power-law model approach is employed, considering the kinetic factor, and driving force required within the simulator:

$$r = (Kinetic\ factor)(driving\ force) \tag{41}$$

$$r = k_0\ exp\left(\frac{-E_A}{R\,T}\right)\ (K_{dir}\Pi_r f_r^{\nu_r} - K_{rev}\Pi_p f_p^{\nu_p}) \tag{42}$$

where r represents the kinetic rate of reaction, k_0 the frequency factor, E_A the activation energy, K_{dir} the forward kinetic constant, $\Pi_r f_r^{\nu_r}$ corresponds to the product of the fugacity of the reactants, K_{rev} the reverse kinetic constant and $\Pi_p f_p^{\nu_p}$ to the product of the fugacity of the products.

It is worth noting that the format of the equilibrium constant expression required by *Aspen Plus* differs from the model by Gillespie and Beatie (1930), which requires an adaptation of the coefficients to enter the kinetic model. Therefore, it is necessary to adjust the units of the driving force and the expression for the equilibrium constant. Within the software, it is only possible to implement the driving force in terms of fugacity (Pa unit) and the expression for the equilibrium constant in the following format:

$$ln\,(K_{eq}) = A + \frac{B}{T} + C\,ln\,(T) + D\,T \quad (43)$$

According to the definition of chemical activity by Equations (25) and (26), it is known that there is a necessary adjustment for dimensioning the kinetic expression within the *Aspen Plus* environment, considering both the format of the expression for the chemical equilibrium constant as the pressure units for the fugacity of the components of the gaseous mixture entering the main reactor. Table 13 details the adapted kinetic parameters used to simulate the ammonia reactor (TRIPODI *et al*., 2018).

The work by Tripodi *et al*. (2018) shows in detail the implementation of kinetic and thermodynamic terms considering the model by Dyson and Simon (1968), in addition to the kinetic model developed by Rosseti *et al*. (2006) for ruthenium-based catalysts. Thus, to corroborate the adjustments made according to Table 13, a dimensional analysis and curve adjustment were performed using the *Python* language, within the *Jupyter Notebook* programming environment.

Table 13 - Kinetic and thermodynamic parameters adapted for simulating the ammonia reactor according to the *Aspen Plus* requirements (adapted from Tripodi *et al*., 2018)

Components	**N_2**	**H_2**	**NH_3**	
Stoichiometry	-0.5	-1.5	1	
Exponents – Driving force				
Direct exponents (v_f)	1	1.5	-1	
Reverse exponents (v_r)	-	-1.5	1	
Equilibrium constant coefficients				
Coefficients	A	B	C	D
(K_{dir})	-4.9	9218	-5.42	7.8×10^{-4}
(K_{rev})	5.76	-	-	-

The output stream from the catalytic bed 03 (PLUG-300) is divided into 2 streams: PROD-S1 and PROD-S2 with SPLIT-02. The first one represents 70% (mass basis) of PROD stream and is sent to the H400 equipment, where the heat exchange takes place between the hot stream leaving the reactor and the cold gas stream (unconverted reactants) arising from the ammonia refrigeration cycle. After H400, PROD-S1B and PROD-S2 streams are mixed again, cooled down to -20ºC (COOL-05)

and then forwarded to the FLASH-02 flash separator. In this way, the liquid stream of ammonia is generated, and conducted to supply the demand of the urea synthesis plant.

The gaseous stream is redirected to the recycle, passing through the H400 heat exchanger to reach the same conditions as the fresh stream FEED-PRO (390 ºC and 200 atm). Due to the low conversion per pass inside the reactor due to thermodynamic limitations, the unconverted reagents are recirculated and there is a purge stream to avoid the concentration of inerts gases (CARVALHO, 2016; PAIXÃO, 2018). The SPLT-01 equipment is responsible for purging the system, with 4.5% of the recycle stream sent for disposal, while the rest is sent to be mixed with the fresh process stream from the MIX-03 mixer. Figure 25 illustrates the simulation model of the synthesis section.

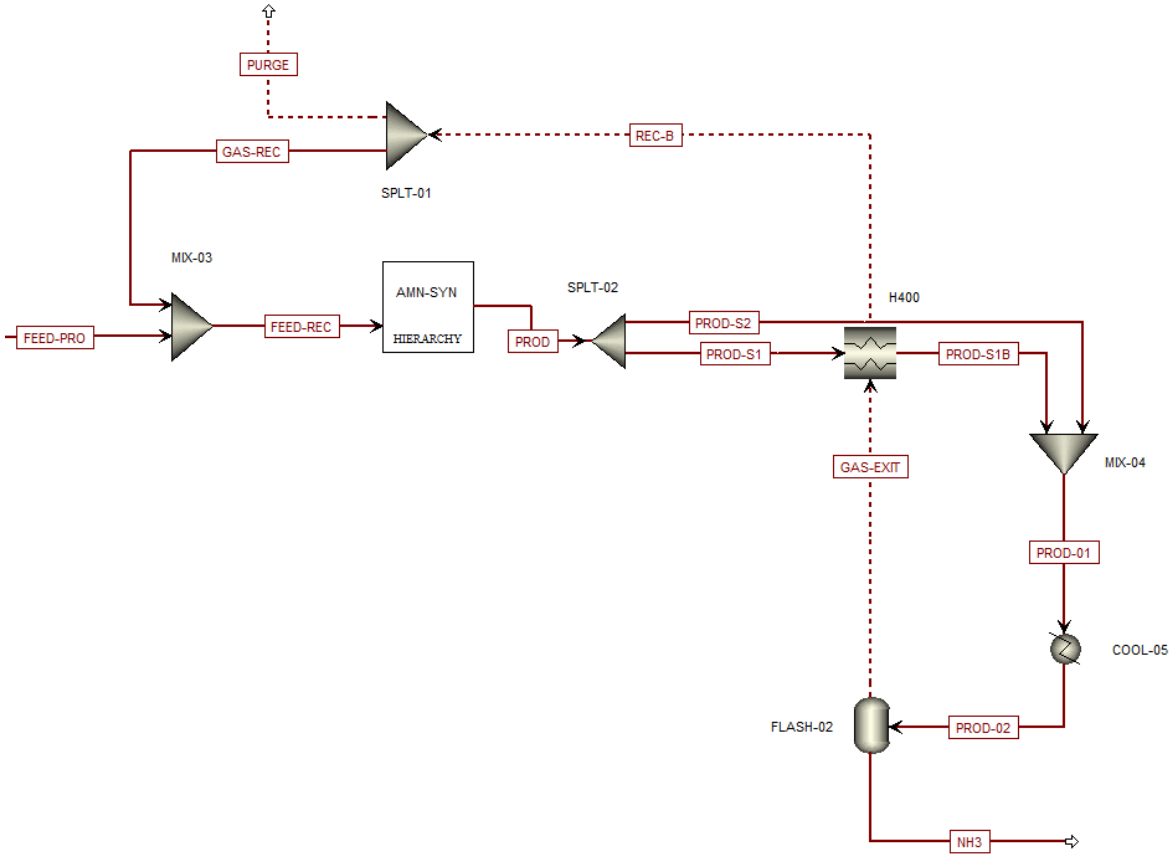

Figure 25 - Simulation model of the synthesis section

3.2 - Urea synthesis

The simulation of the urea synthesis section will be carried out using the Stamicarbon CO_2 Stripping process within the *Aspen Plus* software, based on the following initial assumptions:

- The plant model will be developed in steady state.

- Only two reactions will be considered: carbamate and urea synthesis. Therefore, for this work, biuret production and possible parallel reactions will not be explored.

- In liquid streams, free CO_2 is present to a minimal extent in the form of the intermediate ammonium carbamate.

- The synthesis of urea occurs only in the liquid phase.

- The carbamate condenser participates in the synthesis of urea, that is, it is responsible for both the formation of carbamate and urea.

- The *Aspen Plus* model plant was used as an initial project (ASPEN TECH, 2008b), making necessary adaptations according to the analysis carried out in the literature review.

3.2.1 - Thermodynamic framework

The thermodynamic model used was the Redlich-Kwong-Soave (SRK) equation of state with the Schwartzenruber and Renon mixing rule (SR-Polar) according to Rasheed (2011), Chinda (2015), Edrisi *et al.* (2016) and Koohestanian *et al*. (2018). The SR-Polar model can be applied to non-polar and highly polar components, and non-ideal mixtures. In addition, it is recommended for systems that operate at high temperatures and pressures (KOOHESTANIAN *et al*., 2018; ZAHID *et al*., 2014). This method requires:

- Parameters for polar components. These parameters are determined using vapor pressure data generated by the extended Antoine model.
- Binary parameters for accurate representation of phase equilibrium, being dependent on and variable with temperature.

The SR-Polar method can be used for predictions above 50 bar of pressure. The expectation is to obtain satisfactory results in any condition, if the UNIFAC interaction parameters are available. The set of Equations (44) to (50) briefly represents the description of the SR-Polar method, with more detail found in the following references: Soave (1972), Schwartzentruber and Renon (1989):

$$P = \frac{RT}{V_m + c\ - b} - \frac{a}{(V_m + c)(V_m + c\ + b)} \tag{44}$$

$$a = \sum_{\mathrm{i}} \sum_{j} x_i x_j \left(a_i a_j\right)^{0.5} \left[1 - k_{aij} - l_{ij}\left(x_i - x_j\right)\right] \tag{45}$$

$$b = \sum_{\mathrm{i}} \sum_{j} x_i x_j \frac{b_i + b_j}{2} \left(1 - k_{bij}\right) \tag{46}$$

$$c = \sum_{i} x_i c_i \tag{47}$$

$$a_i = f(T, T_{ci}, P_{ci}, \omega, q_{0i}, q_{1i}, q_{2i}) \tag{48}$$

$$b_i = f(T_{ci}, P_{ci}) \quad (49)$$

$$c_i = f(T, T_{ci}) \quad (50)$$

where P represents the operating pressure of the system, R the ideal gas constant, T the operating temperature of the system, V_m the molar volume, x_i correspond to the molar composition, l_{ij} is temperature dependent binary interaction parameter, k_{aji}, k_{bji} are temperature independent binary interaction parameters, T_c is the critical temperature, P_c the critical pressure, and ω the acentric factor, while q_{0i}, q_{1i}, q_{2i} are polar parameters for the Redlich-Kwong-Soave equation of state. It is important to mention that the data of pure components and parameters of binary interaction of the compounds NH_3, CO_2, ammonium carbamate, urea and H_2O are inserted into the simulator database, and are even used within the model of the initial project of the synthesis plant of urea (ASPEN TECH, 2008; CHINDA, 2015).

3.2.2 - Simulation of the Stamicarbon process

The urea synthesis flowsheet is detailed in Figure 26, the main goal being to represent the equipment and streams when compared to the industrial process. Solid lines represent liquid streams while dashed lines indicate gaseous. The CO_2 stream is fed directly into the high-pressure stripper, upwards and countercurrent to the liquid stream (4) that leaves the top of the reactor. Inside the stripper shell, high pressure saturated steam is supplied. The supplied heat and the counter flow of the CO_2 stream cause the carbamate to decompose into NH_3 and CO_2. In this way, the top stream of the stripper (2) contains the unconverted reactants (NH_3 and CO_2) and water vapor, being sent to the carbamate condenser. The bottom liquid stream (5) has a solution rich in urea, water, and non-decomposed carbamate, being forwarded to the product concentration section (CHINDA, 2015).

The carbamate condenser (pool condenser) receives the stream coming from the ejector (1) and the stream from the top of the stripper (2). This equipment is responsible for the synthesis of a fraction of the total urea produced in the synthesis section. The ejector stream corresponds to the mixture between the fresh stream of NH_3 which arrives from the ammonia plant and the bottom stream of the scrubber (9), which is a solution rich in carbamate and water. Low pressure condensate is supplied to the system for cooling the equipment, and the product stream (3) is conducted to the reactor, that is, to the first CSTR of the series (CHINDA, 2015).

The purpose of the series of CSTRs is to mimic the internal trays of the main urea reactor, being responsible for the synthesis of the major fraction of the urea produced. At the outlet of the last CSTR, there is a separator to split the liquid and gas streams. The stream (4) consists of urea, water,

carbamate, and a small quantity of unreacted gases, and is forwarded to the stripper. The gas stream (5) is composed of unreacted and inert gases, being directed to the scrubber (CHINDA, 2015)

The scrubber is fed by two streams: the gaseous stream (5) coming from the top of the reactor and a liquid stream (7) containing the recirculated carbamate solution. In the equipment's shell there is a supply of medium pressure condensate to remove the heat released by carbamate synthesis. There are two output streams from this equipment: the stream (6) is composed mainly of inerts gases fed to the system and unconverted reagents, while stream (8) is rich in carbamate and goes on to be mixed with the fresh stream of NH_3 (CHINDA, 2015). There is a significant limitation for obtaining operational data for the urea production system. Therefore, there was a need to investigate kinetic models in the open literature. Table 14 has a list of the most recent works in the literature for the synthesis of urea, with different kinetic models to produce ammonium carbamate and urea.

Table 14 - Papers in open literature containing kinetic models for the synthesis of ammonium carbamate and urea

Work Title	**Author**
Gas-Liquid Reactor in the Synthesis of Urea	(Dente *et al.*, 1992)
Simulation of a Urea Synthesis Reactor – 2. Reactor Model	(Irazoqui *et al.*, 1993)
Mathematical Modeling of the Urea Synthesis Reactor	(Abensur, 1996)
Simulation of urea reactor of industrial process	(Zhang *et al.*, 2001)
Modeling and Simulation of High-Pressure Urea Synthesis loop	(Zhang *et al.*, 2005)
Modeling the synthesis section of an industrial urea plant	(Hamidipour *et al.*, 2005)
Revamping Urea Synthesis Reactor using Aspen Plus	(Rasheed, 2011)
A Dual Approach for Modelling and Optimization of Industrial Urea Reactor: Smart Technique and Grey Box Model	(Zendehboudi *et al.*, 2014)
Simulation of the synthesis section of a urea production unit - Stamicarbon Process	(Chinda, 2015)
Process Intensification Applied to Urea Production Process	(Chinda, 2019)

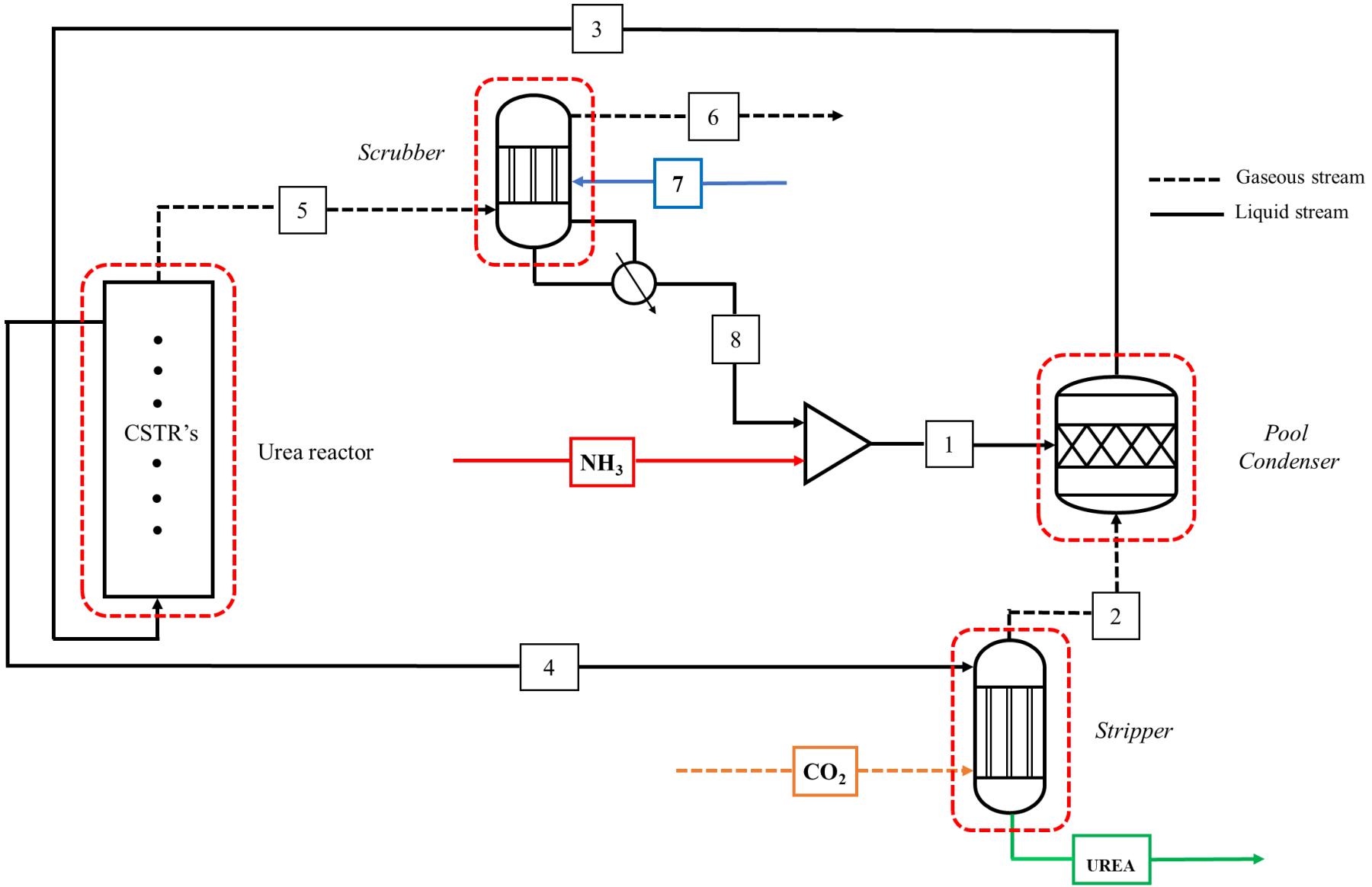

Figure 26 - Flowsheet of the simulated urea synthesis process. Source: Chinda (2015).

Among all the works cited in Table 14, only the authors Abensur (1996), Rasheed (2011) and Chinda (2015) use kinetic data obtained from mathematical adjustments of data from industrial reactors in operation. The work of Chinda (2015) tested the kinetic models of Abensur (1996) and Rasheed (2011), noting that Rasheed (2011) obtained better results considering the data available from FAFEN (Paraná/Brazil). Thus, for this work, the kinetic models of Rasheed (2011) and Chinda (2015) were tested for the kinetic model of the reactor, both of which are described in Table 15 and it was decided to proceed with the model of Rasheed (2011) because it also did not consider the formation of biuret and parallel reactions in the simulation project of the urea section, as well as this work.

Table 15 - Kinetic models tested for the synthesis of ammonium carbamate and urea

Ammonium carbamate synthesis	Urea synthesis	Author
$r_1 = 1628 \exp\left(\frac{-62802}{R\,T}\right) C_{NH_3}^{1.4} C_{CO_2}^{-0.4}$	$r_2 = 12000 \exp\left(\frac{-62802}{R\,T}\right) C_{CARB}^{0.92}$	(Rasheed, 2011)
$r_1 = 1628 \exp\left(\frac{-62802}{R\,T}\right) C_{NH_3}^{0.4} C_{CO_2}^{-0.11}$	$r_2 = 12000 \exp\left(\frac{-62802}{R\,T}\right) C_{CARB}^{0.39}$	(Chinda, 2015)

where r_1 represents the reaction rate for carbamate formation (kmol m^{-3} s^{-1}), C_{NH_3} the ammonia concentration (kmol m^{-3}), C_{CO_2} the carbon dioxide concentration (kmol m^{-3}), r_2 the reaction rate for urea formation (kmol m^{-3} s^{-1}) and C_{CARB} the concentration of ammonium carbamate (kmol m^{-3}), T is the temperature (K) and R is the constant universal of gases (J mol^{-1} K^{-1}).

3.2.3 - Pool Condenser / Carbamate condenser

No data or works were found in the open literature that discussed the study of the operation of the pool condenser for urea synthesis and, therefore, there are no means of comparison/validation of the composition of the inlet and outlet streams of this equipment, as well as the extent of the reactions for the formation of ammonium carbamate and urea. The only work with open data is found in the urea plant project presented by *Aspen Plus*, however the reactor modeling only considers the synthesis of ammonium carbamate, which directly affects the overall performance of the plant (ASPEN TECH, 2008b; CHINDA, 2015).

As highlighted in the literature, the residence time of the reagents is a decisive factor for the composition of the product obtained, with the residence time of the condenser being shorter when compared to the reactor. Thus, the pool condenser was simulated by a stoichiometric reactor, in which

the conversion of ammonium carbamate and urea has a specification conditioned to the performance of the main reactor.

3.2.4 - Reactor

The reactor was simulated from a sequence of 10 continuous stirred-tank reactor (CSTRs) in line with the works in the literature (HAMIDIPOUR *et al*., 2005; RASHEED, 2011; CHINDA, 2015; ZHANG *et al*., 2005; ZENDEHBOUDI *et al*., 2014), so that each reactor represented a reactor tray. Each CSTR had a specified volume of 20 m³, as in the work of Rasheed (2011).

After the flow exits the last reactor, there is a need for a flash tank to separate the liquid and gaseous streams, the first being sent to the high-pressure stripper and the second directed to the scrubber.

The inlet temperature was set at 170 ºC for the first reactor and 185 ºC for the last CSTR, considering a linear temperature profile and constant operating pressure (HAMIDIPOUR *et al*., 2005; RASHEED, 2011; CHINDA, 2015). Figure 27 depicts the simulation of the sequence of CSTRs representing the urea conversion reactor.

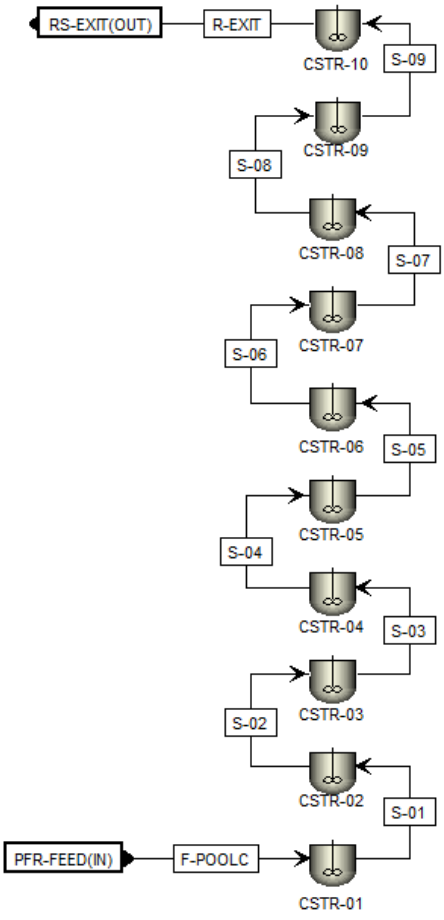

Figure 27 - Schematic diagram of the sequence of CSTR's for simulating the urea conversion reactor.

3.2.5 - Scrubber

This equipment was simulated using a 5-stage RADFRAC block, that solves the MESH (mass balance, thermodynamic equilibrium, sum of molar fractions, and energy balance) equations for each stage, requiring heat removal at the bottom of the equipment by the formation of ammonium carbamate. Usually, the amount of heat withdrawn is calculated from the condensate formed in industrial plants. However, due to the lack of availability of these data, the existence of a reboiler at the bottom of the column and a reflux ratio equal to 10 is specified according to Aspen Plus plant model (ASPEN TECH, 2008b). In addition, the equilibrium reaction of ammonium carbamate formation was assumed in each stage and, thus, all heat generated was removed in the last stage of the equipment.

3.2.6 - Stripper

The high-pressure stripper was also simulated as a RADFRAC block; however, it contained 10 stages (ASPEN TECH, 2008b). To emulate the heat transfer from the high-pressure steam feed, steam was supplied from the second to the penultimate stage of the equipment. In addition, the presence of the equilibrium reaction of decomposition of ammonium carbamate from the first to the penultimate stage was allowed.

It is worth mentioning that the RADFRAC module is the main separation block of *Aspen Plus*, being pointed out by the software itself as a tool for modeling, simulating, and sizing columns with trays and/or packed columns. In this way, equipment such as scrubbers and strippers are usually simulated using the RADFRAC module, which requires different specifications and configurations depending on the output product and the operating conditions determined for the modeled operating system (CHINDA, 2015). Figure 28 illustrates the flowsheet of the urea synthesis plant, with the UREA-SYN block corresponding to the conversion reactor, that is, the sequence of CSTRs described in Section 3.2.4.

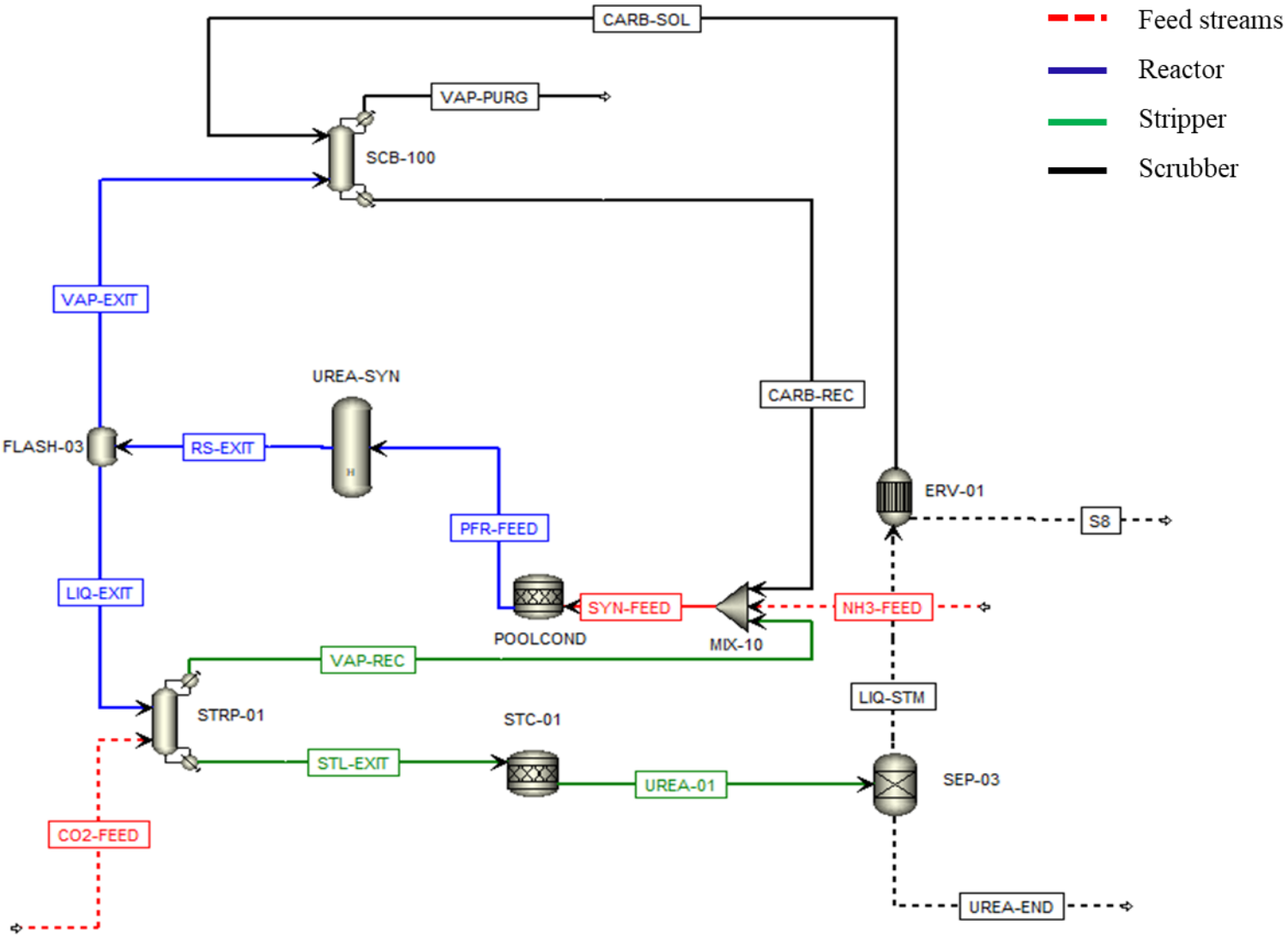

Figure 28 - Flowsheet of the urea synthesis process.

3.3 - Economic evaluation

3.3.1 - Plant total investment

Within the context of chemical engineering projects, it is fundamental to carry out studies on the analysis of the plant's techno-economic viability. Thus, the two main steps are estimating the total investment capital (C_{CTI}) and analyzing the discounted cash flow (DCF). The first consists of the general sum of all costs necessary for the construction and start-up of the industrial plant, while the second corresponds to the calculation of all inputs and outputs arising from the operation of the plant after start-up based on a time window and different proposed scenarios.

The fixed capital cost is made up of aspects:

- Inside Battery Limits (ISBL): Includes all costs related to the installation and regularization of process equipment at the production site. It is possible to cite as direct costs the main process equipment of the plant (pressure vessels, reactors, compressors), accessory items for the construction of the plant (valves, piping, instrumentation), as well as the cost of installation and supervision. It can also be called installed cost (C_I).

- Outside Battery Limits (OSBL): Considers all additional costs related to complementary activities such as allocation of the utilities plant, electrical substations, waste treatment systems, auxiliary facilities for work activities, among other accommodations. It can also be characterized as offsite cost (C_O).

- Engineering costs (C_E): This category includes costs related to general engineering services such as detailing and specification of equipment, supervision and detailing of engineering projects.

- Contingency: Corresponds to the calculation of additional expenses within the project budget considering possible variations in the estimate of the total cost. It is important to note that these calculations are uncertain, and many of them are finalized only after the complete installation. Furthermore, it also contemplates minor modifications in the scope of the project, price and exchange fluctuations and possible contractual/judicial problems.

In the early stages of the project, it is important that the ISBL costs are determined carefully, as the other steps in the total cost estimation are derived from the C_I. Any analysis can be jeopardized if the ISBL costs are poorly dimensioned, impacting the economic feasibility of the project. In this way, this usually becomes the most laborious step, in which the acquisition costs of each piece of equipment present in the process are calculated (TOWLER and SINNOT, 2012).

Naturally, the most assertive option for carrying out this estimate would be through the availability of data from vendors and equipment manufacturers. However, in most cases, there is no reliable open access to this type of information. Therefore, it is necessary to use alternative methods

based on parameterized cost equations, making it possible to establish the price of a given equipment based on the size factor, this metric being variable according to its type and application. Essentially, the formatting of the parameterized equation derives according to three main authors exemplified from the equations below (SEIDER *et al.*, 2003; TOWLER and SINNOT, 2012; PAIXÃO, 2018).

$$C_{EP} = \Xi_1 + \Xi_2 S^{\Xi_3} \tag{51}$$

$$C_{EP} = exp(\Xi_1 + \Xi_2 ln(S) + \Xi_3 \big(ln(S)\big)^2) \tag{52}$$

$$log(C_{EP}) = \Xi_1 + \Xi_2 log(S) + \Xi_3 \big(log(S)\big)^2 \tag{53}$$

where C_{EP} represents the purchase cost of each equipment, Ξ_i are parameters available for different types of equipment according to the authors Seider *et al*. (2003), Towler and Sinnot (2012) and Turton *et al*. (2012) and *S* characterizes the size factor associated with the equipment.

In addition, the individual cost C_{EP} must also consider other aspects for the calculation to be concrete, taking into account expenses related to the installation of the equipment, as well as the selection of construction material and the pressure range in which it operates. It is important to mention that the parameterized equations by Seider *et al*. (2013), Towler and Sinnot (2012) and Turton *et al*. (2012) allow equipment built with carbon steel and operation within the atmospheric pressure range.

$$C_{EP_I} = C_{EP}[(1 + f_T)f_M + f_{IC} + f_C + f_{EP} + f_{PC} + f_E + f_{EL}] \tag{54}$$

$$C_{EP_I} = C_{EP}[\,\beta_1 + \beta_2(f_M f_P)\,] \tag{55}$$

$$C_{EP_I} = C_{EP} f_{BM} f_M \tag{56}$$

Eq. (54) takes into account installation factors for solids and fluids processing plant (Table 16 contains the details of the values for different building materials). It is worth pointing out that the factors highlighted in this equation are computed in a generalized way, disregarding certain particularities found for certain types of equipment. Therefore, Equations (55) and (56) must be used since they consider the singularities of each equipment, in which β_1, β_2 and f_{BM} represent adjusted parameters for the different equipment present in the industrial plant (SEIDER *et al*., 2003; TOWLER and SINNOT, 2012; TURTON *et al*., 2012).

The Capcost method developed by Turton *et al.* (2012) contemplates different desired building materials as well as different operating ranges. The material factor parameter f_M quantifies the change in material choice, requiring an adjustment factor to be added to the calculation (carbon steel follows as the basis if there are no changes in the design). Furthermore, the factor of pressure f_P covers different operating ranges, being portrayed by Eq. (57):

$$log_{10} f_P = \Omega_1 + \Omega_2 log_{10} P + \Omega_3 (log_{10})^2 \quad (57)$$

where Ω_i are parameters found for each piece of equipment detailed by Turton *et al.* (2012) and P represents the operating pressure.

Table 16 - Factor used in Equation (54) developed by Seider *et al*. (2003). Source: Paixão (2018)

Factor	Value
f_{EL}(elevation)	0.5
f_E(electric)	0.2
f_{PC} (painting and covering)	0.1
f_{EP} (structures and building)	0.2
f_C (civil)	0.3
f_{IC} (control and instrumentation)	0.3
f_P (piping)	0.6
f_M (material - carbon steel)	1.0
f_M (material - cast steel)	1.1
f_M(material - 316 stainless steel)	1.3

All the aforementioned equations provide data for calculating the equipment's cost based on tabulated parameters for a given reference year. Therefore, it is necessary that the values obtained are readjusted considering the inflation period so that there is a temporal correction from the natural devaluation of currency(ies). Usually, this process is carried out through the annual update of indices provided by specialized agencies, such as The Chemical Engineering Plant Cost Index (CEPCI) and The Engineering News-Record Construction Cost Index (ENRCCI). In this way, the installed cost C_I is determined from Equation (58). If Eq. (55) is used to calculate the C_{EP}, it is necessary to remove the term $f_{P,i}$ as it is already implicitly incorporated in the estimate (SEIDER *et al*., 2003; TOWLER and SINNOT, 2012; TURTON *et al*., 2012).

$$C_I = \left(\frac{I}{I_{base}}\right) \sum_{i=1}^{NEQ} f_{P,i} C_{CE,i} \quad (58)$$

where I represents the current inflation index, I_{base} the inflation index of the reference year and NQE indicates the total number of pieces of equipment present in the process.

From the determination of C_I, secondary costs within the total capital estimate can be considered. The C_O can vary from 20% to 100% of C_I. This percentage varies according to the conditions of the location where the main plant will be installed and and also the degree of integration with other existing units. The previous structure of the land, available infrastructure in the region and possible logistical limitations are important factors for offsite cost. According to industry practices, engineering costs (C_E) can vary between 10 and 30% based on the size of the industrial plant. On the other hand, contingency (C_C) and startup (C_{SU}) costs are linked to the degree of maturity and complexity of the project. Naturally, both are expected to be higher for new and unestablished technologies. Finally, working capital (C_{WC}) is expected to be quoted at 15% of permanent direct investment (C_{PDI}) within the chemical and petrochemical industry sectors. Table 17 summarizes all costs included in the plant's total fixed investment estimate.

Table 17 - Costs included in the plant's total fixed investment estimate. Sources: Towler & Sinnot (2012)

Investment type	Relations
C_O (offsite *cost*)	$(0.2 \text{ to } 1.0)\ C_I$
C_{PDI}(permanent direct investment))	$C_O + C_I$
C_E (engineering cost)	$(0.1 \text{ to } 0.3)\ C_{PDI}$
C_C (contingency cost)	$(0.1 \text{ to } 0.5)\ C_{PDI}$
C_{CDT} (Total depreciable capital)	$C_{PDI} + C_E + C_C$
C_T (land cost)	$0.02\ C_{CDT}$
C_{SU} (startup cost)	$(0.02 \text{ to } 0.3)\ C_{CDT}$
C_{PTI} (Permanent total investment)	$f_l C_{CDT} + C_T + C_{SU}$
C_{WG} (working capital)	$(0.05 \text{ to } 0.3)\ C_{IPD}$
C_{CTI} (Total investment capital)	$C_{PTI} + C_{CG}$

The calculation of the C_{PTI} must be rectified from the location factor f_l since the calculations for the cost of the equipment are carried out with reference to countries different from the original space where the plant will be built. In addition, the location factor provides a correction parameter for the use of national goods and services, characteristic economic factors, reduction of exchange rate risks, among others. Thus, f_l values can be found for different countries in Towler and Sinnot (2012).

3.3.2 - Total cost of production

The total cost of production (C_{TP}) can be described as the sum of variable costs (C_{CVP}) and fixed cost of production (C_{CFP}). Variable costs are represented by the calculation of expenses related

to the purchase of raw materials, utilities and proper treatment of waste from the production process. The fixed cost of production is determined directly by the cost of labor (C_L), in addition to having other components such as maintenance costs (C_M), supervision and management (C_{SG}), administrative (C_A), sales and marketing (C_{MS}), research and development (C_{RD}), among others.

In order to determine the fixed production cost, it is essential to calculate the operator labor cost (C_{SA}), which is determined by the sum of the month salary (C_{SM}) and the salary charges costs (C_{SC}) indicated by Eq. (59) (TOWLER & SINNOT, 2012, PAIXÃO, 2018):

$$C_{SA} = C_{SM} + C_{SC} \tag{59}$$

After obtaining the C_{SA}, it is possible to establish the total labor cost C_L from Eq. (60), in which the calculation takes into account the number of solid processing units (U_{PS}) and the number of fluid processing units (U_{PF}) (TURTON *et al.*, 2012). In the case of this work, it's assumed that urea synthesis section contributes to 4 piece of equipment described in Section 3 and the existence of equipment for solid processing is disregarded.

$$C_L = 4.5\ (6.29 + 31.7\ U_{PS}^2 + 0.23 U_{PF})^{0.5}\ C_{SA} \tag{60}$$

In addition, other costs are included within the fixed production cost. Table 18 contains the details of the costs included for the sum of the fixed production cost, where S_V represents the total value acquired from the direct sale of products (PAIXÃO, 2018).

Table 18 - Costs included within the fixed production cost. Source: Towler & Sinnot (2012)

Cost type	**Relations**
C_L (labor)	Equation (60)
C_{SG} (Supervising and Management)	0.25 C_L
C_M (Maintenance)	0.05 C_I
C_{BT} (Benefits and training)	0.6 ($C_L + C_{SG}$)
C_{PI} (Property tax and insurance)	0.02 C_{IPD}
C_{RD} (Research and development)	0.05 S_V
C_{MS} (marketing and sales)	0.03 S_V
C_{GA} (administrative)	0.65 ($C_L + C_{SG}$)

3.3.3 - Cash Flow

Cash flow (CF) can be defined in a simplified way as a systematic analysis of a project's revenues and expenses during a time window, which can assume positive and negative values. In this way, the CF allows the visualization of the movement of resources, operating costs, generated revenues and obtained profits/losses. Therefore, it becomes an important tool to ensure economic sustainability from the identification of the main financial difficulties, enabling the development of strategies to minimize and/or avoid them. For industrial projects, the DCF is determined from Eq.(61) :

$$DCF = \sum_{0}^{N} (inputs - outputs) \tag{61}$$

where N represents the time established for the project time window. The portion of cash flow inputs is mainly determined by direct revenue from the sale of products and by-products (S_V), while outputs correspond to the sum of the total production cost (C_{TP}), spent for each year of plant construction, C_{LD} the cost of land and C_{SU} the starting cost of the plant.

Depreciation D is an accounting instrument that consists of reducing the value of a certain asset over time. This loss is realized annually, according to the useful life each asset, distributing its cost over the time window in which it is used. It is worth mentioning that depreciation is a non-cash expense, that is, it does not result in an output of financial resources. However, its value impacts the net result of cash flow since its accounting can help to reduce the payment of taxes (SEIDER *et al.*, 2003; TOWLER and SINNOT, 2012). For the calculation of depreciation, the most used technique corresponds to the linear depreciation method by Eq.(62) where a constant term D_i is calculated for year i considering the total depreciable cost and the operating time of the plant t_{dep}.

$$D_i = \frac{C_{CDT}}{t_{dep}} \tag{62}$$

3.3.4 - Net present value and Internal rate of return

The net present value (NPV) is defined as the sum of all cash flows generated by the project over a period of time. Essentially, the NPV determines the present value of projected cash flows within the project lifetime t_p by discounting these future amounts at a specific rate i called the cost of capital described from Eq. (63):

$$NPV = \sum_{j=1}^{t_p} \frac{CF_j}{(1+i)^j} \tag{63}$$

The NPV is an important decision-making tool as it is an economic metric used to assess whether the project can provide satisfactory returns based on different scenarios and assumptions adopted for the model. This financial performance indicator is directly influenced by the cost of capital i, and may vary according to the financing source used for the project. If all C_{CIT} comes from debt, i can be equivalent to the interest rate. On the other hand, if the C_{CIT} comes from equity sources, the cost of capital (i) can be determined from the combination of debt and equity according to Equation (64):

$$i = \left(FF \; i_f\right) + (1 - FF)\, i_{cp} \tag{64}$$

where i_f is the interest rate for financed capital, i_{cp} is the rate of return on equity investment, and FF represents the fraction of financed capital.

In addition, the internal rate of return (IRR) is a financial metric calculated from Eq. (61) and represents the discount rate so that the NPV value is zero, that is, it provides the minimum expected return for the project to be considered viable given certain assumptions adopted (SEIDER *et al*., 2003; TOWLER and SINNOT, 2012; TURTON *et al.*, 2012).

3.4. - Economic Equations

3.4.1 - Installed cost

The installed cost was calculated based on different methodologies applied to chemical engineering cost estimates, considering different attributes and specifications of each equipment within the integrated plant project. Furthermore, it is necessary to quantify the effect of inflation on the total cost of equipment as explained by Eq. (58), with the CEPCI index equal to 708.0 (corresponding to the year 2021) used in this work.

Table 19 contains a summary of the methodologies used for all simulated equipment within the integrated plant. It is important to highlight that a list containing all the technical coefficients used for each type of equipment is available in Appendix A.

Table 19 - Estimation methodology of capital cost adopted for each equipment

Equipment Type	Equipment Name	Section	C_{EP} Method
Pump	PUMP-01	Raw Materials	Capcost
Compressor	COMP-01	Raw Materials	Capcost
Compressor	COMP-02	Raw Materials	PTW[a]
Compressor	COMP-CO2	CO_2-Removal	Capcost
Compressor	COMP-03	Methanation	PTW[a]
Compressor	COMPRESS	Ammonia synthesis	Capcost
Reformer Furnace	SRM-01	Steam Reforming	Capcost
Pyrolysis Furnace	SRM-02	Steam Reforming	Capcost
Vertical Vessel	FLASH-01	CO_2-Removal	Capcost
Vertical Vessel	FLASH-02	Ammonia synthesis	Capcost
Horizontal Vessel	PLUG-01	Ammonia synthesis	Capcost
Horizontal Vessel	PLUG-02	Ammonia synthesis	Capcost
Horizontal Vessel	PLUG-03	Ammonia synthesis	Capcost
Heat Exchanger	HEAT-01	Raw Materials	Icarus
Heat Exchanger	H100	Raw Materials	Icarus
Heat Exchanger	H200	Raw Materials	Icarus
Heat Exchanger	H300	Raw Materials	Icarus
Heat Exchanger	H400	Raw Materials	Icarus
Heat Exchanger	COOL-01	Shift Converter	Icarus
Heat Exchanger	COOL-02	Shift Converter	Icarus
Heat Exchanger	COOL-03	Ammonia Synthesis	Icarus
Heat Exchanger	COOL-04	Ammonia Synthesis	Icarus
Heat Exchanger	COOL-05	Ammonia Synthesis	Icarus
Acid Gas Removal	CO2-SEP	CO_2-Removal	Gadelha (2013)
Urea synthesis	-	-	Zhang (2021)[b]

[a] PTW: Petter, Timmerhaus & West, [b] Installed capital cost for urea synthesis section will be determined according to the total installed cost for ammonia plant (Zhang, 2021)

As indicated by Table 19, the majority of estimating the installed costs follows the Capcost methodology (Turton *et al.*, 2012). However, for the compressor class there is a need to use an auxiliary method to complement the cost estimated to the technical specification given by *Aspen Plus*. The Capcost methodology indicates as a maximum limit of application of its formula a specific power of 3000 kW. Some equipment has a specified value higher than the maximum limit proposed by the Capcost method, which requires the application of a method that has a higher validity interval. The methodology implemented by Peter, Timmerhaus and West meets this need, having a validation interval between 75-6000 kW for power specified for industrial compressors (EPE, 2018). Eq. (65) contemplates the method described above.

$$C_{EP} = \exp(A\,ln(p) + B)\;F_m \tag{65}$$

where p represents the power (kW), A e B are design factors for different types of compressors and F_m indicates the factor of the chosen material. The factors for the Peter, Timmerhaus and West methodology is still indicated in Appendix A.

For heat exchangers, the chosen methodology is called Icarus. This choice is because the *Aspen Plus* software also uses this technique for the estimated calculation of the necessary investment considering the operating conditions described. Eq. (66) has the general formulation employed.

$$C_{EP} = \exp[\,A\,ln(x)^3 + B\,ln(x)^2 + C\,ln(x) + D]\,F_m \tag{66}$$

where x represents the thermal exchange area, A, B, C and D are parameters defined for different types of heat exchangers (shell-tube, air exchanger) and F_m indicates the factor of the chosen material. The factors for the Icarus methodology are indicated in Appendix A. Besides, special relations for f_m and f_p will be used.

Finally, for the CO_2 removal stage, CAPEX estimate is performed from the methodology used for Gadelha *et al*. (2014) derived from an economic study conducted to CO_2 treatment units by washing with amines considering MDEA as the main solvent employed. Eq. (67) indicates the adjusted function as a function of CO_2 (Q) flow quantified in $MMnm^3\ dia^{-1}$ flow, being the cost base raised from 2013.

$$CAPEX = 23.553\;Q + 0.5229 \tag{67}$$

where Q is the $MMnm^3$/day of each CO_2 removal unit implemented at this work. The factors assumed are indicated in Appendix A.

Moreover, the methanation reactor cost is considerable despicable due to low investment needed proportionally to other sections and the cost associated with shift converters is assumed to be 2% of ammonia synthesis installed cost (ZHANG *et al*., 2020; ZHANG *et al.*, 2021). Finally, the total installed cost regarding urea synthesis will be assumed as 15% of total ammonia synthesis installed cost. This hypothesis was made based on the lack of open data and complexity of Stamicarbon process (CHINDA, 2015; MOURA *et al*., 2021). Zhang *et al*. (2021) estimated the urea synthesis cost as 6% of the total installed cost regarding conventional methane to urea plant. In that work, a more conservative premise was adopted.

All methods for estimating CI described in this section have detailed description in work conducted by the Energy Research Company (EPE). This manual has the compilation of several correlations for different types of equipment for industrial natural gas installations (EPE, 2018), and can be used for different areas of the chemical industry as the basis for initial investment estimate.

3.4.2 - Total Depreciable Cost

The C_{CDT} calculation is calculated according to the relationships established by Table 17, and C_O is determined from 50% of C_I by the operating conditions of high pressure and temperature imposed by the integrated plant, and there is a need for a robust structure for power supply and utilities. From there, the C_E variable was established as 20% of C_{PDI} jointly with C_C as 25% of C_{IPD}. Although ammonia and urea synthesis processes are considered fully established technologies, the introduction of biogas as a raw material provides a higher degree of uncertainty for the project mainly in terms of adaptations necessary for pretreatment step. In addition, locality factor (f_l) was required equal to 1.4 considering the United States reference for plant construction (TOWLER AND SINNOT, 2012, MOURA, 2021).

3.4.3 - Total Fixed Cost

The C_{CFP} is determined from the calculation of all items contained in Table 18, with C_L being calculated directly from Eq. (60), returning the need for 16 operators. For the variable C_{SM}, the value of R$ 5000/month was established considering the average salary of an operation technician within the Brazil's reality industry. Furthermore, three additional positions are considered for the plant's labor cost structure: supervisor, process engineer, and plant manager. In addition, it is still necessary to include the costs of salary charges (C_{SC}) considering the 13th salary, Service Time Guarantee Fund (FGTS) and the rates of the National Social Security Institute (INSS), which represents approximately

70 % of C_{SC}. Therefore, C_{SA} can be calculated (LUZ *et al*., 2015). The data from Table 20 indicates cost structure associated with the plant's labor costs.

Table 20 - Estimated labor cost structure

Position	Employees	Month Salary (k R$)	Reference
Operators	16	5	Glassdoor (2024)
Supervisor	1	10	Glassdoor (2024)
Process Engineer	1	12	Glassdoor (2024)
Plant Manager	1	30	Glassdoor (2024)

3.5.4 - Variable Production Cost

The C_{CVP} is determined from the sum of the costs of raw materials, utilities, and wastewater treatment. The main raw material costs are the supply of biogas and process water, detailed in Table 21. The price range specified for biogas considers a series of technical aspects raised by CIBiogás such as origin of the substrate, technology used, percentage of biomethane and other technical aspects that directly affect the sales price charged for biogas. For this work, the maximum value was assumed due to biogas feed conditions (composed only of CH_4 and CO_2) and logistic/access limitations regarding biogas supply.

Table 21 - Raw materials costs

Raw materials	Unit	Price	Reference
Biogas	Nm³	0.20-0.65 R$/Nm³	CIBiogás (2023)
Water	ton	4.42 $ / ton	Moura *et al*. (2021)
Natural Gas	ton	0.6 $ / m³	ANP (2024)

Furthermore, the integrated plant to produce urea and ammonia has intensive use of utilities to keep operational conditions. Therefore, the integrated plant requires the supply of electricity (ELEC), Fired Heat (FH), low (LPS), medium (MPS) and high-pressure steam (HPS), and cooling water (CW). Moreover, due to the low temperature of the refrigeration cycle in ammonia synthesis loop, an refrigerant fluid is also needed. The main related costs are detailed in Table 22. The conditions regarding each utility are in Appendix B.

Table 22 - Plant utility costs

Utility	Unit	Price[a]	Reference[b]
Electricity (ELEC)	kWh	$ 0.08	Aspen Plus
Low-pressure steam (LPS)	GJ	$ 1.9	Aspen Plus
Medium-pressure steam (MPS)	GJ	$ 2.2	Aspen Plus
High-pressure steam (HPS)	GJ	$ 2.5	Aspen Plus
Fired Heat (FH)	GJ	$ 4.06	Aspen Plus
Refrigerant Fuild	CJ	$ 3.36	Aspen Plus

[a]Prices declared based in dollar; [b]The work used as reference used data provided directly by the Aspen Plus software.

3.4.5 - Sales products revenue

The S_V corresponds to the sum collected from the sales of products, by-products and possible waste that have a certain added value. In the present work, urea is synthesized as the main product, however there is the possibility of commercializing surplus carbon dioxide generated as waste during the production process (CO_2 residual trading was only considered in the sensibility analysis). Table 23 contains the prices charged for the products.

Table 23 - Products/by-products prices used for selling

Product	Unit	Price[a]	Reference
Urea	ton	400	IHS Markit
CO_2	ton	60	Moura *et al*. (2021)

[a]Prices declared based in dollar; [b]Values updated for year 2021.

3.4.6 - Discounted Cash Flow

Net Present Value (NPV) was used as the main criterion for the project economic evaluation, with the investor interest rate (i) being established at a value of 10%. The time determined for the project corresponds to a period of 25 years, 3 of which are for construction of the plant and the remainder for operation (ZHANG *et al.*, 2020; ZHANG *et al*., 2021). Furthermore, it is considered that the plant will operate 7920 hours annually (330 days), and the annual depreciation of the plant is calculated from Eq. (62).

During the plant construction period, it is assumed that 70% of the capital will come from external financing and the remaining 30% will come from equity. For the financed capital, an interest

rate of 10% p.y. will be applied on the debt assumed. During plant's construction period, it is assumed that no interest payments will be done due to the lack of income. From the first year of operation, there will be an annual payment of the amortization constant tax from the financial debt assumed and financial expenses related to the interest payments.

The financing rate takes into account the National Consumer Price Index (IPCA) along with the inclusion of the credit risk rate, in which represents a strategic and well-founded approach to the current context of credit granting and financing. Firstly, by anchoring the interest rate to the IPCA index, it's possible to adopt solid benchmark to mitigate the effects of inflation. Moreover, the value assumed considers not only the capital cost, but also the operational and administrative costs involved. The inclusion of the credit risk rate is crucial to reflect market realities and the inherent risks in financial transactions. This rate, determined based on the borrower's credit analysis, considers factors such as payment history, financial capacity, and macroeconomic conditions, allowing for a more accurate assessment of the risk involved in the transaction. Thus, by incorporating this rate, we are ensuring more appropriate pricing of the financing, reflecting the actual risks involved and strengthening the sustainability of the credit system as a whole (BNDES, 2024).

The accumulated NPV is directly influenced by the assumptions adopted for the annual cash flow during the project's duration. Equation is used to calculate the DCF, considering an income tax rate (t_{ir}) of 34%. It is important to mention that income tax is calculated based on the Income Statement (IE). In this way, the calculation of the annual DCF follows the schedule shown in Table 24 considering the time stipulated for plant construction and normalized operation.

Table 24 - Schedule and assumptions established for discounted cash flow

Year	Cost	Income	Stage
1	0.3 C_{CIT}	0	Construction
2	0.5 C_{CIT}	0	Construction
3	0.2 C_{CIT}	0	Construction
4	C_{CFP}+ 0.5 C_{CVP}	0.5 S_V	*Startup*
5	C_{CFP}+ 0.9 C_{CVP}	0.9 S_V	Plant Stabilization
6-24	C_{TP}	S_V	Normal operation
25	C_{TP}	$S_V + C_{WC}$	Normal operation and project's end

Moreover, Table 25 contains the details regarding the main assumptions made during DCF analysis of the work.

Table 25 - Main assumptions made for techno-economic assessment

Variable	Value
Interest rate (%)	10
Project years	25
Plant construction period	3
Financed capital (%)	70
Interest Rate applied to financed capital (%)	10
Income tax (%)	34
National factor	1.4
Annual hours of operation (hours/days)	7920/330

4. Results and Discussion

4.1 - Ammonia reactor

As described, the ammonia plant was designed to produce approximately 500 ton/day to supply the urea plant. All stages before the reactor section aimed to produce and purify the synthesis gas, as well as to adjust the H_2/N_2 molar ratio close to the stoichiometry of the reaction. Thus, the synthesis cycle is the main stage of the plant. Ammonia synthesis presents complex operating conditions due to the exothermic and reversible characteristic of the reaction, limiting the conversion rate due to thermodynamic equilibrium (CARVALHO, 2016). Figure 29 illustrates the variation in molar composition, temperature, and conversion profile throughout the reactor. The operating conditions were 200 atm pressure, purge/recycle ratio equal to 0.045 and H_2/N_2 molar ratio equal to 3 in the reactor inlet stream. Also, Table 26 indicates the composition of inlet and outlet stream of the ammonia reactor.

Table 26 - Molar composition of inlet/outlet stream in the ammonia synthesis loop

Components	Inlet stream (% molar)	Outlet stream (% molar)
N_2	23.8	19.5
H_2	71.3	58.6
CH_4	2.4	2.8
Ar	1.1	1.3
NH_3	1.4	17.6

In Figure 29, it is important to notice the presence of the physical limitation of the catalytic beds, characterizing the existence of intermediate cooling according to the description made in Section 3.1.5. Figure 29a shows the gradual decrease in the molar fraction of reactants N_2 and H_2 and the progressive increase in the molar fraction due to the reaction progress as expected in the literature (AZARHOOSH *et al.*, 2014; PAIXÃO, 2018).

Figure 29b shows the temperature profile with the physical boundaries of the reactors being well characterized. Firstly, there is an increase in temperature during the operation of the catalytic beds and the discontinuities in the graph reflect the presence of intermediate heat exchangers. Depending on the exothermic characteristics of the reaction and the adiabatic operation of the reactors, it is necessary to cool the output streams of the intermediate beds to maximize the conversion considering the restriction imposed by the thermodynamic equilibrium. It is verified that the exit

temperature in each catalytic bed does not exceed 500 ºC and $\Delta T \leq 100$ ºC according to the established operational safety rules (AZARHOOSH *et al.*, 2014; CHEEMA *et al.*, 2018; YOSHIDA *et al.*, 2021).

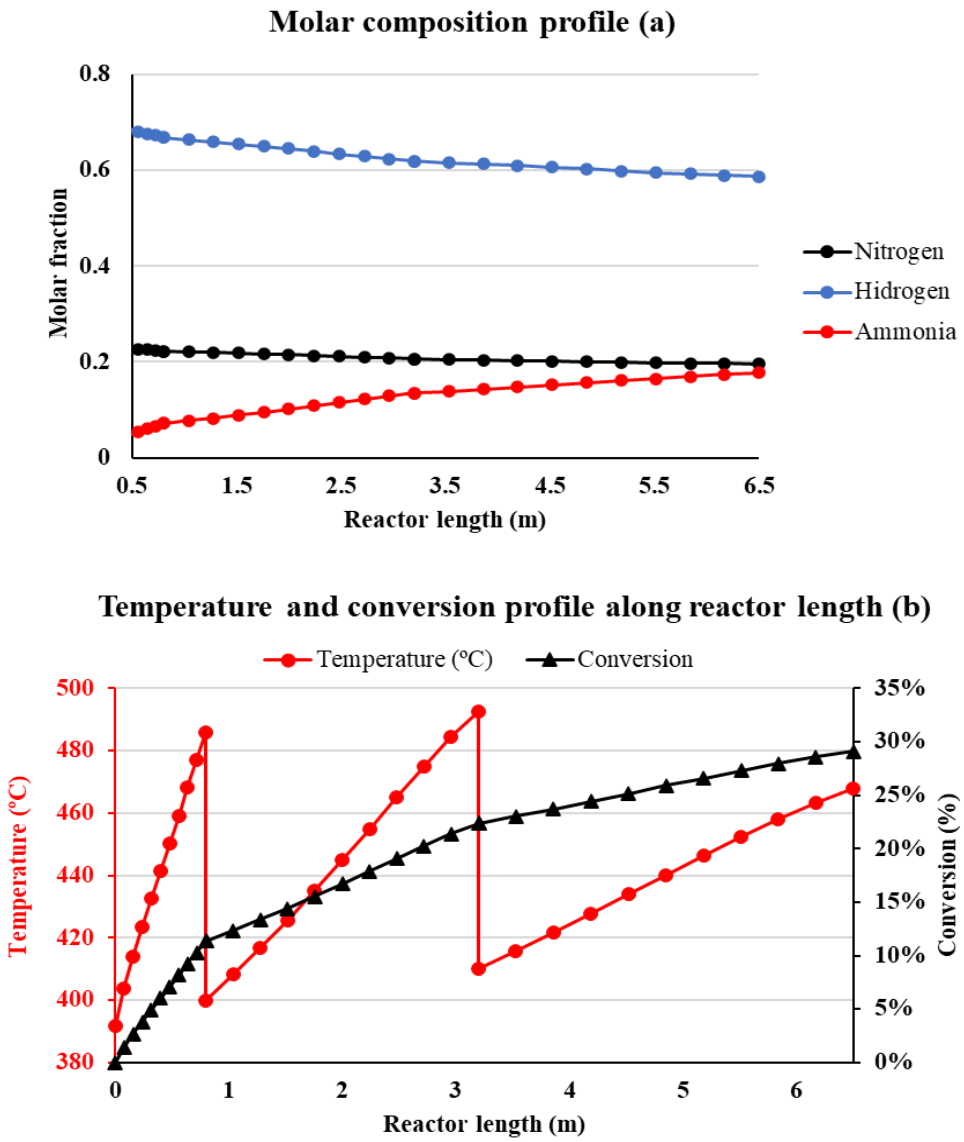

Figure 29 - Molar composition profile of the main components (N_2, H_2 e NH_3) (a), temperature and conversion (b) alongside reactor's length (200 atm, purge/recycle ratio: 0.045 e H_2/N_2 molar ratio: 3).

Furthermore, Figure 29b also illustrates the conversion profile. A gradual decrease in the conversion rate is observed along the reactor beds, which can be directly explained by the continuous formation of ammonia and the restriction imposed by reverse reaction. This behavior is confirmed at the physical boundary between the catalytic beds, being indicated by the slope of the conversion curves (black lines). A conversion per pass of approximately 29% was obtained, in line with the values reported in the literature and within the expected range of 25-30% (AZARHOOSH *et al.*, 2014; CARVALHO, 2016; CHEEMA *et al.*, 2018; MOURA *et al.*, 2021; YOSHIDA *et al.*, 2021).

Besides, data on the progress of the reaction through conversion and temperature can also be expressed in relation to the reaction volume as shown in Figure 30. It is interesting to note a behavior very similar to that observed in Figure 29b, showing the gradual decrease in conversion with increasing reaction volume as explained by Cheema *et al*. (2018) and Yoshida *et al*. (2021).

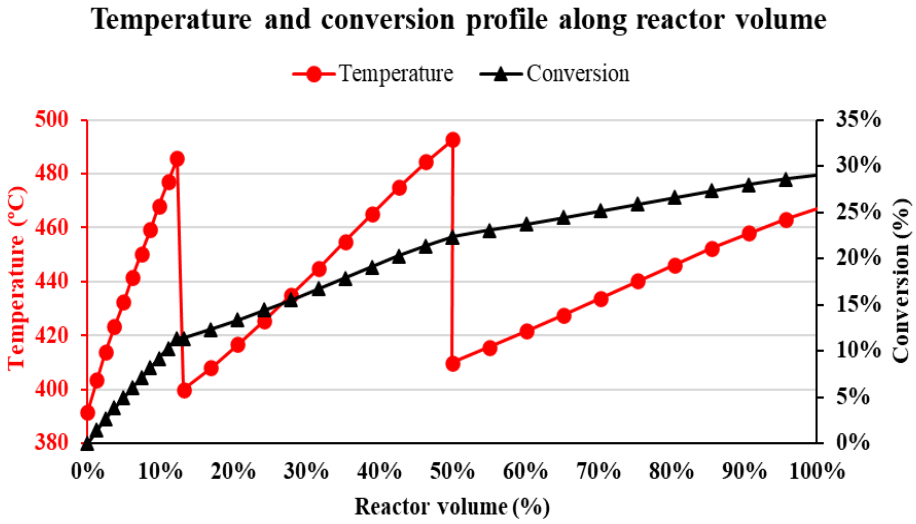

Figure 30 - Temperature profile and conversion by reaction volume (200 atm, purge/recycle: 0.045 e H_2/N_2 molar ratio: 3).

4.2 - Stamicarbon process

Like the ammonia synthesis loop, the urea production process is also conducted under high pressure conditions (135-140 atm), however the operating temperature conditions of the equipment are milder, varying between 150 and 200 ºC. As illustrated in Figure 28, the system is interconnected to promote the recycle of unconverted reactants and benefit from CO_2 as a stripping agent. In this way, the entire process operates under the same pressure condition (140 atm) due to the connection of existing equipment and streams.

The carbamate condenser, also known as pool condenser, is fed by the gaseous stream coming from the high-pressure stripper (recirculated unconverted reactants) and the liquid stream containing the mixture of fresh ammonia inlet and the carbamate solution processed in the scrubber. This equipment participates in the synthesis of urea in the STAC unit. However, information on the specification for both the formation of ammonium carbamate and urea is very limited, which makes it difficult to provide a basis for direct comparison even for a qualitative analysis. The works done by Chinda (2015, 2019) address the difficulty in obtaining detailed operational information about the equipment, validating the simulation based on the steam generated with data made available by FAFEN. Furthermore, the plant design provided by the *Aspen Plus* software (ASPEN TECH, 2008b)

does not consider the synthesis of urea in the condenser pool, that is, it only specifies the formation of ammonium carbamate.

As detailed previously (Section 3.2.3), the carbamate condenser was simulated as a stoichiometric reactor operating at a temperature of 170ºC. The conversion of each reaction was conditioned on the operation of the reactor, with the CO_2 conversion and mass fraction of urea in the liquid outlet stream of the reactor determining the extent of the reactions in this equipment. In industrial plants, the pool condenser has two outputs for the liquid and gaseous lines, while for this work only one output stream was adopted containing both liquid and vapor streams. This is a result from the modeling of the pool condenser as a stoichiometric reactor and the two-phase operation of the main reactor where occurs the necessary mass transfer from reactants into the liquid phase (ASPEN TECH, 2008b).

The carbamate condenser represents an important piece of equipment for the efficient operation of urea synthesis as discussed previously, but the scarcity of data in the open literature limits a more detailed and accurate analysis regarding the influence of this equipment on the general performance of urea synthesis. Therefore, a simplified representation was adopted for the pool condenser, considering the intrinsic phenomenology, and linking its operation to important operating parameters of the urea reactor (CHINDA, 2019).

The main equipment of the Stamicarbon process is the urea reactor, modeled and simulated from a sequence of CSTRs reactors to reproduce the internal trays in the industrial equipment (CHINDA, 2015; HAMIDIPOUR *et al.*, 2005; RASHEED, 2011; ZHANG *et al.*, 2005; ZENDEHBOUDI *et al.*, 2014). The urea reactor has a two-phase operating condition, receiving gaseous reactants (NH_3 and CO_2) and a liquid stream containing ammonium carbamate, urea, and water. Both streams come from the carbamate condenser. The inlet (170 ºC) and outlet (185 ºC) temperatures were chosen to emulate the temperature behavior throughout the equipment, assuming a linear profile during the sequence of CSTRs (BROUWER, 2009a; DENTE *et al.*, 1992; HAMIDIPOUR *et al.*, 2005). The increase of temperature throughout the CSTRs is explained by the characteristic of the urea synthesis reaction system, since the formation of ammonium carbamate represents a fast and exothermic reaction, while the dehydration of the intermediate for urea synthesis is endothermic and corresponds to the slow stage of the process. Therefore, the urea reactor operates with long residence times for urea synthesis to occur, and the energy released for the synthesis of ammonium carbamate is reused to promote the synthesis of urea. Thus, an gradual increase in temperature throughout the reactor is expected.

To calculate the reactor operating parameters, the data obtained at the exit of the liquid stream were evaluated: analysis of the mass composition, NH_3/CO_2 (N/C) molar ratio and CO_2 conversion to urea, using Equations (68) and (69):

$$\chi_{CO_2} = \frac{wt\ urea}{wt\ urea + 1.365\ wt\ CO_2} \quad (68)$$

$$\frac{NH_3}{CO_2} = \frac{2\ wt\ urea + 3.53\ wt\ NH_3}{wt\ urea + 1.365\ wt\ CO_2} \quad (69)$$

where wt represents the mass fraction of the components in the liquid outlet of the reactor. It is worth noting that due to the hypothesis that CO_2 exists in a minimal extent in the liquid phase, it is expected that CO_2 is converted in the form of the intermediate ammonium carbamate. Therefore, it was necessary to recalculate the mass fractions of CO_2 and NH_3 according to the stoichiometric relationship regarding Eq. (29) and each compound molar mass, adapting the original expressions found for Equations (68) and (69), being rewritten based on Equations (70) and (71):

$$\chi_{CO_2} = \frac{wt\ urea}{wt\ urea + 0.76\ wt\ carbamate} \quad (70)$$

$$\frac{NH_3}{CO_2} = \frac{2\ wt\ urea + 3.53\ (wt\ NH_3 + 0.44\ wt\ carbamate)}{wt\ urea + 0.76\ wt\ carbamate} \quad (71)$$

This consideration was also assumed for the work of Rasheed (2011) and Chinda (2015), with the objective of quantifying the composition of ammonium carbamate present in the system's liquid streams, being extremely useful information in scrubber and stripper equipment. Table 27 contains molar and mass composition data at the exit of the liquid stream from the reactor.

Table 27 - Molar and mass composition of the liquid exit stream from the urea reactor

Components	Molar composition (%)	Mass composition (%)
CO_2	1.5	2.0
NH_3	40.0	20.6
Ammonium carbamate	12.2	28.8
Urea	18.2	33.1
H_2O	28.1	15.3

Urea has the highest mass percentage at the exit of the reactor's liquid stream, reaching a value close to 33%. Hamidipour *et al.* (2005) obtained a simulated value of 33% for urea at the outlet of the reactor's liquid stream, while data from the real plant indicated a mass composition close to 34%. Rasheed *et al*. (2011) and Zhang *et al*. (2001) also obtained values greater than 30% for urea mass composition. Furthermore, the CO_2 conversion and the N/C ratio were also calculated at the reactor's liquid stream outlet, reaching values of 60% and 3.3, respectively. The results for both parameters are also in line with the literature as the conversion χ_{CO_2} generally varies between 55 % and 70% due

to the thermodynamic limitations of the urea synthesis process, while the N/C parameter normally varies in a range between 3.0 and 5.0 (BROUWER, 2009a; RASHEED, 2011; ZHANG *et al*., 2001; ZHANG *et al*., 2005; ZENDEHBOUDI *et al*., 2014). Figure 31 represents the molar composition profile throughout the series of CSTRs.

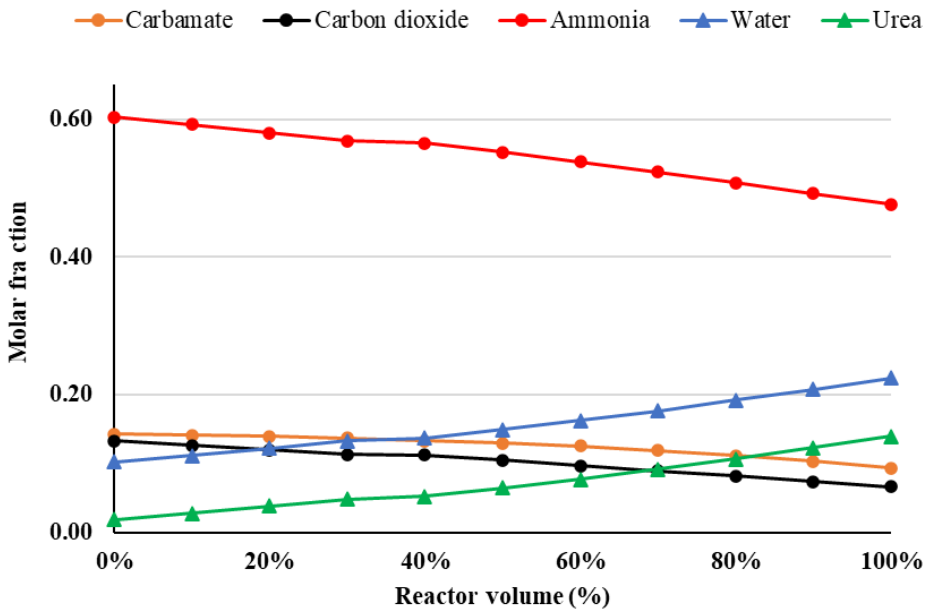

Figure 31 - Molar composition profile alongside reactor volume.

As expected, there is consumption of reactants (ammonia, carbon dioxide and ammonium carbamate) throughout the reaction volume and, consequently, the generation of products (water and urea) resulting from the dehydration of ammonium carbamate. The observed behavior is also seen in the work of different authors such as Chinda (2015), Zhang *et al.* (2005) and Zendehboudi *et al.* (2014). Furthermore, Figure 32 contains data relating to the distribution of residence time throughout the trays/CSTRs, in which is observed a trend of a progressive increase in the residence time due to the decrease in the vapor volume and the continuous mass transfer of reactants to liquid phase and the progress of the reaction. In absolute terms, the total residence time reached a value of 0.50 h (30 min) at the exit of the last tray. This value is also corroborated by the literature due to the slow characteristic of the urea synthesis reaction, where residence time values vary between 20 and 40 minutes and the volume used for the tray/CSTRs reflects data obtained from industrial plants (DENTE *et al*., 1992; CHINDA, 2015; RASHEED, 2011).

The liquid effluent from the reactor contains urea, water, and unconverted reactants (carbamate, ammonia, and carbon dioxide in small concentrations). This stream is directly routed to the high-pressure stripper, where the fresh carbon dioxide stream is fed in countercurrent to provide the decomposition of unconverted carbamate.

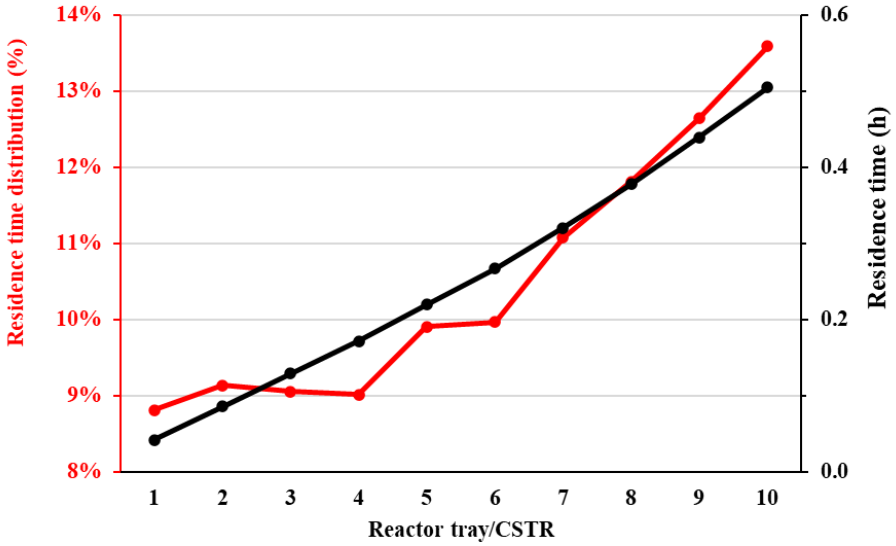

Figure 32 - Distribution of residence time throughout the urea reactor.

Figure 33 represents the temperature profile in relation to the number of stages in the high-pressure stripper. This behavior is explained by the constant MPS steam supply between stage 2 and 9 to decompose the residual ammonium carbamate (Appendix B). Stages 1 and 10 only have the inlet of liquid and vapor streams, respectively. The liquid stream is fed to the top of the stripper (stage 1) with high temperature (185 ºC) and there is a large amount of material coming from the main reactor. On the other hand, the last stage (stage 10) feeds the CO_2 flow in countercurrent in a lower temperature (100ºC). (ASPEN TECH, 2008b; CHINDA, 2015).

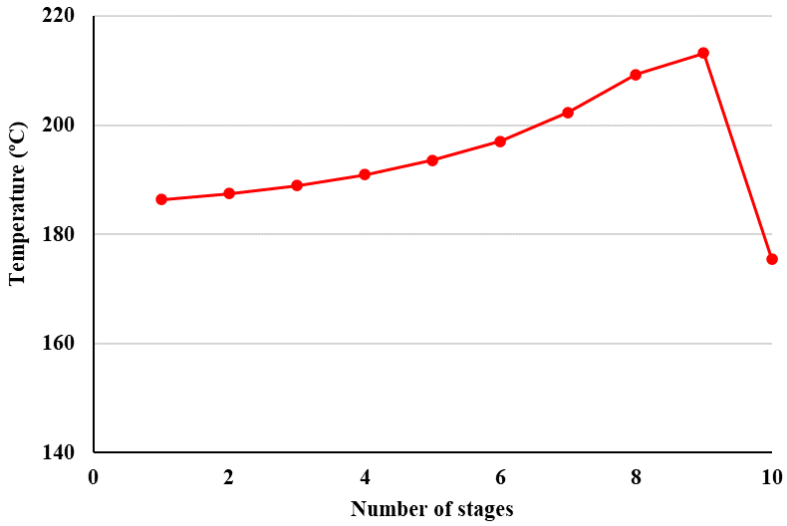

Figure 33 - Temperature profile in relation to the number of high-pressure stripper stages.

This operational configuration makes it possible to maximize mass transfer between the liquid and gaseous phases, in which the constant decomposition of unreacted carbamate occurs throughout

the stages of the high-pressure stripper. The profile of the vapor molar composition along the stripper is illustrated in Figure 34. It can be seen, according to the data provided, that CO_2 has the maximum molar composition in the lower stage (stage 10), which is an expected behavior considering the gaseous supply at the bottom of the equipment. Besides, NH_3 presents the minimum molar composition in stage 10, with an increase observed until the upper stage, that is, at the top of the high-pressure stripper. This phenomenon is justified by the upward flow of ammonia in a gaseous state resulting from the decomposition of residual carbamate in the liquid phase. The molar composition profile of the liquid phase along the stripper (Figure 35) complements and validates the results analyzed in Figure 34.

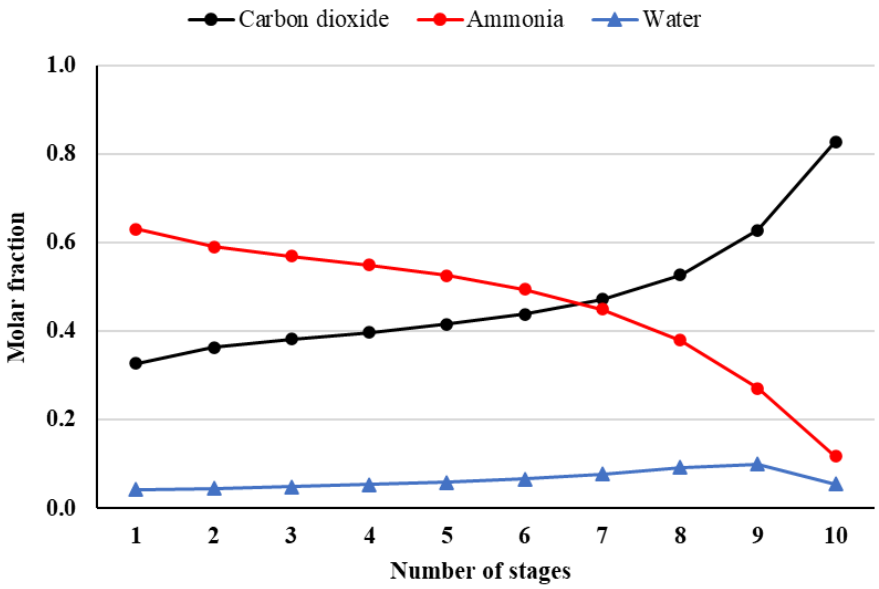

Figure 34 - Molar composition profile in the vapor phase alongside stripper stages.

The gradual increase in the molar fraction of urea and water in the liquid phase is noticeable throughout the high-pressure stripper, with the maximum observed at the bottom of the column where the concentrated stream exits. Furthermore, the progressive reduction of ammonium carbamate is also observed due to its decomposition into the reactants ammonia and carbon dioxide, being transferred to the gaseous phase and recirculated to the synthesis system from the top of the equipment. The behavior observed in both the vapor and liquid phases is corroborated by the works of Chinda (2015) and Zhang *et al* (2005), showing that the simulation strategy used based on the constant supply of thermal load between stages 2 and 9 was capable to reproduce the phenomenology of the equipment. Under stripper operating conditions, urea is found only in the liquid phase, and its chemical affinity with water means that both components are represented as just a single component in ternary diagrams associated with the system's phase equilibrium. This interaction between the two compounds also justifies the small variation of water in the composition of the vapor phase (BROUWER, 2009b,

CHINDA, 2015). The bottom stream has the concentrated liquid stream containing the product of interest, and in this work the mass fraction of urea was established to reach the value of 77% (EDRISI *et al.*, 2016, ZHANG *et al.*, 2021).

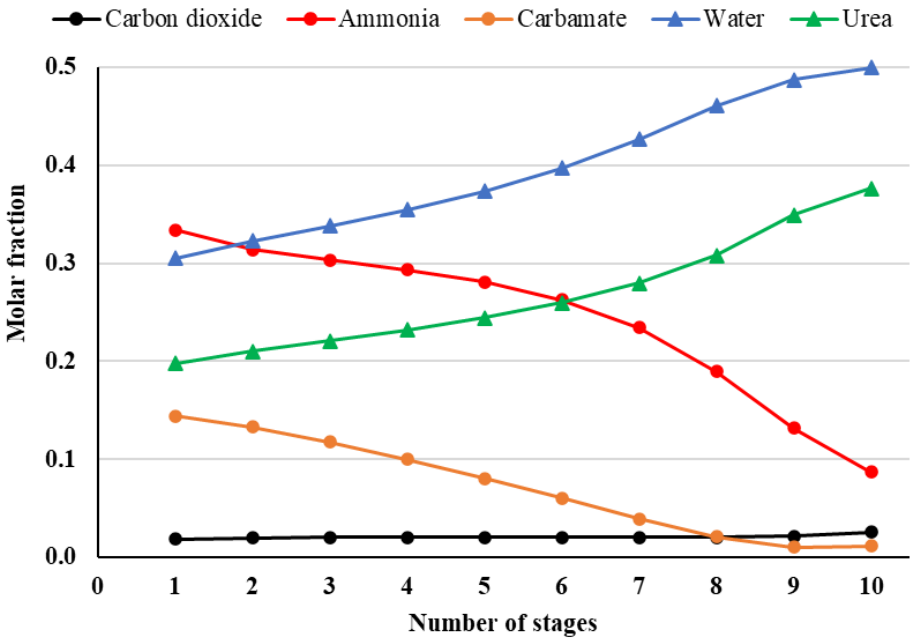

Figure 35 - Molar composition profile of liquid phase alongside stripper.

Finally, the role of the scrubber is to promote the condensation of unconverted vapors coming from the reactor and entering the last stage of the equipment, while the top receives the carbamate solution recirculated from the product concentration section. The countercurrent flow facilitates mass transfer between the phases, with the synthesis of ammonium carbamate occurring along the scrubber profile, where the liquid solution is led to direct mixing with the fresh ammonia stream that enters the Stamicarbon system. At the top of the equipment, the gas stream contains the fed inerts and a small percentage of the reactants that are not dissolved into the liquid phase. However, like the carbamate condenser, there is no open data in the literature for validation and direct comparison of the results involving the scrubber.

4.3 - Operational results regarding the ammonia-urea integrated plant

As previously discussed, a flow of 1000 kmol/h (~ 22300 Nm^3/hr) containing 60 and 40% CH_4 and CO_2 was used as a benchmark. It was established that methane is completely separated from the CO_2 stream, which is a direct by-product of the process with a flow rate of 400 kmol/h (~ 422 ton/day). The biogas and water feed rates are intended to keep the H_2O/CH_4 molar ratio equal to 3 to increase the useful life of the catalysts used in methane reforming. With this performance indicator as a

guideline, the plant operates continuously with a total steam flow rate in the range of 1800 kmol/h (considering the 600 kmol/h feed in the biogas stream). The total amount is composed of a make-up stream and the residual water stream coming from the CO_2 removal section after FLASH-01. This water stream is separated and recirculated past the shift reactors with a total flow rate of 965 kmol/h (~17.4 ton/h), while the make-up water stream provides a continuous feed of 841 kmol/h (~15.2 ton/h). It is also worth highlighting that CO_2 removal section is responsible for cleaning the gaseous effluent that will be sent to the synthesis loop. Therefore, a concentrated CO_2 stream of 585 kmol/h (25.7 ton/h) is produced as a direct by-product of the shift stage and can be sent to the urea synthesis section and is completely absorbed by the urea plant.

Furthermore, atmospheric air flow is introduced into the secondary reforming stage to supply the necessary nitrogen in the synthesis loop and enough oxygen demand to complete methane combustion in the secondary reformer. All syngas preparation steps work together to promote the adjustment of the H_2/N_2 molar ratio in stoichiometric proportions for the synthesis loop. Therefore, the atmospheric air flow rate required is approximately 850 kmol/h (~ 24.5 ton/h) to guarantee that operating condition before the gas stream enters the synthesis loop. Table 28 contains the main data regarding operational parameters of syngas preparation section, detailing raw material flow rates.

Table 28 - Main results from ammonia plant regarding syngas preparation

Variables	Values
Air flow rate (kmol/h)	850
CO_2 flow rate (kmol/h)	985[a]
Water steam flow rate (kmol/h)	~1800
H_2O/CH_4 molar ratio	3
H_2/N_2 molar ratio	3

[a] Sum of residual CO_2 purification stream and CO_2 removal section.

At the end of the syngas preparation process, the inlet stream of synthesis loop has as its majority molar composition the presence of the reactants N_2 and H_2, corresponding to a value close to 95%. The remaining percentage is made up of reactants recirculated after leaving the last stage of the main reactor. The main reactor strategy involves the existence of three catalytic beds coupled with heat exchangers. Ammonia synthesis presents complex operating conditions due to the exothermic and reversible characteristic of the reaction, limiting the conversion rate due to thermodynamic equilibrium. The goal is to maximize conversion considering the restriction imposed by thermodynamic equilibrium (temperature and conversion profiles alongside reactor are illustrated in

Figure 29) (AZARHOOSH *et al*., 2014; CARVALHO, 2016; CHEEMA *et al*., 2018; PAIXÃO, 2018; YOSHIDA *et al*., 2021).

A daily production of 480 ton/day (~1175 kmol/h) of ammonia with a purity of 98.5% on a molar basis is observed after the refrigeration cycle, with the remainder of the composition consisting of unreacted gases and inert gases. The purge/recycle ratio is relevant because it promotes the recovery of unconverted gases and control of the concentration of inert gases present in the feed stream of the first catalytic bed. Therefore, the value of 0.045 was defined because it is possible to reconcile a value for the global reactor conversion close to 29% and the product stream conditions (flow and purity) desired to supply the demand coming from the urea synthesis section. Values lower than 0.045 for the purge/recycle ratio promote an increase in the inerts concentration in the reactor feed stream and, consequently, a decrease in the overall conversion of the process and in the purity of the ammonia product stream (CARVALHO, 2016; PAIXÃO, 2018). Table 29 contains the main results regarding ammonia plant.

Table 29 - Main results regarding ammonia plant

Variables	Values
Purge/recycle ratio	0.045
Pressure (atm)[a]	200
NH_3 production (ton/day / kmol/h)	480 / 1175
Purity (% mol/mol)	98.5
Conversion (%)	~29

[a] Loop synthesis and refrigeration cycle pressure.

According to the logical sequence of the process, the two raw materials necessary for urea synthesis are fully supplied by the ammonia plant. The CO_2 and NH_3 feed flow rates were 600 and 1.175 kmol/h, respectively, following a stoichiometric NH_3/CO_2 molar ratio close to 2. Table 30 describes the main results regarding urea synthesis.

All the validation results were discussed before (Section 4.2) to highlight the difficulties about getting open data regarding Stamicarbon process. In this context, some assumptions were made to try to represent the intrinsic phenomenology of each piece of equipment. The carbamate condenser and scrubber are the two pieces of equipment which very have limited open data. On the other hand, the reactor and stripper both can be modeled with more accuracy giving that more studies are available to compare different approaches (CHINDA, 2015; HAMIDIPOUR *et al*., 2005; RASHEED, 2011; ZENDEHBOUDI *et al*., 2014). The flow rate of urea produced in the synthesis section was approximately 840 ton/day.

Table 30 - Urea synthesis main results

Variables	Values
CO_2 flow rate (kmol/h)	600
NH_3 flow rate (kmol/h)	1175
Urea production (ton/day)	840
Conversion (%)	60

Figure 36 details the plant's energy demand profile broken down by equipment and process section. In fact, the energy demand of reformers added to that of coolers/condensers represents more than 60% of total energy demand. This fact is explained by the need for successive cooling streams inside ammonia production process and the high endothermic characteristic of the methane reforming reaction. Besides, power equipment (compressors) and the equipment from Stamicarbon are responsible for approximately 37% of the plant's total energy demand due to the operating conditions detailed above (pumps contribution to energy consumption is despicable compared to compressors).

Furthermore, according to the results obtained for Figure 36b, both ammonia synthesis (~27%) and steam reforming (~23.7%) sections are responsible for almost 50% of total energy demand. For the first, the operational complexity discussed previously in this work stands out due to the severe conditions of pressure, temperature, and several heat exchange stages necessary. Besides, the urea synthesis also has a major contribution (~18%) to the total integrated plant total energy demand due to the high-pressure steam feed into the stripper and the heat removed from the scrubber.

Figure 37 illustrates the differences between conventional process and new concept using biogas as main feedstock. As described in previous sections, the integrated plant considers full replacement of natural gas by biogas as raw material without modifying existing technologies. Regarding conventional process, the main change is related to raw-material pre-treatment due to the higher concentration of CO_2 in the feed stream. In the natural gas plant, there is no need for an upgrade process due to the higher methane concentration.

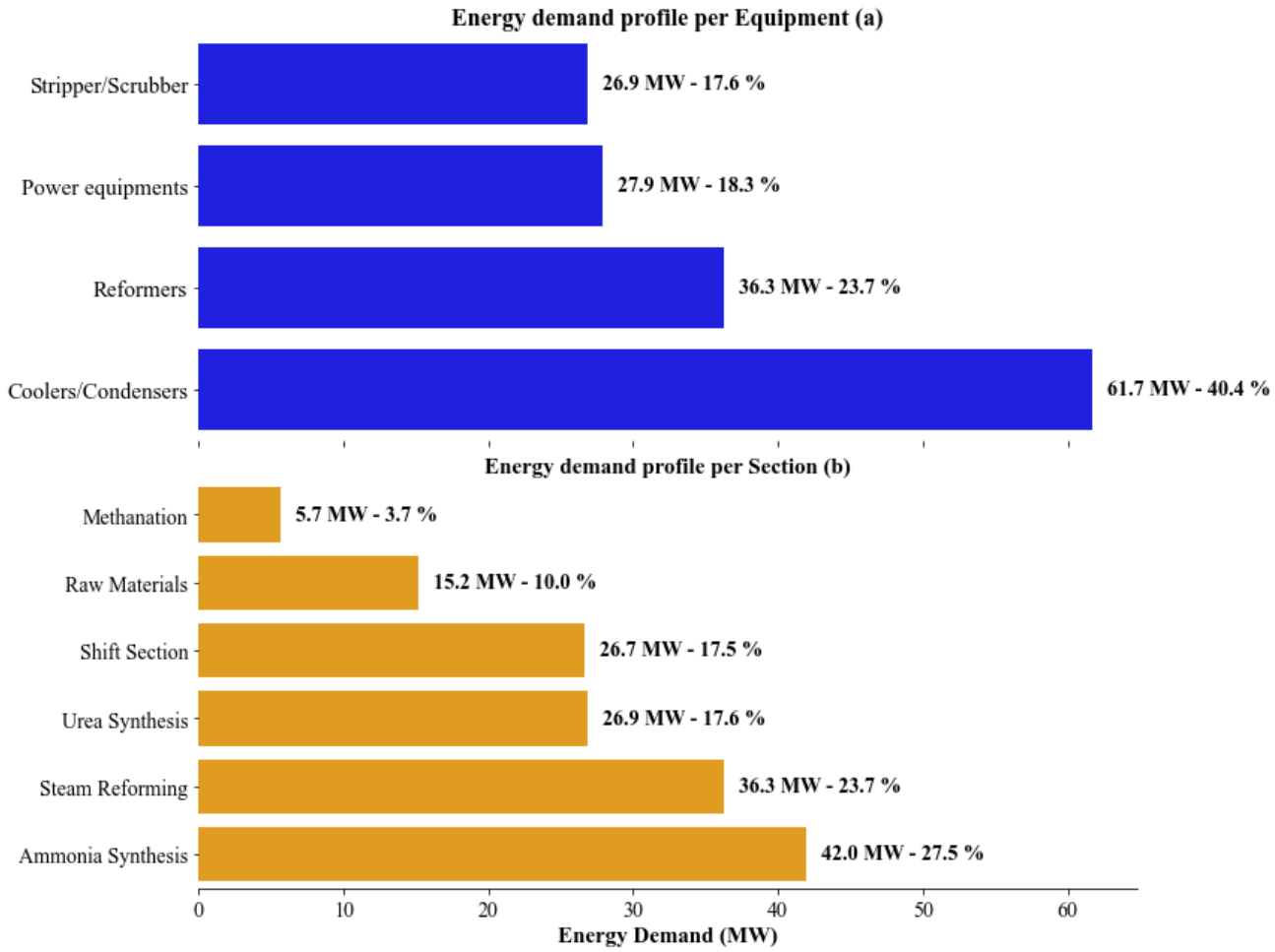

Figure 36 - Energy demand profile of integrated plant per equipment (a) and process section (b).

Another relevant challenge is to guarantee the continuous supply of the unit fed by biogas considering the availability of raw materials and coordinated operation of a series of biodigesters. Plant's location becomes a relevant aspect to ensure a high availability of biogas production, which requires its own infrastructure of surge tanks and gas pipelines to avoid any supply chain problems. Furthermore, another relevant topic refers to the large surplus of almost 400 kmol/h CO_2 from the biogas upgrading. The ammonia plant is capable of supplying urea synthesis due to the presence of methane steam reforming, causing CO_2 to become an unwanted waste if it is not sold. Therefore, residual CO_2 monetization would lead to an increase in the total revenue and an improvement in the project economic metrics. This should be important as recurring revenue considering CO_2 is a by-product and should not need a huge additional investment due to products specifications regarding the first separation step. However, there are challenges which are related to prospect nearby customers and the technical specification required for trading. Besides, the residual CO_2 comes directly from a renewable source, what means it would also be possible to store that amount and sell carbon credits in the open market. From this perspective, it has an interesting path to certificate urea production as a low carbon product and possibly increase the selling price.

After pre-treatment of raw material, the new process becomes very similar to the traditional process, without the need to replace technologies due to the technological maturity existing in industry. New alternatives have been studied to reduce energy expenditure and environmental impact, such as the implementation of bi-reforming reactors to replace the traditional steam reforming process (MOURA, 2021), integrated plant concepts for the production of urea from biomass in a fully renewable process (ZHANG *et al.*, 2020; ZHANG *et al*, 2021) and the use of wind energy sources and electrolysis to obtain the necessary hydrogen (CARVALHO, 2016; PAIXÃO, 2018; REESE *et al*., 2016). However, there are still technological challenges to compete economically with the traditional process in the coming years, requiring greater investment for the gradual establishment of new concepts.

4.3 - Economic Assessment

Table 31 includes the main indicators related to the economic breakdown of the integrated plant considering the natural gas and biogas as the main feedstocks. The base scenario only involves urea as the main product, without any revenue being obtained from byproducts (carbon dioxide). Seeking a fair comparison, the same assumptions were established to evaluate both biogas and natural gas scenarios.

From the results, the plant's operation with natural gas presents worse economic and financial indicators when compared to the plant integrated with biogas. The results show that in the price scenario used in this work, biogas presents itself with a more competitive raw material in an integrated plant to produce urea. This's mainly explained by the low competitiveness of the national natural gas prices compared to the international scenario, which directly hinders investments in the Brazilian chemical industry.

Table 31 - Economic parameters for techno-economic assessment considering natural gas and biogas

Raw Material	NPV (MM $)	IRR (%)	Payback (years)
Natural Gas[a]	-335	-43.4	-
Biogas	-98	3.5	-

*Both scenarios have the same economic and operating conditions; [a]Natural Gas composition is considered 100% methane.

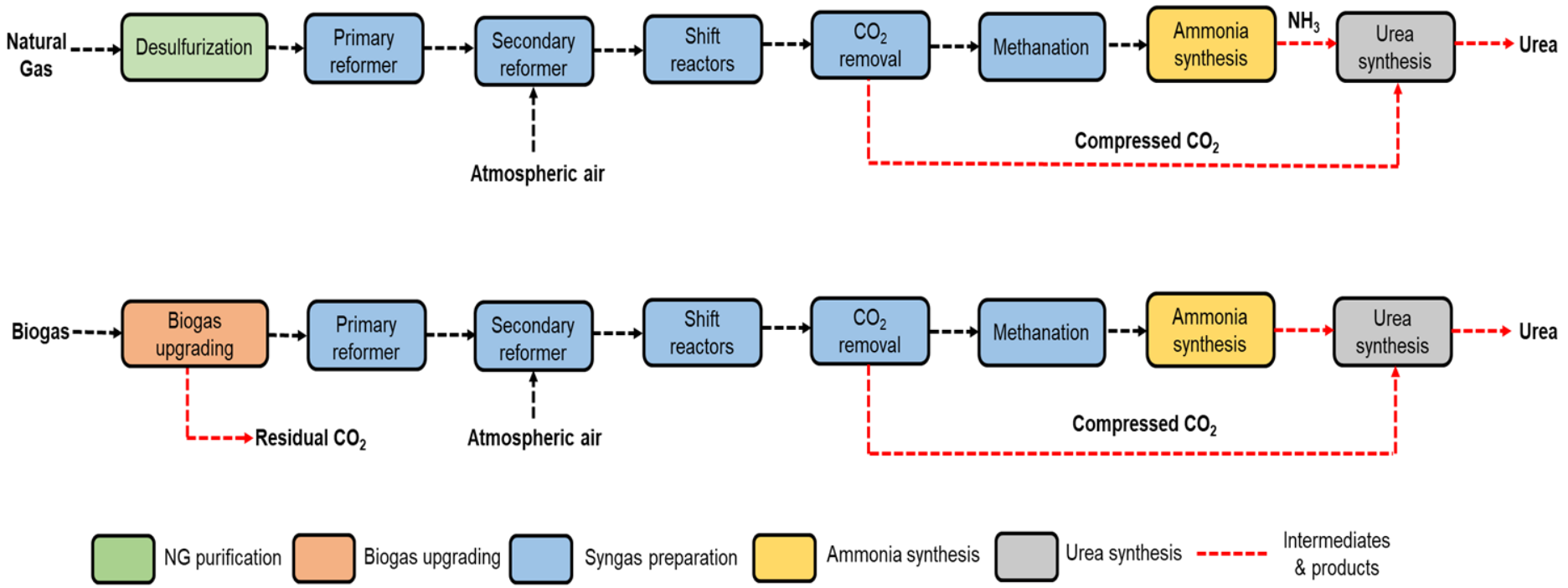

Figure 37 - Conventional and innovative configuration for ammonia and urea synthesis.

For large scale chemical industries, the price of raw materials is the main component of the operating cost. Any variation in price directly affects cash flow, being a detractor for the operating margin. The availability of natural gas under suitable conditions is increasingly a decisive factor for the country's competitiveness and directly affects the development of national industry (FIRJAN, 2011; ANP, 2024).

A study conducted by FIRJAN (2011) reported natural gas consumption prices from 18 distributors operating in 15 federal units. It was possible to determine the average natural gas tax for industry in Brazil: US$ 16.84/MMBtu. This value was 17% higher than the average of US$ 14.35/MMBtu found for a set of 23 countries with available data. When compared to the other BRICS countries, the national industrial natural tax was more than twice the average of China, India, and Russia (US$ 7.24 US$/MMBtu). Furthermore, EPE (2019) conducted a study related to the competitiveness of natural gas within the nitrogen fertilizer industry. The case study was carried out based on a Petrobras nitrogen fertilizer unit with a capacity of 3600 ton/day and demand of 2.2 MM m^3/day of natural gas. Considering the sales price of 294 USD/ton of urea, it was found that the price of natural gas viable for investments in the plant would be in the range between 4 - 7 USD/MMBtu, indicating values well below the reality of national natural gas market according to the historical series provided by the ANP and available reports.

The results reported above indicate a highly concerning scenario for the national industry and rule out the possibility of using natural gas as an affordable raw material source the fertilizer industry. The use of biogas is directly affected by the availability of secure sources for transition, thereby ensuring the continuous supply of industrial-scale plants. The findings outlined in the studies reaffirm the importance of natural gas for the national nitrogenous fertilizer segment, where the relative cost of raw materials is a significant factor in the decision to invest in a new plant. Addressing the challenges surrounding natural gas affordability and accessibility is crucial not only for maintaining competitiveness in the fertilizer industry but also for fostering a more sustainable and resilient energy ecosystem conducive to long-term industrial growth and development (FIRJAN, 2011; EPE,2019).

The biogas plant scenario presents a financial perspective marked by a negative NPV(~98 MM). Such a scenario typically suggests that the project under consideration is yielding returns below the initial investment, as indicated by the financial metrics. The results obtained show the impact of the high investment required on the plant’s total cost due to the necessary operational conditions. Furthermore, it is worth mentioning that the estimated IRR was 3.5%. Consequently, while the project indicates that isn’t financially lucrative in absolute terms, the positive IRR implies that it still holds some potential for generating returns, albeit at a lower rate than expected. Figure 38 illustrates the temporal evolution of cash flow throughout the established project horizon (25 years).

As indicated from the results in Table 31, Figure 38 shows that there is no payback considering the base scenario (the curve sign would have to change if that happens and NPV would turn positive). Furthermore, the significant negative value recorded for the NPV during the first years of the project results from the investment required to build the plant, while the gradual decrease of the negative amount is due to the profitable operation in subsequent years. The calculated operating margin is greater than 30% from the years in which the plant operates at capacity above 90%, and the calculated operating break-even point represents 270 ton/day (Appendix B contains the details of operational performance). Therefore, even assuming the highest biogas price in the interval assumed (Table 21), the values indicate a healthy operation in the stipulated price range. The financing structure adopted as a condition on the project schedule plays an important role in leveraging the cash flow result. The total investment of an ammonia and urea production project is significantly high, making external capital financing a viable alternative and impacting recent cash flow incomes.

Therefore, financing is essential to make large projects viable due to the high total investment cost involved. Access to adequate financial resources is important to ensure initial cash flow inputs of the project. The financial debt structure is paid during the established project horizon, consisting of the amortization rate and financial expenses. The amortization rate is assumed constantly during the years of plant operation (during the plant's construction years there is not payment of finance expenses due to the absence of revenue). In this way, the financial debt is carried out through the payment of a linear fixed portion and a variable one corresponding to the loan interest rate applied to the total debt remaining.

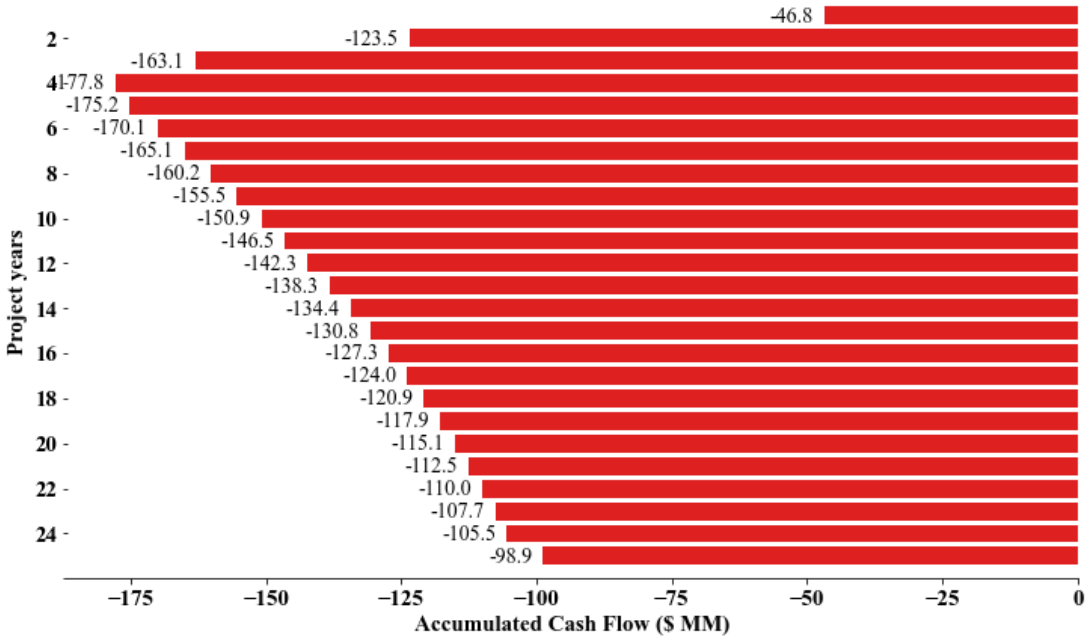

Figure 38 - Accumulated cash flow during project years.

Figure 39 details the composition of the total investment for construction of the plant. As indicated, the installation cost corresponds to approximately 34% of the total estimated investment, totaling an amount of MM $ 118. This component provides the sum of the expenditure associated with the plant's main equipment and is used as a basis for estimating the other components. Furthermore, it can be observed that the direct permanent cost (C_{PDI}) (sum of C_I and C_O) corresponds to a percentage above 50%, adding up to MM $ 177 of the total estimated amount.

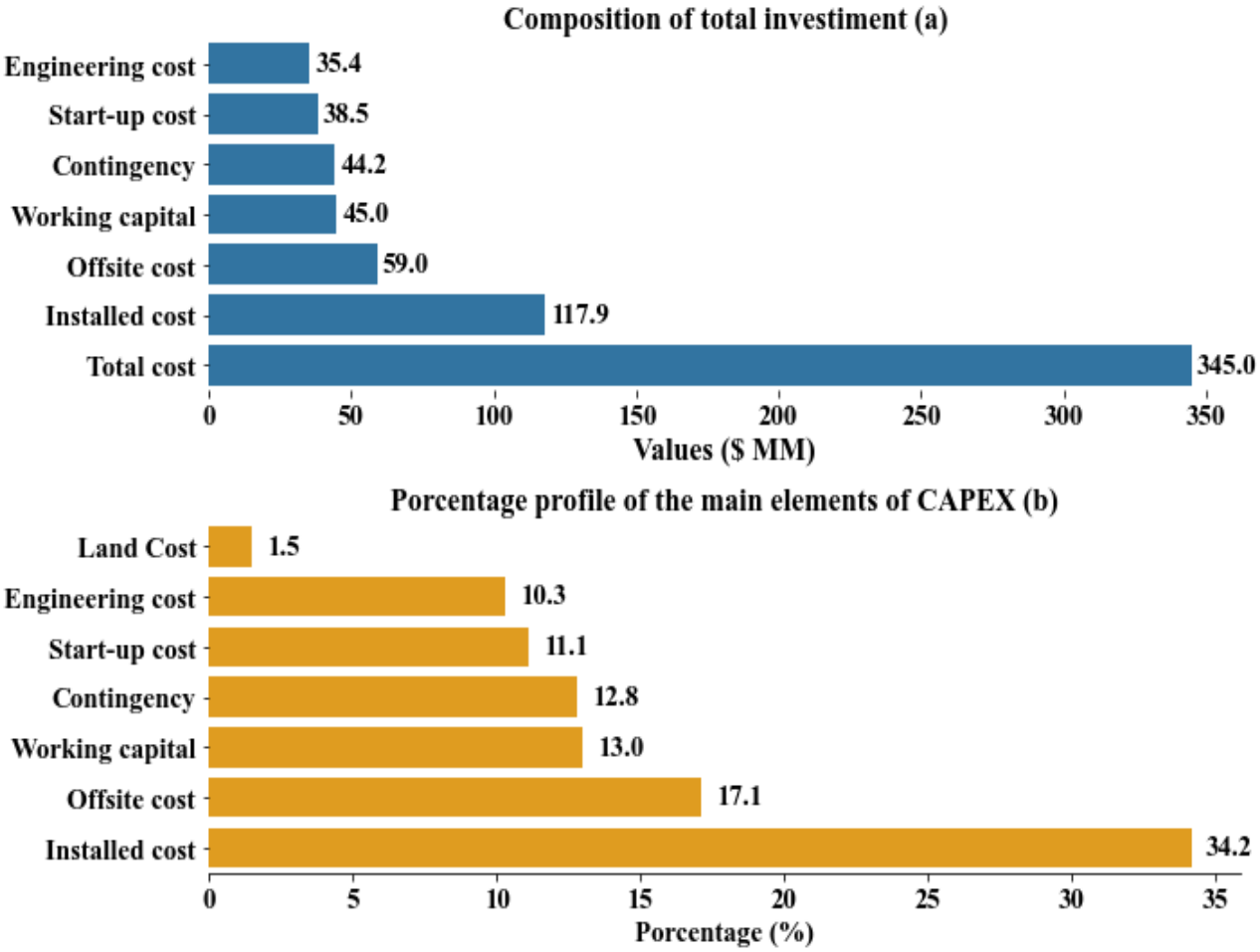

Figure 39 - Composition of the plant's total fixed investment (CAPEX) (a) and distribution of the main elements of the plant's investment (b).

Table 32 provides details of variable costs relating an annual period. As expected for large industrial plants, the cost of supplying the biogas feedstock is the largest contributor to the variable cost of the plant (~ MM$ 23). Furthermore, it is possible to observe the relevance of utilities since a series of power (compressors) and heat exchange equipment operate in conditions that require intense energy supply. The negative values refer to the generating potential of utilities that can be redirected to the plant's energy integration and, consequently, contribute positively to the plant's cash flow.

Table 32 - Composition of plant variable costs (annual period)

Cost	Class	Description	Values
RAW MATERIALS	VOLUME FLOW	Biogas	22,990,968.0
RAW MATERIALS	MASS FLOW	Process Water	529,471.8
UTILITIES	ELEC	PUMP-01	15,840.0
UTILITIES	ELEC	COMP-01	1,457,280.0
UTILITIES	ELEC	COMP-02	2,043,360.0
UTILITIES	ELEC	COMP-CO2	570,240.0
UTILITIES	ELEC	COMP-03	3,619,440.00
UTILITIES	ELEC	COMPRESS	4,546, 080.0
UTILITIES	CW	COMP-01	4095.5
UTILITIES	CW	COMP-02	11,735.5
UTILITIES	CW	COMP-CO2	8,071.2
UTILITIES	HPS	HEAT-01	320,112.0
UTILITIES	FH	HEAT-01	544,066.0
UTILITIES	FH	SRM-01	3,612,829.7
UTILITIES	LPS	COOL-01	-454,780.7
UTILITIES	CW	COOL-02	106,877.2
UTILITIES	CW	COMPRESS	26,568.3
UTILITIES	HPS	COOL-03	-444,003.1
UTILITIES	HPS	COOL-04	-422,547.8
UTILITIES	HPS	STRIPPER	1,358,810.6
UTILITIES	LPS	SCRUBBER	-425,960.7
UTILITIES	AGR	AGR	12,884,318.7
UTILITIES	REF1	COOL-05	1,923,037.9

[a]ELEC: Eletricity, [b]CW: Cooling Water, [c]HPS:High Pressure Steam; [d]FH:Fired Heat; [e]LPS: Low Pressure Steam; [f]AGR:Acid Gas Removal [g]REF: Refrigerant Fluid.

According to the results highlighted in Figure 40, the sum of expenses related to raw materials represents 43% of the plant's variable costs (~MM $ 23). On the other hand, the costs associated with utilities also represent the major portion of the total estimated variable cost for the plant with almost 57% and ~ MM $ 31. Therefore, the operation of the integrated plant has significant costs both for purchasing biogas as raw material and maintaining the plant's operation through the continuous supply of utilities. Individually, it is important to notice that the purchase of biogas cost has the major contribution to the plant annual cost, as expected for large scale industrial plants. In the second place, AGR units also have an significant impact in the total variable cost. The correlation assumed to AGR

OPEX (Appendix A) takes into both energy and make-up solvent aspects to have an accumulated estimation cost about biogas clean and CO_2 removal section base (EPE, 2018).

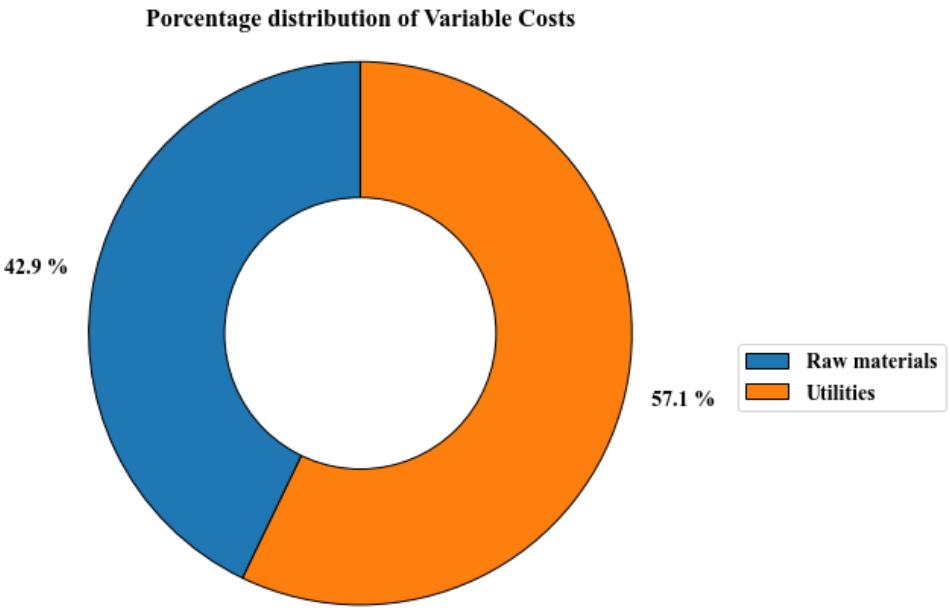

Figure 40 - Percentage distribution of variable costs (annualized period).

Table 33 contains the plant's fixed costs considering the annualized cash flow analysis period. Comparatively, fixed costs have less impact when compared to the variable's ones, however, items related to maintenance and R&D stand out. The two items correspond to the largest contribution related to the composition of fixed costs, totaling an amount greater than MM $ 10 because they are calculated based on the installed cost. Fixed costs arising from the operation of the integrated plant represent values close to MM $ 17.9. Figure 41 shows the greater contribution of variable costs to the detriment of fixed costs, with the former being the main detractor for the estimated operating margin for regular operation of the plant.

Therefore, considering the base scenario for the plant's operation, the economic feasibility of the integrated plant is intrinsically linked to the time horizon established for evaluating the project according to the main financial metrics used (payback, NPV and IRR). The estimated total investment for the plant is around MM $ 345, with the largest important portion related to the installation cost of the plant's equipment. In turn, all other components of the total investment are derived directly from the plant's CI.

Besides, according to the plant's operational parameters, variable costs are the main detractors of the operating margin as expected. In this way, the costs of biogas and utilities can be indicated as the main contributor. Thus, to carry out the economic sensitivity analysis of the project, some factors

such as the price of biogas, the selling price of urea and interest rate applied will be considered to evaluate the elasticity and robustness of the plan when considering from different scenarios.

Table 33 - Distribution of fixed and variable costs (annualized period)

Fixed costs	Values ($)
Labor cost	292,931.5
Supervision and Management	73,232.9
Maintenance	5,895,304.1
Training and Benefits	219,698.6
Property tax	2,358,121.6
Administrative	238,006.8
Research and Development	5,682,600.0
Sales & Marketing	3,409,560.0
Total fixed cost	17,900,000.0

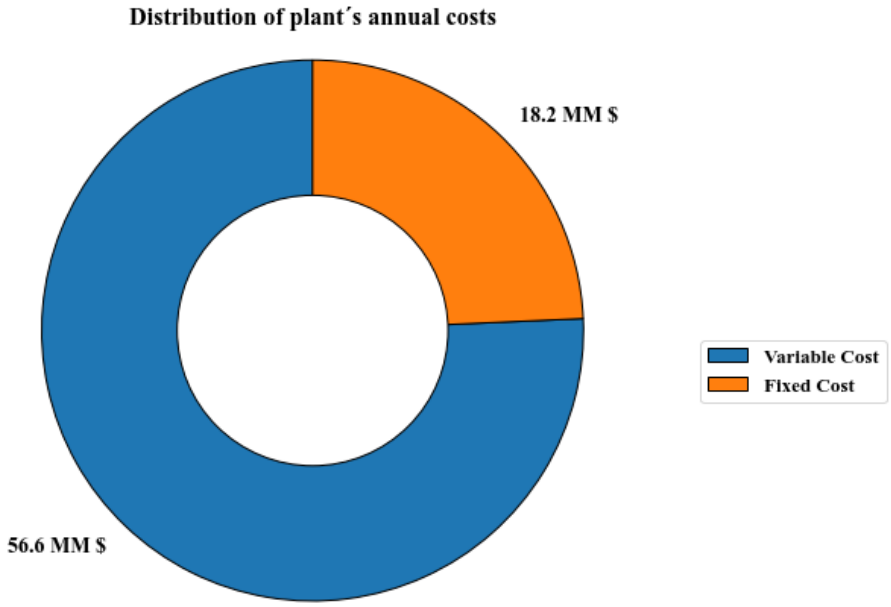

Figure 41 - Distribution of fixed and variable costs.

4.4 - Sensitivity analysis

A plant construction project within the chemical industry is a complex operation, with its economic feasibility linked to the need for high initial investment. Furthermore, several external factors (*e.g.*, fluctuations in the price of raw materials and changes in government legislation) can significantly affect the financial success of these industrial plants. Therefore, sensitivity analysis

proves to be an important strategy in the management of these projects, allowing the evaluation of different scenarios and the impact of changes in the main economic variables detected during the conceptual phase of the project. In this context, understanding the complexity and the need to consider economic and financial variables in its evaluation is essential to guarantee the success of chemical engineering projects. For each topic discussed below, it is highlighted that the other assumptions remained constant to exclusively evaluate the individual effect of the selected variables.

4.4.1 - Sale of residual CO_2

As previously discussed, the integrated plant for producing urea from biogas has a significant amount of CO_2 from both the biogas pre-treatment stage and the steam reforming of methane within the ammonia synthesis process. A portion is compressed and fed directly to the urea synthesis section, while the residual percentage has no use within the process flowsheet. Therefore, there is a relevant monetization (Section 3.4.5) opportunity for the residual flow of CO_2 generated, illustrated in Figure 42 considering the impact of the percentage of sales of the residual portion of CO_2 on the main economic indicators evaluated.

As expected, it is possible to verify the impact on the project's financial health. The addition of a new revenue line results in an increase in the total recurring revenue generated by the plant, causing a direct improvement in the key financial metrics. However, the viability of the project is not yet concrete. This result is significant given that CO_2 is a byproduct inherent to the structural conditions of the process, without the need for relevant additional investment to include this new line of revenue. However, it is worth highlighting that there are challenges beyond considering this recurring revenue, given that there is the challenge of total product's sale, prospecting nearby customers and the having all the technical specification required.

Furthermore, it would be possible to sell this residual CO_2 as carbon credit (1 ton of CO_2) which is the currency used inside the carbon market derived from the biogas pre-treatment since the gas produced is no longer emitted and can be used as biomethane. Companies which emit large amounts of carbon dioxide and have difficulty reducing these emissions can purchase carbon credits as a way of indirectly reducing their environmental impact. Thus, the more an organization strives to reduce pollutant emissions, more credit can be generated, being able to negotiate with other partners which have not achieved their reductions targets

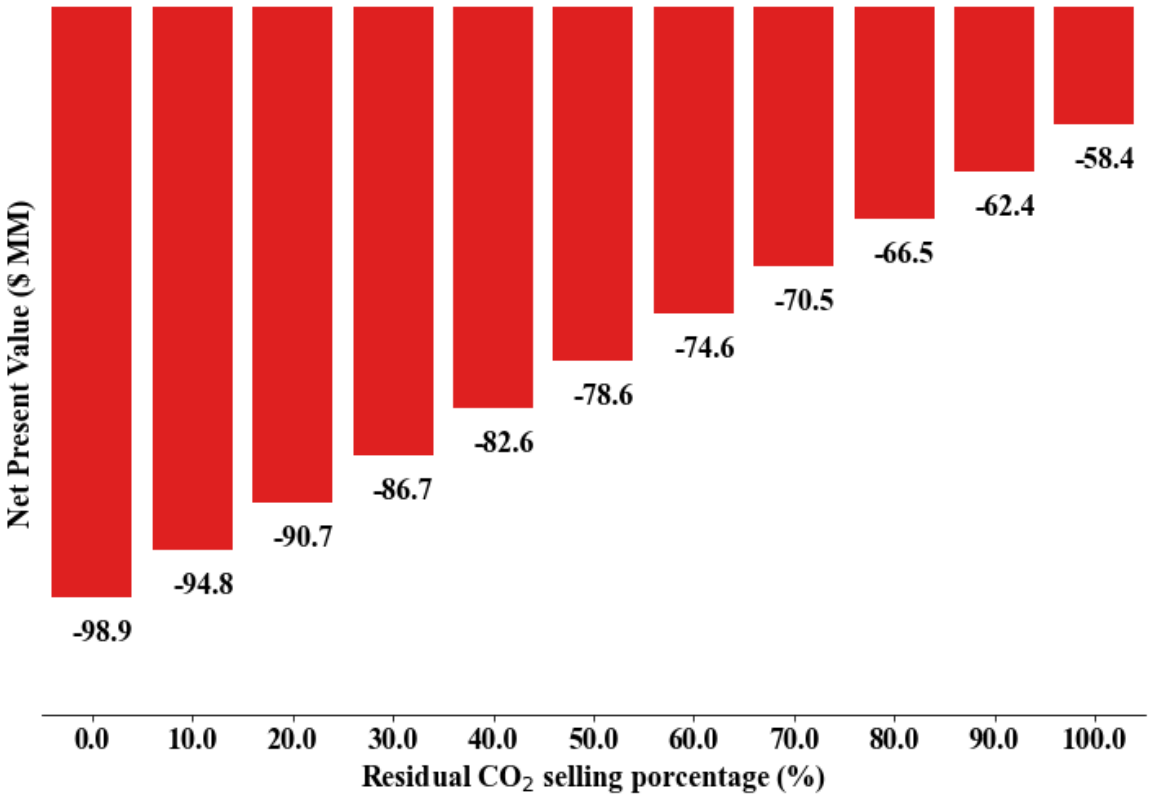

Figure 42 - Effect of percentage of residual CO_2 on NPV.

Brazil has a huge potential to become an important player inside the carbon market, being able to supply a significant amount of global demand in the next years. In the actual scenario, Europe represents the highest carbon market in the world and carbon credits are priced in euro. Considering the period from April 2019 to February 2024, the carbon credit price rose from 30 to 90 euros as the maximum price reached. Currently, it is in a range of 50-60 euros in the last 6 months (Sep/23-Feb/24). Therefore, considering a simplification of monetary parity between euro and dollar, it can be stated that the price for carbon credit would be in a range close to the CO_2 sales price for the study implemented above (Figure 42). In this context, considering the possibility of selling CO_2 as a raw material or carbon credit, the impacts on the NPV would be similar given the price range of the carbon credit negotiated within the European market (INVESTING.com, 2024; SEBRAE, 2023).

4.4.2 - Biogas/urea price

From the results discussed for the base scenario in Section 4.3, it is known that the prices of raw materials and the main product are preponderant in determining the profitability of the industrial plant project. Price variations in commodities and intermediaries are likely scenarios due to the influence of external factors and must be considered to verify the elasticity and robustness of the established assumptions. Figure 43 highlights the impact on the percentage variation in the price of biogas and urea in relation to the NPV.

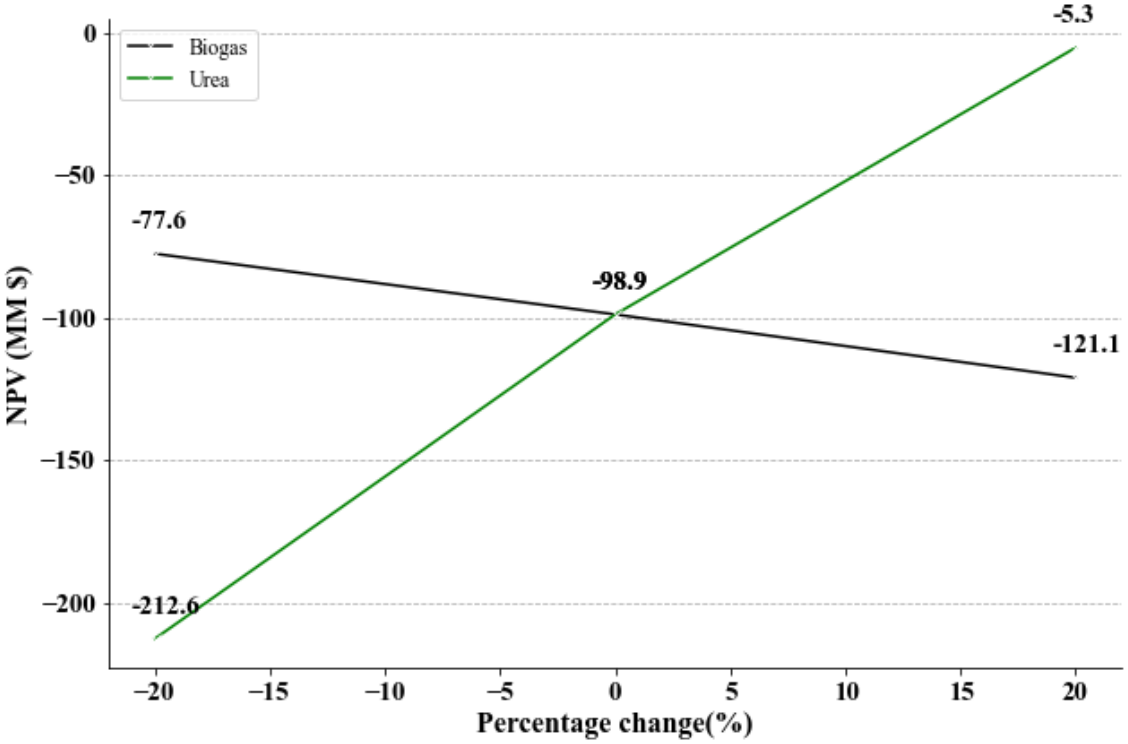

Figure 43 - Assessment of biogas/urea price variation over NPV.

The graph reveals the difference in magnitude between the likely changes in scenario between the two main chemical compounds involved in the project. It becomes evident that any effect on the variation in the price of urea has greater sensitivity on the viability of the project, since it is the main input in the calculation of the plant's cash flow. The effect on an increase in the price of biogas is also deleterious to the economic performance of the plant project, given that it is the main component accounted for in the total costs of the plant.

Therefore, it is important to highlight those variations in the price of raw materials, which although important, do not have the same impact as variations in the price of the main product. Although a change in the price of biogas contributes negatively to economic viability, the cost of raw materials represents a smaller portion of cash flow compared to the revenues generated from the urea production and trading. It is essential to consider the strong dependence on the price of the main product and its possible fluctuations during the sensitivity analysis, to minimize risks and evaluate economic elasticity considering the time horizon for financial return on industrial plant projects.

4.4.3 - Interest Rate

The interest rate is a parameter used by investors to evaluate the expected financial return of a project, taking into account the risks involved. In the context of industrial plant projects, the IR is particularly important because it represents the cost of opportunity of invested capital. The

relationship between the IR and the financial return is inversely proportional, that is, the higher the interest rate, the lower the potential financial return. This occurs by increasing the rate applied to the project's future revenues, reducing the present value. As a result, the payback period may become longer and the NPV may turn negative, making the project financially unfeasible. This relationship is exemplified in Figure 44, illustrating the impact of increasing the IR on the project's NPV.

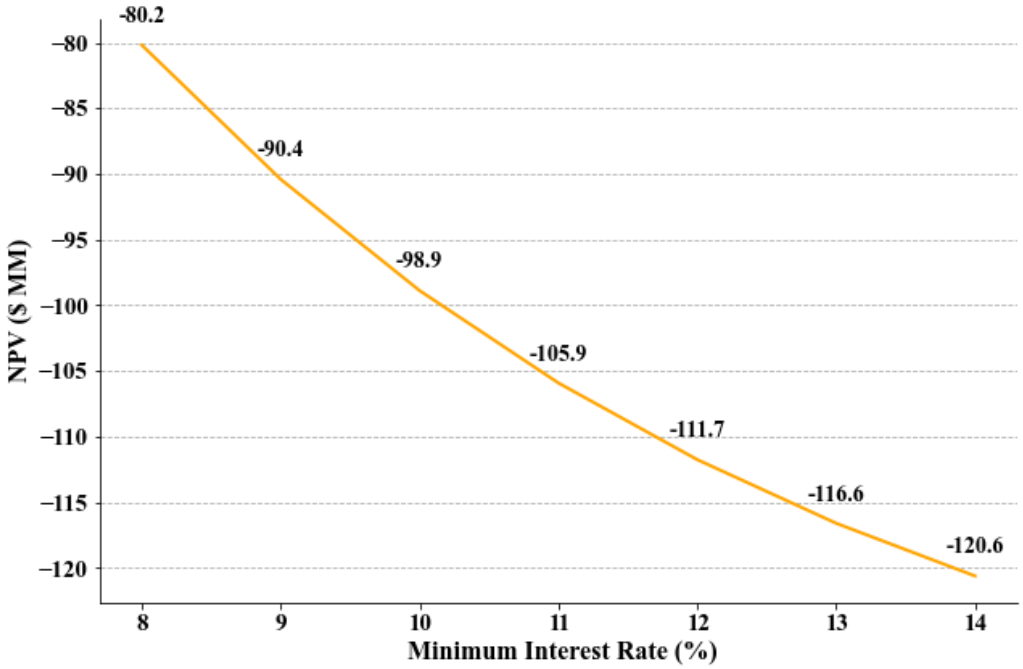

Figure 44 - Impact of the IR on the NPV.

For the reality of industrial projects, interest rates have a significant effect on the expected financial return. When they are at lower levels, the opportunity cost is reduced and, therefore, the interest rate can be reduced. This can make the project financially attractive, providing a greater return. When interest rates are high, the cost of opportunity of capital is higher, reducing the project's return. In short, interest rates have a critical impact on the financial return of a chemical plant project.

In short, the interest rate represents the lowest expected return for an investment given the initial assumptions of a given project. Analyzing, specifically, the context of the integrated plant for the production of urea from biogas, it is clear that the main challenge in terms of the process flowsheet arises from the pre-treatment and purification of the biogas and the guarantee of a continuous supply of raw material. Therefore, the existing technological challenge proves the need to apply a greater MRR when compared to a urea synthesis plant fed directly by natural gas due to the stage of process maturity achieved through the coupling of the Haber-Bosch and Stamicarbon processes.

5. Conclusion

Currently, Brazil presents itself as one of the world's pillars regarding agribusiness. Even considering the recent years of stagnation in the Brazilian economy, this sector has a growing share of the national GDP, corresponding to a percentage greater than 25%. On the other hand, there is a decreasing scenario in the national production of fertilizers in the last 10 years, increasing, annually, the Brazilian dependence on the importation of this relevant asset for agricultural productivity. The country has enormous potential to use biogas to build a sustainable chemical platform to produce ammonia and fertilizers, promoting the use of this product beyond the generation of electrical energy. The main change is related to the biogas pre-treatment stage to remove CO_2 and guarantee the continuous supply of biogas for the full functioning of the plant.

It is possible to observe that the proposal to integrate plants using biogas has relevant potential inside Brazil's economy context. The ammonia plant is capable of fully meeting the demand of the urea synthesis section. Furthermore, due to the high CO_2 content in the biogas feed, there is an excess generation of this byproduct that cannot be fully absorbed by the urea plant. Therefore, it is necessary to evaluate different strategies for monetizing surplus CO_2 to increase the economic viability of the plant. The economic sensitivity analysis highlights the potential for generating a new line of recurring revenue for the plant without the need for relevant changes to the production process. The main challenges regarding the trading of residual CO_2 are related to the location of the plant to prospect nearby customers and the technical specification necessary for sale.

The simulation strategy for the integrated plant presented results in line with the literature, being validated based on important operational variables for both ammonia and urea synthesis. However, a significant limitation is observed for obtaining reliable open data regarding the simulation of the urea synthesis plant, especially in relation to the carbamate condenser and scrubber. The lack of references for direct comparison makes it difficult to more accurately validate the results of all equipment used and evaluate their contribution to the overall performance of the system. The availability of information on the behavior of the carbamate condenser is essential to progress with studies on the total conversion of the plant as it actively participates in the synthesis of urea before the currents enter the main reactor.

The results of the economic evaluation reveal that at the current price level there is no economic viability of the integrated plant project for both biogas. Despite demonstrating a healthy operational result, the high investment required still proves to be the main challenge in implementing the investment. that there is economic potential despite the technological risk involved in the project. As with the construction of traditional ammonia and urea synthesis plants, the operational complexity of

the process requires a high estimated CAPEX, which directly affects the NPV and payback within the proposed time horizon. Furthermore, it is observed that the variable costs related to the consumption of biogas and plant utilities are the main detractors of the operating margin. From the sensitivity analysis, there is the impact of percentage variations on the purchase price of the raw material (biogas) and the sale price of urea, the latter being the factor with the greatest impact on the financial viability of the project as it represents the main line of cash flow revenue.

6. Suggestions for future work

Considering Brazil economic framework, biogas reflects a huge asset to build a sustainable chemical platform. As explored during this work, there is an extensive field that can be developed and open new lines of research. Below follows some suggestions for future work in this area:

- ✓ Operational and energy optimization of the integrated plant based on the integration of the *Aspen Plus* tool and open programming framework (*e.g.*, Python) based on the proposition of different needs.
- ✓ Analysis of different biogas compositions and their effect on the plant's operational performance and economic viability (especially in relation to the potential for monetizing residual CO_2 generated during the pre-processing stage).
- ✓ Implementation of a methane bi-reforming reactor to replace the primary/secondary reforming stages.
- ✓ Assessment of the potential for locating the plant in Brazilian territory to analyze the logistical gains in relation to the continuous supply of biogas to the plant from gas pipelines.
- ✓ Specific operational study on the carbamate condenser and its effects within the urea synthesis section.
- ✓ Assessment of the plant's operational performance considering the presence of biuret in urea synthesis.
- ✓ Implementation of the kinetic model of the ammonia reactor considering ruthenium catalysts instead of traditional ferrous catalysts and possible combinations of multiple reactors.
- ✓ Evaluation of predictive control and real-time optimization strategies for the main equipment of the integrated plant and evaluation of economic gains.

7. Bibliographic References

Abensur, S. *Modelagem Matemática do Reator de Síntese de Ureia*. Doctoral Thesis– Polytechnic School– USP, São Paulo, 1996.

ANDA – National Fertilizer Association. Pesquisa Setorial. Available in http://anda.org.br/pesquisa_setorial/., 2022.

ANP - National Oil, Gas and Biofuels Agency. Available in https://www.gov.br/anp/pt-br/assuntos/movimentacao-estocagem-e-comercializacao-de-gas-natural/acompanhamento-do-mercado-de-gas-natural/publicidade-dos-precos-de-gas-natural/ Access in 15/03/2024.

Andersson, J., & Lundgren, J. *Techno-economic analysis of ammonia production via integrated biomass gasification*. **Applied Energy**, v. 130, p. 484–490, 2014.

Angira, R., 2011, *Simulation and Optimization of an Auto-Thermal Ammonia Synthesis Reactor*. **International Journal of Chemical Reactor Engineering**, v. 9, n. 1, 2011.

Araújo, A.; Skogestad, S. *Control structure design for the ammonia synthesis process*. **Computers and Chemical Engineering**, v. 32, n. 12, p. 2920–2932, 2008.

Arora, P., Hoadley, A. F. A., Mahajani, S. M., & Ganesh, A. *Small-Scale Ammonia Production from Biomass: A Techno-Enviro-Economic Perspective*. **Industrial and Engineering Chemistry Research**, v. 55, p. 6422–6434, 2016.

ABiogás – Brazilian Biogas Association. Technical report - *O potencial brasileiro de biogás*. São Paulo, SP. 2020.

ASPEN TECH *Aspen Plus Ammonia Model*, 2008a.

ASPEN TECH. *Aspen Plus Urea Synthesis Loop Model*, 2008b.

Azarhoosh, M. J.; Farivar, F.; Ale Ebrahim, H. *Simulation and optimization of a horizontal ammonia synthesis reactor using genetic algorithm*. **RSC Advances**, v. 4, n. 26, p. 13419–13429, 2014.

BNDES - National Bank for Economic and Social Development. Available in https://www.bndes.gov.br/wps/portal/site/home/financiamento/guia/taxa-de-juros/. Acess in 04/03/2024.

Brouwer, M., 2009a. *Thermodynamics of the Urea Process*. **Urea Know How**.

Brouwer, M., 2009b. *Phase Diagrams of the Urea Process*. **Urea Know How**.

Cardoso, F. S. *Elaboração de Roadmaps Tecnológicos da Produção de Biogás a partir de Palha e Vinhaça* (Master Degree in Chemical and Biochemical Process Enginnering) – Chemistry School, UFRJ, 2017.

Carvalho, E.P., Borges, C., Andrade, D., *et al*. *Modeling and optimization of an ammonia reactor using a penalty-like method.* **Applied Mathematics and Computation**, v.237, pp. 330-339, 2014.

Carvalho, M. *Análise de desempenho de um reator de síntese de amônia*. Master's degree for Chemical Engineering Program (PEQ), COPPE/UFRJ, 2016.

Cheema, I. I., & Krewer, U. *Operating envelope of Haber-Bosch process design for power-to-ammonia*. **RSC Advances**, v.8, p. 34926–34936., 2018.

Chinda, R.C. *Simulação da seção de síntese de uma unidade de produção de ureia – processo Stamicarbon*. (Master Degree in Chemical and Biochemical Process Enginnering) – Chemistry School, Federal University of Rio de Janeiro, 2015.

Chinda, R.C. *Process intensification applied to urea production process*. Doctoral thesis in Chemical and Biochemical Process Enginnering – Chemistry School - Federal University of Rio de Janeiro, 2019.

CIBiogás – International Renewable Energy Center. Technical report: Nº 001/2021 – *Panorama do biogás no Brasil 2020*. Foz do Iguaçu, PR, 2021.

CIBiogás – International Renewable Energy Center. Technical report: Nº 001/2022 – *Panorama do biogás no Brasil 2021*. Foz do Iguaçu, PR, 2022

CIBiogás – International Renewable Energy Center. Technical report: Nº 001/2022 – *Panorama do biogás no Brasil 2022*. Foz do Iguaçu, PR, 2023

Costa, L. M., Silva, M. F. O. A indústria química e o setor de fertilizantes. Rio de Janeiro: BNDES, 2012.

Cooper, W. H., 1967, Hydrocarbon Process & Petrol. Ref., n. 46, pp.159.

Dente, M. *et al*., 1988. *Simulation Program for Urea Plants*. **Comput. Chem. Eng**., v. 12, p. 389-400, 1988.

Dente, M., Rovaglio, M., Bozzano, G., Sogaro, A., & Isimbaldi, A. (1992). *Gas-liquid reactor in the synthesis of urea*. **Chemical Engineering Science**, v.47, p. 2475–2480, 1992.

Dyson, D. C., Simon, J. M. *A kinetic expression with diffusion correction for ammonia synthesis on industrial catalyst*. **I & EC Fundamentals**, v.7, n.4, pp. 605-610, 1968.

Edrisi, A., Mansoori, Z., & Dabir, B. *Urea synthesis using chemical loop ing process - Techno-economic evaluation of a novel plant configuration for a green production*. **International Journal of Greenhouse Gas Control**, vol. 44, pag. 42–51, 2016.

EPE – Energy Research Company. Technical report: Nº 001/2019 – *Competitividade do Gás Natural: Estudo de Caso na Indústria de Fertilizantes Nitrogenados*. Rio de Janeiro, RJ, 2019.

EPE – Energy Research Company. Compilação de correlações de custos de equipamentos – Instalações Industriais de Gás Natural, Rio de Janeiro, RJ, 2018.

EXAME JOURNAL. Available in https://exame.com/agro/agro-gera-27-das-riquezas-do-brasil-e-e-setor-seguro-e-promissor-para-quem-quer-investir-veja-oportunidades/ Acess in 11/14/2022.

Esturilio, G. G. *Modelagem e controle preditivo econômico de um reator de amônia*. Master Degree – Polytechnic School of São Paulo University. Chemical Engineering Program. São Paulo, 2011.

Farias, P.I.V. *Aspectos Técnicos e Econômicos da Indústria de Fertilizantes NPK no Brasil*. Chinda, R.C. *Process intensification applied to urea production process*. Master's degree in chemical and Biochemical Process Enginnering – Chemistry School - Federal University of Rio de Janeiro, 2019.

FIRJAN - Federation of Industries of the State of Rio de Janeiro. *Quanto custa o gás natural para a indústria no Brasil?*, Rio de Janeiro, 2011.

Flórez-Orrego, D., de Oliveira Junior, S. *Modeling and optimization of an industrial ammonia synthesis unit: An exergy approach*. **Energy**, v. 137, p. 234–250, 2017.

Gadelha, T. S., Araújo, O. F. e Medeiros, J. L. Captura de CO_2 do gás natural por absorção pela amina MDEA: uma análise técnico-econômica. Rio de Janeiro: Rio Oil & Gas 2014.

Glassdoor. Available in https://www.glassdoor.com.br/Vaga/index.html/. Acess in 04/03/2024.

Gillespie, L., J Beattie, J. A. *The thermodynamic treatment of Chemical equilibria in systems composed of real gases. II. A relation for the heat of reaction applied to the ammonia synthesis reaction. The energy and entropy constants for ammonia*. **Physical Review**, v. 36, pp. 1008-1013, 1930.

Hamidipour, M., Mostoufi, N., & Sotudeh-Gharebagh. *Modeling the synthesis section of an industrial urea plant*. **Chemical Engineering Journal**, vol. 106, p. 249–260, 2005.

Heiker, M., Kraume, M., Mertins, A., Wawer, T., & Rosenberger, S. *Biogas Plants in Renewable Energy Systems — A Systematic Review of Modeling Approaches of Biogas Production*. **Applied Sciences**, 2021.

IHS MARKIT. Ammonia | *Ammonia Fertilizer Market and Price Analysis*. Available in https://www.spglobal.com/commodityinsights/en/ci/products/fertilizers-urea.html. Acess in 07/10/2023

IHS Markit. *Urea Fertilizer Market and Price Analysis*. Available in https://www.spglobal.com/commodityinsights/en/ci/products/fertilizers-urea.html. Acess in 07/10/2023.

INVESTING.COM. Available in https://www.investing.com/commodities/carbon-emissions. Acess in 02/17/2024.

Isla, M. A., Irazoqui, H. A., Genoud, C. M. *Simulation of a Urea Synthesis Reactor. 1. Thermodynamic Framework*. **Industrial and Engineering Chemistry Research**, v. 32, n. 11, p. 2662–2670, 1993.

Khan, I. U., Othman, M. H. D., Hashim, H., Matsuura, T., Ismail, A. F., Rezaei-DashtArzhandi, M., & Wan Azelee, I. *Biogas as a renewable energy fuel – A review of biogas upgrading, utilisation and storage*. **Energy Conversion and Management**, vol. 150, pag. 277–294, 2017.

Koohestanian, E., Sadeghi, J., Mohebbi-Kalhori, D., Shahraki, F., & Samimi, A. *A novel process for CO_2 capture from the flue gases to produce urea and ammonia*. **Energy**, vol. 144, pag. 279–285, 2018.

Kunz, A., Steinmetz R. L. R., Amaral, A.C. *Fundamentos da digestão anaeróbia, purificação do biogás, uso e tratamento do digestato*. Brazilian Agricultural Research Company (Embrapa), Ministry of Agriculture, Livestock and Food Supply, Concórdia, Santa Catarina (SC), 2019.

Jorqueira, D.S.S. *Investigação de modelo pseudo-homogêneo para síntese da amônia: uso de uma abordagem composicional*. Master Degree, State University of Campinas, Chemical Engineering Department, Campinas, SP, 2018.

Luz, F. C., Rocha, M. H., Lora, E. E. S., *et al*. *Techno-economic analysis of municipal solid waste gasification for electricity generation in Brazil*. **Energy Conversion and Management**, v. 103, pp. 321–337, 2015.

Malmali, M., Wei, Y., McCormick, A., & Cussler, E. L. *Ammonia Synthesis at Reduced Pressure via Reactive Separation*. **Industrial and Engineering Chemistry Research**, vol. 55, pag. 8922–8932, 2016.

Mariani, Leidiane. *Biogás: diagnóstico e propostas de ações para incentivar seu uso no Brasil*. Doctoral Thesis – State University of Campinas, Mechanical Engineering Department, Campinas, SP, 2018.

Morone, A., Apte, M., & Pandey, R. A. *Levulinic acid production from renewable waste resources: Bottlenecks, potential remedies, advancements and applications*. **Renewable and Sustainable Energy Reviews**, vol. 51, pag. 548–565, 2015.

Moura, I.P., Reis, A.C, Bresciani, A. E., *et al. Carbon dioxide abatement by integration of methane bi-reforming process with ammonia and urea synthesis*. **Renewable and Sustainable Energy Reviews,** v. 151, 2021.

Moura, I.P. *Integration of bi-reforming of methane with ammonia and urea process*. Master Degree, Polytechnic School of São Paulo University, USP, 2021.

Newton, R. H., **Ind. Eng. Chem,** n.27, pp. 302, 1935.

Nielsen, A. *An Investigation on Promoted Iron Catalysis for the Synthesis of Ammonia*. **Jul. Giellerups forlang,** 1968.

Oliveira, F. S. *Avaliação do potencial de utilização do biogás gerado em estação de tratamento de esgoto para conversão em energia elétrica*. Master Degree (Technology of Chemical and Biochemical Processes) – Chemistry School, UFRJ, 2013.

Paixão, V.P. *Análise retro-tecno-econômica de uma planta de produção de amônia baseada na gaseificação de resíduo sólido urbano*. Master Degree of Chemical Engineering Program (PEQ), COPPE/UFRJ, 2018.

Peters, M. S., Timmerhaus, K. D. e West, R. E. Equipment Costs. New York: McGraw-Hill, 2014.

Poblete, I.B.S. *Simulação e Análise de Produção e Condicionamento de Biogás.* Master Degree (Technology of Chemical and Biochemical Processes) – Chemistry School, UFRJ, 2019.

Pwc, *The green hydrogen economy: Predicting the decarbonisation of tomorrow.* Available in https://www.pwc.com/gx/en/industries/energy-utilities-resources/future-energy/green-hydrogen-cost.html/, Acess in 04/03/2024.

Rabelo, C. *O fomento do biogás como fonte de energia renovável*. **Revista Videre**, vol. 11, p. 79-91, 2019.

Rasheed, S. A. *Revamping Urea Synthesis Reactor using Aspen Plus*. **UreaKnowHow**, pag. 1–15, 2011.

Reese, M., Marquart, C., Malmali, M., Wagner, K., Buchanan, E., McCormick, A., & Cussler, E. L. *Performance of a Small-Scale Haber Process*. **Industrial and Engineering Chemistry Research**, vol. 55, pag. 3742–3750, 2016.

Rossetti, I. Pernicone, N., Ferrero, F., Forni, L. *Kinetic study of ammonia synthesis on a promoted Ru/C catalyst*. **Industrial and Engineering Chemistry Research**, v. 45, n. 12, p. 4150–4155, 2006.

SAE – Special Secretariat for Strategic Affairs. *Produção Nacional de Fertilizantes*. Paraná, PR, 2020.

Sartore, P. E. *Otimização Energética de uma planta de produção de amônia* (UFN V). Master Degree (Technology of Chemical and Biochemical Processes) – Chemistry School, UFRJ, 2017.

Seider, W. D., Seader, J., Lewin, D. R. *Product and Process Design Principles*. John Wiley ans Sons, Inc, 2003.

SEBRAE, 2023. How does carbon credit trading work? Available in https://sebrae.com.br/sites/PortalSebrae/como-funciona-a-comercializacao-de-credito-de-carbono,88dbbc6d15757810VgnVCM1000001b00320aRCRD. Access in 02/17/24.

Schiaroli, N., Volanti, M., Crimaldi, A., *et al*. *Biogas to Syngas through the Combined Steam/Dry Reforming Process: An Environmental Impact Assessment*. **Energy and Fuels**, vol. 35, n. 5, p. 4224–4236, 2021.

Schwartzentruber, J. & Renon H. *Extension of UNIFAC to High Pressures and Temperatures by the Use of a Cubic Equation-of-State.* **Ind. Eng. Chem. Res**., vol. 28, p. 1049-1955, 1989.

Serrano-Ruiz, J. C., Luque, R., Campelo, J. M., & Romero, A. A. (2012). *Continuous-Flow Processes in Heterogeneously Catalyzed Transformations of Biomass Derivatives into Fuels and Chemicals*. **Challenges**, vol. 3, 114–132, 2012.

Shirmohammadi, R., Aslani, A., Ghasempour, R., & Romeo, L. M. CO_2 *utilization via integration of an industrial post-combustion capture process with a urea plant: Process modelling and sensitivity analysis*. **Processes**, vol. 8, p. 1144, 2020.

Soave, G. *Equilibrium Constants for Modified Redlich-Kwong Equation-of-State.* **Chem. Eng. Sci.**, v. 27, p. 1196-1203, 1972.

Tavares, F. W.; Medeiros, F. A., Segtovich, I. S. V. **Termodinâmica na Engenharia Química**. COPPE – UFRJ, June 2020.

Tavares, F., Monteiro, L., Mainier, F. *Indicators of energy efficiency in ammonia production plants.* **American Journal of Engineering Research**, vol. 2, pag. 116-123, 2013.

Temkin, M.L., Pyzhev, V.J. **Acta Physichochim (USSR)**, n.12, pp.327, 1940.

Tripodi, A., Compagnoni, M., Bahadori, Elnaz, *et al*. *Process simulation of ammonia synthesis over optimized Ru/C catalyst and multibed Fe + Ru configurations*. **Journal of industrial and Engineering Chemistry**, v. 66, p. 176–186, 25 out. 2018.

Towler, G., Sinnot, R. K. *Chemical engineering design: principles, practice and economics of plant and process design*. Segunda ed. Waltham, USA, Elsevier, 2012.

Turton, R., Bailie, R. C., Whiting, W. B., et al. *Analysis, synthesis and design of chemical processes*. Quarta ed. Michigan, USA, Pearson Education, 2012.

Vianna, C. E. D. *Análise exegética de processos químicos industriais : produção de amônia pelo processo de reforma a vapor.* Master Degree, Polytechnic School of São Paulo University, USP, 2017.

Woods, D. R., 2007, Rules of thumb in engineering practice. Weinheim, Wiley VCH.

Yoshida, M., Ogawa, T., Imamura, Y. *et al*. *Economies of scale in ammonia synthesis loop s embedded with iron- and ruthenium-based catalysts*. **International Journal of Hydrogen Energy**, v. 46, n. 57, p. 28840–28854, 18 ago. 2021.

Zahid, S., Ramzan, N., Rustam, M. *Simulation and Parametric Study of Urea Decomposition Section*. **Proceedings of the Pakistan Academy of Sciences**, vol. 51, p. 277-288, 2014.

Zendehboudi, S., Zahedi, G., Bahadori, A., Lohi, A., Elkamel, A., & Chatzis, I. *A dual approach for modelling and optimisation of industrial urea reactor: Smart technique and grey box model*. **Canadian Journal of Chemical Engineering**, vol. 92, pag. 469–485, 2014.

Zhang, X., Zhang, S., Yao, P., & Yuan, Y. *Modeling and simulation of high-pressure urea*

synthesis loop . **Computers and Chemical Engineering**, vol. 29, pag. 983–992, 2005.

Zhang, H., Wang, L., Van herle, J., Maréchal, F., & Desideri, U. Techno-economic comparison of green ammonia production processes. **Applied Energy**, 259, 2020.

Zhang, H., Wang, L., Van herle, J., Maréchal, F., & Desideri, U. *Techno-economic comparison of 100% renewable urea production processes*. **Applied Energy**, 284, 2021.

Appendix A - Equipment installed cost

A.1 - Pumps and Compressors (Power Equipments)

Table A.1.1 - Economic parameters of pumps/compressores for calculus of C_I

Equipment	PUMP-01	COMP-01	COMP-02	COMP-03	COMP-CO_2	COMPRESS
Equipment type	Pump	Comp[a]	Comp[a]	Comp[a]	Comp[a]	Comp[a]
Ξ_1	3.39	2.2891	2.2891	2.2891	2.2891	2.2891
Ξ_2	0.05	1.3604	1.3604	1.3604	1.3604	1.3604
Ξ_3	0.15	-0.1027	-0.1027	-0.1027	-0.1027	-0.1027
S (kW)	28.2	2763	4772	7114	1109	6170
Ω_1	-0.39	-	-		-	-
Ω_2	0,4	-	-		-	-
Ω_3	0,0	-	-		-	-
Pressure (atm)	25	25	25	25	200	200
β_1	1,89	-	-		-	-
β_2	1,35	-	-		-	-
Methood	Capcost	Capcost	PTW[b]	PTW[b]	Capcost	PTW[b]
CEPCI	397.5	397.5	576.1	576.1	397.5	576.1

[a]Comp: Compressor; [b]PTW: Peter, Timmerhaus & West

Table A.1.2 – Parameters assumed for Peters, Timmerhaus e West correlation considering design factors (A, B) e material factor (F_m) (adapted de EPE (2018))

Trigger	Gas combustion	Eletric engine	Steam turbine
A	0.9467	0.9138	0.9567
B	7.3553	7.2692	6.7937
Material	**Carbon steel**	**Stainless steel**	**Nickey alloy**
F_m	1.00	2.50	5.10

A.2 - Primary and Secondary Reformers

Tabela A.2.1 - Economic parameters of primary and secondary reformer for the calculus of C_I

Equipment	**SRM-01**	**SRM-02**
Equipment Type	Primary reformer	Secondary reformer
Ξ_1	3.0680	2.3859
Ξ_2	0.6567	0.9721
Ξ_3	0.0194	-0.0206
S unity (kW)	34331	2000
Ω_1	0.1405	0.1017
Ω_2	-0.2698	-0.1957
Ω_3	0.12930	0.09403
Pressure (atm)	25	25
β_1	-	-
β_2	-	-
Method	Capcost	Capcost
S (kW)	34331	2000
CEPCI	397.5	397.5

A.3 - Vertical Vessels

Table A.3.1 - Economic parameters of vertical vessels for the calculus of C_I (gas-liquid separators)

Equipment	FLASH-01	FLASH-02
Equipment Type	Flash Separator	Flash Separator
Ξ_1	3.4974	3.4974
Ξ_2	0.4485	0.4485
Ξ_3	0.1047	0.1047
S unity	-	-
Ω_1	-	-
Ω_2	-	-
Ω_3	-	-
Pressure (atm)	25	200
Temperature (ºC)	50	-20
β_1	2.25	2.25
β_2	1.82	2.25
Method	Capcost	Capcost
CEPCI	397.5	397.5

FLASH-01 and FLASH-02 separators perform two-phase separation (liquid and gas) for partially condensed mixtures. Usually. a *demister* is used in the gas outlet stream in order to increase separation efficiency. To size this equipment. the set of Equations (1) and (2) were used from the calculation of the settling velocity and vessel diameter:

$$u_t = 0.07 \sqrt{\frac{\rho_l - \rho_v}{\rho_v}} \tag{1}$$

$$D_v = \sqrt{\frac{4\, V_v}{\pi\, u_t}} \tag{2}$$

where the subscripts l and v represent the liquid and vapor phases. respectively; ρ_l e ρ_v correspond to the liquid and gas density (kg/m³); $u_t$is the settling velocity; V_v the gas volumetric flow rate(m³/s) and D_v the mininum vessel diameter (m).

After calculating D_v. the L/d ratio can be calculated based on the criteria adopted by WOODS

(2007). For pressures below 400 kPa. L/d is in the range of 2 and 3 and for pressures above 400 kPa. L/d is between 4 and 5. For this work. due to the operating pressure. the second criteria was adopted (PAIXÃO, 2018).

Once you have calculated the dimensions of the vessel. it is possible to calculate the equipment's purchase cost. as well as determining the calculation of the pressure factor according to the criteria of the Capcost method for vertical vessels (EPE. 2018; TURTON *et al.*. 2012):

$$f_p = \left[\frac{(P+1)\,D}{2\left(849.6 - 0.6\,(P+1)\right)} + 0.00315\right] \tag{3}$$

$$C_{BM} = C_{PE}\left(\beta_1 + \beta_1 f_m f_p\right) \tag{4}$$

Where P is the operational pressure (barg). D is the vessel diameter (m) and f_p is the pressure factor.

A.4 - Horizontal Vessels

Table A.4.1 - Economic parameters for horizontal pressure vessels for the calculus of C_I

Equipment	**PLUG-01**	**PLUG-02**	**PLUG-03**
Equipment type	Ammonia Reactor	Ammonia Rector	Ammonia Reactor
Ξ_1	3.556	3.556	3.556
Ξ_2	0.378	0.378	0.378
Ξ_3	0.0905	0.0905	0.0905
S Unity (m^3)	1.4	4.8	5.8
Ω_1	-	-	-
Ω_2	-	-	-
Ω_3			
Pressure (atm)	200	200	200
Temperature (ºC)	480	475	465
β_1	1.49	1.49	1.49
β_2	1.52	1.52	1.52
Method	Capcost	Capcost	Capcost
CEPCI	397.5	397.5	397.5

A.5 - Heat Exchangers

Table A.5.1 - Parameters assumed for heat exchangers considering Icarus methodology for C_{EP}. Source: EPE (2018).

Type	Shell-Tube	Air cooler
A	-0.0111	0
B	0.3539	0.0913
C	-2.769	-0.7632
D	15.872	11.558
x minimum (ft^2)	100	100
x maximum (ft^2)	70.000	10.000

In order to calculater the installed cost of heat exchangers. different f_m and f_p expressions where used to calculate the C_{BM} because Capcost method has limitations considering size attributes for shell-tube heat exchangers in the Capcost method for shell-tube exchangers (PAIXÃO, 2018; TURTON). In that regard, Equations (5) and (6) were used:

$$f_m = \tau_1 + \left(\frac{A}{100}\right)^{\tau_2} \quad (5)$$

$$f_p = 0.9803 + 0.1018\left(\frac{P}{100}\right) + 0.0017\left(\frac{P}{100}\right)^2 \quad (6)$$

where $\tau_1 . \tau_2$ are parameters chosen for each heat exchanger. P is the pressure (psig) and A is the heat exchange area (ft^2).

Table A.5.2 contains the description for each heat exchangers with the details for the parameters assumed, material description and cost estimated.

Table A.5.2 – Heat exchangers parameters for f_m

Equipment	τ_1	τ_2	Material Description	A(m^2)
HEAT-01	1.55	0.05	Alloy steel with Cr and Mo	163
H100	1.55	0.05	Alloy steel with Co and Mo	317
H200	1.55	0.05	Alloy steel with Cr and Mo	475
H300	1.55	0.05	Alloy steel with Cr and Mo	230

Table A.5.2 – Heat exchangers parameters for f_m (continue)

H400	1.55	0.05	Alloy steel with Cr and Mo	1988
COOL-01	1.55	0.05	Alloy steel with Cr and and Mo	285
COOL-02	1.55	0.05	Alloy steel with Cr and and Mo	223
COOL-03	1.75	0.13	316 stainless steel	55
COOL-04	1.75	0.13	316 stainless steel	51
COOL-05	2.7	0.07	316 stainless steel	718

A.6 - Acid Gas Removal Unit

The work from Gadelha *et al*. (2014) developed correlations to estimate CAPEX and OPEX costs from a Acid Gas Removal Unit considering derived from an economic study conducted to CO_2 treatment units by washing with amines considering MDEA as the main solvent employed. Equation (7) e (8) indicates the adjusted function as a function of CO_2 (Q) flow quantified in $MMnm^3\ day^{-1}$ flow, being the cost base raised from 2013.

$$CAPEX = 23.553\ (Q) + 2.6532 \tag{7}$$

$$OPEX = 14.493\ (Q) + 0.5229 \tag{8}$$

where CAPEX and OPEX costs are in MM $.

Table A.6.1 contains both AGR parameters in the equations to estimate both costs.

Table A.6.1 – Acid Gas Removal parameters

Section	**CO_2 molar flow (kmol/hr)**	Q (MMnm³/day)
BIOGAS-CLEAN	400	0.214
CO2-REMOVAL	585	0.312

Table A.7 – Utilities consumption according to Aspen Plus classification

Equipment	Utilities	Values	Unity
PUMP-01	ELEC	28.2	kW
COMP-01	ELEC	2763	kW
COMP-02	ELEC	4772	kW
COMP-CO2	ELEC	1109	kW
COMP-CO2	CW	684	kW
HEAT-01	FH	4700	kW
SRM-01	FH	34331	kW
SRM-02	HPS	-2000	kW
COOL-01	LPS	-8395	kW
COOL-02	CW	-17850	kW
FLASH-01	CW	482	kW
COMP-03	ELEC	7114	kW
COMPRESS	ELEC	6169	kW
COMPRESS	CW	4881	kW
COOL-03	HPS	-6229	kW
COOL-04	HPS	-5928	kW
COOL-05	REF	-18135	kW
STRIPPER	MPS	19063	kW
SCRUBBER	CW	-7863	kW

Appendix B - Economic analysis

B.1 - Utilities specifications

Table B.1 – Utilities specifications from *Aspen Plus*

Utility	Type	Tin (ºC)	Tout (ºC)	Inlet Vapor fraction	Outlet vapor fraction	Pressure (bar)	Price ($/GJ)
ELEC	-	-	-	-	-	-	21.5[a]
LPS	Hot	125	124	1	0	2.3	1.9
MPS	Hot	175	174	1	0	8.9	2.2
HPS	Hot	250	249	1	0	39.8	2.5
FH	Hot	-	-	-	-	-	4.06
LPSg	Cold	124	125	0	1	2.3	-.1.9
MPSg	Cold	174	175	0	1	8.9	-2.2
HPSg	Cold	249	250	0	1	39.8	-2.5
CW	Cold	20	25	0	0	1	0.212
REF	Cold	-40	-30	0	0	-	3.06

[a]Equivalent to 0.08 $

Table B.2 – Equipment cost breakdown

Equipment Type	Equipment Name	Section	CEPCI-base	Cost CEPCI ($)
Pump	PUMP-01	Raw Materials	397.5	73,947.26
Compressor	COMP-01	Raw Materials	397.5	1,258,478.64
Compressor	COMP-02	Raw Materials	576.1	7,732,854.63
Compressor	COMP-03	Methanation	576.1	13,228,736.89
Compressor	COMP-CO2	CO2-Removal	397.5	643,511.73
Compressor	COMPRESS	Ammonia Synthesis	397.5	16,406,917.75
Reformer Furnace	SRM-01	Steam Reforming	397.5	15,844,090.37
Pyrolysis furnace	SRM-02	Steam Reforming	397.5	2,741,561.95
FLASH-01	FLASH-01	CO2-Removal	397.5	316,506.74
FLASH-02	FLASH-02	Ammonia Synthesis	397.5	984,005.01
Horizontal Vessel	HTS-01	Shift Section	397.5	210,860.28
Horizontal Vessel	LTS-01	Shift Section	397.5	248,784.47
Horizontal Vessel	PLUG-01	Ammonia Synthesis	397.5	728,944.94
Horizontal Vessel	PLUG-02	Ammonia Synthesis	397.5	1,266,572.57
Horizontal Vessel	PLUG-03	Ammonia Synthesis	397.5	1,513,152.95
Heat-Exchanger	HEAT-01	Raw Materials	395.6	709,988.84
Heat-Exchanger	H100	Raw Materials	395.6	758,053.02
Heat-Exchanger	H200	Raw Materials	395.6	1,632,385.13
Heat-Exchanger	H300	Methanation	395.6	595,456.13
Heat-Exchanger	H400	Ammonia Synthesis	395.6	4,092,706.89
Heat-Exchanger	COOL-01	Shift Section	395.6	1,056,999.04
Heat-Exchanger	COOL-02	Shift Section	395.6	652,336.63
Heat-Exchanger	COOL-03	Ammonia Synthesis	395.6	626,731.55
Heat-Exchanger	COOL-04	Ammonia Synthesis	395.6	606,153.38
Heat-Exchanger	COOL-05	Ammonia Synthesis	395.6	5,015,827.04
Acid Gas Removal Unit	CO2-SEP	CO2-Removal	564.7	13,816,481.96
Acid Gas Removal Unit	CO2-RES	BIOGAS-CLEAN	564.7	9,764,982.24

Table B.3 – Income Statement (DRE) regarding biogas plant in the base scenario

Liquid Income	Variable Costs	Fixed Costs	Gross Operating Profit	Operational Expenses	Operational Profit	Financial Expenses	Investment Depreciation	Profit before tax	Income Tax	Liquid Profit
0.0	0.0	0.0	0.0	0.0	0.0	6.3	0.0	0.0	0.0	0.0
0.0	0.0	0.0	0.0	0.0	0.0	16.8	0.0	0.0	0.0	0.0
0.0	0.0	0.0	0.0	0.0	0.0	21.0	0.0	0.0	0.0	0.0
55.4	27.4	17.9	10.1	0.1	10.1	20.0	13.6	-23.6	0.0	-15.6
99.8	49.4	17.9	32.5	0.1	32.5	19.1	13.6	-0.3	0.0	-0.2
110.9	54.9	17.9	38.1	0.1	38.1	18.1	13.6	6.3	2.1	4.1
110.9	54.9	17.9	38.1	0.1	38.1	17.2	13.6	7.2	2.5	4.8
110.9	54.9	17.9	38.1	0.1	38.1	16.2	13.6	8.2	2.8	5.4
110.9	54.9	17.9	38.1	0.1	38.1	15.3	13.6	9.1	3.1	6.0
110.9	54.9	17.9	38.1	0.1	38.1	14.3	13.6	10.1	3.4	6.7
110.9	54.9	17.9	38.1	0.1	38.1	13.4	13.6	11.1	3.8	7.3
110.9	54.9	17.9	38.1	0.1	38.1	12.4	13.6	12.0	4.1	7.9
110.9	54.9	17.9	38.1	0.1	38.1	11.5	13.6	13.0	4.4	8.6
110.9	54.9	17.9	38.1	0.1	38.1	10.5	13.6	13.9	4.7	9.2
110.9	54.9	17.9	38.1	0.1	38.1	9.5	13.6	14.9	5.1	9.8
110.9	54.9	17.9	38.1	0.1	38.1	8.6	13.6	15.8	5.4	10.4
110.9	54.9	17.9	38.1	0.1	38.1	7.6	13.6	16.8	5.7	11.1
110.9	54.9	17.9	38.1	0.1	38.1	6.7	13.6	17.7	6.0	11.7
110.9	54.9	17.9	38.1	0.1	38.1	5.7	13.6	18.7	6.4	12.3
110.9	54.9	17.9	38.1	0.1	38.1	4.8	13.6	19.7	6.7	13.0
110.9	54.9	17.9	38.1	0.1	38.1	3.8	13.6	20.6	7.0	13.6
110.9	54.9	17.9	38.1	0.1	38.1	2.9	13.6	21.6	7.3	14.2
110.9	54.9	17.9	38.1	0.1	38.1	1.9	13.6	22.5	7.7	14.9
110.9	54.9	17.9	38.1	0.1	38.1	1.0	13.6	23.5	8.0	15.5
110.9	54.9	17.9	38.1	0.1	38.1	-0.0	13.6	24.4	8.3	16.1

Table B.4 – Discounted Cash Flow for biogas plant in the base scenario

Liquid Income	Financing	Financial Income	Variable Costs	Fixed Costs	Financial Expense	CAPEX	Working Capital	Amortization	Income Tax	NPV	Total NPV
0.0	63.0	0.0	0.0	0.0	6.3	90.0	13.5	0.0	0.0	-46.8	-46.8
0.0	105.0	0.0	0.0	0.0	16.8	150.0	22.5	0.0	0.0	-76.6	-123.5
0.0	42.0	0.0	0.0	0.0	21.0	60.0	9.0	0.0	0.0	-39.7	-163.1
55.4	0.0	0.0	27.4	17.9	20.0	0.0	0.0	9.5	0.0	-14.7	-177.8
99.8	0.0	0.0	49.4	17.9	19.1	0.0	0.0	9.5	0.0	2.6	-175.2
110.9	0.0	0.0	54.9	17.9	18.1	0.0	0.0	9.5	2.1	5.1	-170.1
110.9	0.0	0.0	54.9	17.9	17.2	0.0	0.0	9.5	2.5	5.0	-165.1
110.9	0.0	0.0	54.9	17.9	16.2	0.0	0.0	9.5	2.8	4.9	-160.2
110.9	0.0	0.0	54.9	17.9	15.3	0.0	0.0	9.5	3.1	4.7	-155.5
110.9	0.0	0.0	54.9	17.9	14.3	0.0	0.0	9.5	3.4	4.6	-150.9
110.9	0.0	0.0	54.9	17.9	13.4	0.0	0.0	9.5	3.8	4.4	-146.5
110.9	0.0	0.0	54.9	17.9	12.4	0.0	0.0	9.5	4.1	4.2	-142.3
110.9	0.0	0.0	54.9	17.9	11.5	0.0	0.0	9.5	4.4	4.0	-138.3
110.9	0.0	0.0	54.9	17.9	10.5	0.0	0.0	9.5	4.7	3.8	-134.4
110.9	0.0	0.0	54.9	17.9	9.5	0.0	0.0	9.5	5.1	3.7	-130.8
110.9	0.0	0.0	54.9	17.9	8.6	0.0	0.0	9.5	5.4	3.5	-127.3
110.9	0.0	0.0	54.9	17.9	7.6	0.0	0.0	9.5	5.7	3.3	-124.0
110.9	0.0	0.0	54.9	17.9	6.7	0.0	0.0	9.5	6.0	3.1	-120.9
110.9	0.0	0.0	54.9	17.9	5.7	0.0	0.0	9.5	6.4	3.0	-117.9
110.9	0.0	0.0	54.9	17.9	4.8	0.0	0.0	9.5	6.7	2.8	-115.1
110.9	0.0	0.0	54.9	17.9	3.8	0.0	0.0	9.5	7.0	2.6	-112.5
110.9	0.0	0.0	54.9	17.9	2.9	0.0	0.0	9.5	7.3	2.5	-110.0
110.9	0.0	0.0	54.9	17.9	1.9	0.0	0.0	9.5	7.7	2.3	-107.7
110.9	0.0	0.0	54.9	17.9	1.0	0.0	0.0	9.5	8.0	2.2	-105.5
110.9	0.0	0.0	54.9	17.9	-0.0	0.0	0.0	9.5	8.3	6.6	-98.9

Table B.5 – Income Statement (DRE) regarding natural gas plant in the base scenario

Liquid Income	Variable Costs	Fixed Costs	Gross Operating Profit	Operational Expenses	Operational Profit	Financial Expenses	Investment Depreciation	Profit before tax	Income Tax	Liquid Profit
0.0	0.0	0.0	0.0	0.0	0.0	5.7	0.0	0.0	0.0	0.0
0.0	0.0	0.0	0.0	0.0	0.0	15.2	0.0	0.0	0.0	0.0
0.0	0.0	0.0	0.0	0.0	0.0	19.0	0.0	0.0	0.0	0.0
55.4	50.8	17.1	-12.5	0.1	-12.5	18.1	12.3	-43.0	0.0	-28.4
99.8	91.5	17.1	-8.8	0.1	-8.8	17.3	12.3	-38.5	0.0	-25.4
110.9	101.6	17.1	-7.8	0.1	-7.9	16.4	12.3	-36.7	0.0	-24.2
110.9	101.6	17.1	-7.8	0.1	-7.9	15.5	12.3	-35.8	0.0	-23.6
110.9	101.6	17.1	-7.8	0.1	-7.9	14.7	12.3	-34.9	0.0	-23.1
110.9	101.6	17.1	-7.8	0.1	-7.9	13.8	12.3	-34.1	0.0	-22.5
110.9	101.6	17.1	-7.8	0.1	-7.9	13.0	12.3	-33.2	0.0	-21.9
110.9	101.6	17.1	-7.8	0.1	-7.9	12.1	12.3	-32.3	0.0	-21.3
110.9	101.6	17.1	-7.8	0.1	-7.9	11.2	12.3	-31.5	0.0	-20.8
110.9	101.6	17.1	-7.8	0.1	-7.9	10.4	12.3	-30.6	0.0	-20.2
110.9	101.6	17.1	-7.8	0.1	-7.9	9.5	12.3	-29.8	0.0	-19.6
110.9	101.6	17.1	-7.8	0.1	-7.9	8.6	12.3	-28.9	0.0	-19.1
110.9	101.6	17.1	-7.8	0.1	-7.9	7.8	12.3	-28.0	0.0	-18.5
110.9	101.6	17.1	-7.8	0.1	-7.9	6.9	12.3	-27.2	0.0	-17.9
110.9	101.6	17.1	-7.8	0.1	-7.9	6.0	12.3	-26.3	0.0	-17.4
110.9	101.6	17.1	-7.8	0.1	-7.9	5.2	12.3	-25.4	0.0	-16.8
110.9	101.6	17.1	-7.8	0.1	-7.9	4.3	12.3	-24.6	0.0	-16.2
110.9	101.6	17.1	-7.8	0.1	-7.9	3.5	12.3	-23.7	0.0	-15.6
110.9	101.6	17.1	-7.8	0.1	-7.9	2.6	12.3	-22.8	0.0	-15.1
110.9	101.6	17.1	-7.8	0.1	-7.9	1.7	12.3	-22.0	0.0	-14.5
110.9	101.6	17.1	-7.8	0.1	-7.9	0.9	12.3	-21.1	0.0	-13.9
110.9	101.6	17.1	-7.8	0.1	-7.9	0.0	12.3	-20.3	0.0	-13.4

Table B.6 – Discounted Cash Flow for natural gas plant in the base scenario

Liquid Income	Financing	Financial Income	Variable Costs	Fixed Costs	Financial Expense	CAPEX	Working Capital	Amortization	Income Tax	NPV	Total NPV
0.0	57.0	0.0	0.0	0.0	4.7	81.4	12.2	0.0	0.0	-42.3	-42.3
0.0	95.0	0.0	0.0	0.0	12.4	135.7	20.4	0.0	0.0	-69.3	-111.7
0.0	38.0	0.0	0.0	0.0	15.6	54.3	8.1	0.0	0.0	-35.9	-147.6
55.4	0.0	0.0	50.8	17.1	14.8	0.0	0.0	8.6	0.0	-29.5	-177.1
99.8	0.0	0.0	91.5	17.1	14.1	0.0	0.0	8.6	0.0	-23.7	-200.9
110.9	0.0	0.0	101.6	17.1	13.4	0.0	0.0	8.6	0.0	-20.5	-221.3
110.9	0.0	0.0	101.6	17.1	12.7	0.0	0.0	8.6	0.0	-18.1	-239.4
110.9	0.0	0.0	101.6	17.1	12.0	0.0	0.0	8.6	0.0	-16.0	-255.5
110.9	0.0	0.0	101.6	17.1	11.3	0.0	0.0	8.6	0.0	-14.2	-269.6
110.9	0.0	0.0	101.6	17.1	10.6	0.0	0.0	8.6	0.0	-12.5	-282.2
110.9	0.0	0.0	101.6	17.1	9.9	0.0	0.0	8.6	0.0	-11.0	-293.2
110.9	0.0	0.0	101.6	17.1	9.2	0.0	0.0	8.6	0.0	-9.7	-302.9
110.9	0.0	0.0	101.6	17.1	8.5	0.0	0.0	8.6	0.0	-8.6	-311.5
110.9	0.0	0.0	101.6	17.1	7.8	0.0	0.0	8.6	0.0	-7.5	-319.1
110.9	0.0	0.0	101.6	17.1	7.1	0.0	0.0	8.6	0.0	-6.6	-325.7
110.9	0.0	0.0	101.6	17.1	6.4	0.0	0.0	8.6	0.0	-5.8	-331.5
110.9	0.0	0.0	101.6	17.1	5.7	0.0	0.0	8.6	0.0	-5.1	-336.6
110.9	0.0	0.0	101.6	17.1	4.9	0.0	0.0	8.6	0.0	-4.5	-341.1
110.9	0.0	0.0	101.6	17.1	4.2	0.0	0.0	8.6	0.0	-3.9	-345.0
110.9	0.0	0.0	101.6	17.1	3.5	0.0	0.0	8.6	0.0	-3.4	-348.4
110.9	0.0	0.0	101.6	17.1	2.8	0.0	0.0	8.6	0.0	-3.0	-351.4
110.9	0.0	0.0	101.6	17.1	2.1	0.0	0.0	8.6	0.0	-2.6	-354.0
110.9	0.0	0.0	101.6	17.1	1.4	0.0	0.0	8.6	0.0	-2.2	-356.2
110.9	0.0	0.0	101.6	17.1	0.7	0.0	0.0	8.6	0.0	-1.9	-358.2
110.9	0.0	0.0	101.6	17.1	0.0	0.0	0.0	8.6	0.0	2.5	-355.7

Appendix C – Mass Flow, pressure, temperature and molar fraction of streams

Table C.1 – Stream conditions from ammonia synthesis

Stream	AIR	AIR-B	BIOGAS	CH4-FEED	CO2-RES	FEED-H2O	MAKE-UP	WAT-RES
From	-	COMP-02	-	SEP-01	SEP-01	MIX-02	-	CO2-SEP
To	COMP-02	STM-REF	SEP-01	COMP-01		PUMP-01	MIX-02	VALV-01
Temperature (K)	298	482	298	298	298	300	298	323
Pressure (atm)	1	25	1	1	1	1	1	25
Vapor Fraction	1	1	1	1	1	0	0	0
Mole Fractions								
CO_2	-	-	0.4	-	1	-	-	-
NH_3	-	-	-	-	-	-	-	-
H_2O	-	-	-	-	-	1	1	1
N_2	0.78	0.78	-	-	-	-	-	-
O_2	0.21	0.21	-	-	-	-	-	-
CH_4	-	-	0.6	1	-	-	-	-
H_2	-	-	-	-	-	-	-	-
CO	-	-	-	-	-	-	-	-
Argon	0.01	0.01	0	-	0	-	0	-
Mass Flow (kg/hr)	24,565	24,565	27,230	9626	17,604	32,430	15,140	17,290

Table C.1 – Stream conditions from ammonia synthesis (continue)

Stream	**S-01**	**S-01B**	**S-02**	**S-03**	**SRM-FEED**	**SRM-EXIT-01**	**FEED-02**	**SRM-EXIT-02**
From	PUMP-01	H200	COMP-01	MIX-01	H100	SRM-01	MIX-02	SRM-02
To	H200	MIX-01	MIX-01	H100	STM-REF	MIX-02	SRM-02	-
Temperature (K)	322	497	673	550	823	1,093	986	1273
Pressure (atm)	25	25	25	25	25	25	25	25
Vapor Fraction	0	1	1	1	1	1	1	1
Mole Fraction								
CO_2	-	-	-	-	-	0.058	0.046	0.046
NH_3	-	-	-	-	-	-	-	-
H_2O	1	1	-	0.75	0.75	0,36	0.287	0.320
N_2	-	-	-	-	-	-	0.161	0.155
O_2	-	-	-	-	-	-	0.043	-
CH_4	-	-	1	0.25	0.25	0,052	0.040	-
H_2	-	-	-	-	-	0,455	0.361	0.381
CO	-	-	-	-	-	0,074	0.059	0.093
Argon	-	-	-	-	-	-	-	-
Mass Flow (kg/hr)	32,430	32,430	9,625	42,056	42,056	42,056	66,621	66,621

Table C.1 – Stream conditions from ammonia synthesis (continue)

Stream	SRM-EXIT	S-04	S-04B	S-04C	HTS-EXIT	HTS-B	LTS-EXIT	LTS-B
From	SRM-REF	H100	H200	HEAT-01	HTS-100	COOL-01	LTS-100	COOL-02
To	H100	H200	SHIFT-RF	HTS-100	COOL-01	LTS-100	COOL-02	FLASH-01
Temperature (K)	1,273	1,091	482	603	673	473	493	323
Pressure (atm)	25	25	25	25	25	25	25	25
Vapor Fraction	1	1	1	1	1	1	1	1
Mole Fraction								
CO_2	0.046	0.046	0.046	0.046	0.120	0.120	0.137	0.137
NH_3	-	-	-	-	-	-		
H_2O	0.320	0.320	0.320	0.320	0.246	0.246	0.229	0.229
N_2	0.155	0.155	0.155	0.155	0.155	0.155	0.155	0.155
O_2	-	-	-	-	-	-	-	-
CH_4	-	-	-	-	-	-	-	-
H_2	0.381	0.381	0.381	0.381	0.455	0.455	0.473	0.473
CO	0.093	0.093	0.093	0.093	0.019	0.019	0.019	0.002
Argon	-	-	-	-	-	-	-	-
Mass Flow (kg/hr)	66,621	66,621	66,621	66,621	66,621	66,621	66,621	66,621

Table C.1 – Stream conditions from ammonia synthesis (continue)

Stream	**FLS-EXIT**	**CO2-REM**	**CO2-UREA**	**S-05**	**S-05B**	**S-06**	**MET-RES**	**S-06B**	**S-06C**
From	FLASH-01	SEP-01	COMP-CO2	SEP-01	H300	MET-01	SEP-02	SEP-02	COMP-03
To	SEP-01	COMP-CO2	STRP-100	H300	MET-01	SEP-02	-	COMP-03	H300
Temperature (K)	323	323	373	323	573	573	573	573	815
Pressure (atm)	25	25	140	25	25	25	25	25	65
Vapor Fraction	1	1	1	1	1	1	1	1	1
Mole Fraction									
CO_2	0.177	1	1	-	-	-	-	-	-
NH_3	-	-	-	-	-	-	-	-	-
H_2O	0.005	-	-	0.005	0.005	-	0.665	-	-
N_2	0.200	-	-	0.243	0.243	0.245	0.083	0.247	0.247
O_2	-	-	-	-	-	-	-	-	-
CH_4	-	-	-	0.002	0.002	0.005	0.002	0.006	0.006
H_2	0.611	-	-	0.742	0.742	0.736	0.249	0.743	0.743
CO	0.003	-	-	0.003	0.003	-	-	-	-
Argon	0.002	-	-	0.003	0.003	0.003	0.001	0.003	0.003
Mass Flow (kg/hr)	49,332	25,748	25,748	23,583	23,583	23,583	592	22,991	22,991

Table C.1 – Stream conditions from ammonia synthesis (continue)

Stream	S-07	FEED-PRO	GAS-REC	FEED-REC	EXIT-01	EXIT-01B	EXIT-02	EXIT-02B	PROD
From	H300	COMPRESS	SPLIT-01	MIX-03	PLUG-100	COOL-03	PLUG-200	COOL-04	PLUG-300
To	COMPRESS	MIX-03	MIX-03	PLUG-100	COOL-03	PLUG-200	COOL-04	PLUG-300	SPLT-02
Temperature (K)	564	663	663	663	754	673	767	683	741
Pressure (atm)	65	200	200	200	200	200	200	200	200
Vapor Fraction	1	1	1	1	1	1	1	1	1
Mole Fraction									
CO_2	-	-	-	-	-	-	-	-	-
NH_3	-	-	0.020	0.014	0.070	0.070	0.134	0.134	0.176
H_2O	-	-	-	-	-	-	-	-	-
N_2	0.247	0.247	0.232	0.0237	0.223	0.223	0.206	0.206	0.195
O_2	-	-	-	-	-	-	-	-	-
CH_4	0.006	0.006	0.034	0.025	0.027	0.027	0.028	0.028	0.029
H_2	0.743	0.743	0.698	0.712	0.669	0.669	0.619	0.619	0.586
CO	-	-	-	-	-	-	-	-	-
Argon	0.003	0.003	0.014	0.011	0.012	0.012	0.012	0.012	0.013
Mass Flow (kg/hr)	22,991	22,991	55,505	78,496	78,496	78,496	78,496	78,496	78,496

Table C.1 – Stream conditions from ammonia synthesis (continue)

Stream	PROD-S1	PROD-S2	PROD-S1B	PROD-01	PROD-02	GAS-EXIT	REC-B	PURGE	NH3
From	SPLT-02	SPLT-02	H400	MIX-04	COOL-05	FLASH-02	H400	SPLT-01	FLASH-02
To	H400	MIX-04	MIX-04	COOL-05	FLASH-02	H400	SPLT-01	-	-
Temperature (K)	741	741	295	427	-253	253	663	663	253
Pressure (atm)	200	200	200	200	200	200	200	200	200
Vapor Fraction	1	1	1	1	0.74	1	1	1	0
Mole Fraction									
CO_2	-	-	-			-	-	-	
NH_3	0.176	0.176	0.176	0.176	0.176	0.020	0.020	0.020	0.985
H_2O	-	-	-	-	-	-	-	-	-
N_2	0.195	0.195	0.195	0.195	0.195	0.232	0.232	0.232	0.002
O_2	-	-	-	-	-	-	-	-	
CH_4	0.029	0.029	0.029	0.029	0.029	0.034	0.034	0.034	0.004
H_2	0.586	0.586	0.586	0.586	0.586	0.698	0.698	0.698	0.005
CO	-	-	-	-	-	-	-	-	-
Argon	0.013	0.013	0.013	0.013	0.013	0.014	0.014	0.014	0.003
Mass Flow (kg/hr)	54,947	23,548	23,548	78,496	78,496	58,120	58,120	2,615	20,358

Table C.2 – Stream conditions from urea synthesis

Stream	CO2-FEED	LIQ-EXIT	STL-EXIT	VAP-REC	NH3-FEED	CARB-REC	SYN-FEED	PFR-FEED
From	-	FLASH-03	STRP-100	STRP-100	-	SCB-100	MIX-100	POOLCOND
To	STRP-100	STRP-100	STC-100	MIX-100	MIX-100	MIX-100	POOLCOND	UREA-SYN
Temperature (K)	373	458	448	460	313	446	415	443
Pressure (atm)	140	140	140	140	140	140	140	140
Vapor Fraction	1	0	0	1	0	0	0.702	0.436
Mole Fraction								
Urea	-	0.182	0.372	-	-	-	-	0.019
Ammonium Carbamate	-	0.121	0.012	-	-	0.300	0.05	0.143
CO_2	1	0.015	0.023	0.0326	-	0.012	0.196	0.132
NH_3	-	0.400	0.088	0.630	1	0.418	0.680	0.603
H_2O	-	0.281	0.498	0.042	-	-	0.071	0.102
Mass Flow (kg/hr)	26,405	105,932	54,459	72,133	20,010	30,892	128,779	128,779

Table C.2 – Stream conditions from urea synthesis (continue)

Stream	RS-EXIT	VAP-EXIT	LIQ-EXIT	CARB-REC	CARB-SOL	UREA-01	LIQ-STM	UREA-END
From	UREA-SYN	FLASH-03	FLASH-03	SCB-100	ERV-01	STC-100	SEP-03	SEP-03
To	FLASH-03	SCB-100	STRP-100	MIX-100	SCB-100	SEP-03	ERV-01	-
Temperature (K)	458	458	458	446	345	345	345	345
Pressure (atm)	140	140	140	140	140	140	140	140
Vapor Fraction	0.178	1	1	0	0	0	0	0
Mole Fraction								
Urea	0.139	-	0.182	-	-	0.642	-	0.501
Ammonium Carbamate	0.093	-	0.121	0.300	0.507	-	-	-
CO_2	0.066	0.231	0.015	0.012	-	0.047	0.138	-
NH_3	0.477	0.727	0.400	0.418	0.106	0.054	0.408	-
H_2O	0.224	0.04	0.281	0.269	0.386	0.256	0.454	0.499
Mass Flow (kg/hr)	128,781	22,856	105,924	30,898	9,024	54,455	9,024	45,430